ISAS - INTERNATIONAL SCHOOL
FOR ADVANCED STUDIES

Network activity in the hippocampus during development: modulatory role of acetylcholine.

Thesis submitted for the degree of "Doctor Philosophiae"

CANDIDATE
Avignone Elena

SUPERVISOR
Prof. Enrico Cherubini

SISSA - SCUOLA
INTERNAZIONALE
SUPERIORE
DI STUDI AVANZATI

TRIESTE
Via Beirut 2-4

TRIESTE

Table of contents

Acknowledgements

I wish to express my gratitude to Prof. Enrico Cherubini for its patient and careful supervision. His contagious enthusiasm always played a fundamental role during my PhD. I thank Prof. A. Cattaneo and A. Nistri for helpful and stimulating discussions.

A special thanks goes to Dr. Nicola Berretta for friendly and open discussions and for all the advices that he gave me during these years. Finally I would like to thank Dr. Margherita Molnar for introducing me to the field of molecular biology.

NOTE

The work described in this dissertation was carried out at the International School for Advanced Studies, Trieste, between January 1995 and June 1998. All work reported, with the exception listed below, arises solely from my own experiments and this work has not been submitted in whole or in part to any other University

The immunohystochemical experiments were carried out by Margherita Molnar (section 4.2.2), the release experiments by Fiorella Casamenti and Costanza Prosperi (section 4.2.4)

Part of the data reported in the present thesis have been published or submitted in the articles listed below.

Avignone E., Molnar M., Berretta N., Casamenti F., Prosperi C., Ruberti F., Cattaneo A. and Cherubini E.
Cholinergic function in the hippocampus of juvenile rats chronically deprived of NGF.
Dev. Brain Res. In press

Molnar M., Tongiorgi E., **Avignone E.**, Gonfloni S., Ruberti F., Domenici L., & Cattaneo A.
The effects of anti-NGF monoclonal antibodies on developing basal forebrain neurons are transient and reversible
Eur. J. Neurosci.In press

Bolea S., **Avignone E.**, Sanchez-Andres J.V., Berretta N. and Cherubini E.
Glutamate controls the induction of GABA-mediated giant depolarising potential through AMPA receptor
Submitted

Rosati A.M., Guarnieri E., **Avignone E.**, Cherubini E., Cattaneo A. and Traversa U.
Increased density of M1 receptors in the hippocampus of juvenile rats chronically deprived of NGF
Dev. Brain Res. In press

Avignone E. and Cherubini E.
Muscarinic modulation of GABA-mediated Giant Depolarizing Potentials in the neonatal rat hippocampus
In preparation

Abbreviations used in the text

ACh: Acetylcholine

AChE: acetylcholine esterase

ACSF: artificial cerebrospinal fluid

AMPA: (*RS*)-α-amino-3-hydroxy-5-methyl-4-isoxadepropionate

AP-5: D(-)2-amino-5-phosphovaleric acid

ATPA: ((RS)-2-amino-3-(3-hydroxy-5-tert-butylisoxazol-4-yl) propanoic acid

BF: basal forebrain

ChAT: choline acetyl transferase

CNQX: 6-cyano-7-nitroquinoxaline-2,3-dione

CPP: (+)-3-(2-carboxy-piperazin-4-yl)-propyl-1-phosphonic acid

Cyclothiazide: 6-chloro-3,4dihydro-3-[2-norbornen-5-yl]-2H-1,2-4benzothiadiazine-7-sulfonamide 1,1-dioxide

D-AP5: D(-)-2-amino-5-phosphonopentanoic acid

DCG-IV: 2-(2,3-dicarboxycyclopropyl) glycine

DG: dentate gyrus

DNQX: 6,7-dinitroquinoxaline-2,3(1H,4H)-dione

EC: enthorinal cortex

EPSP: excitatory postsynaptic potentials

GABA: γ-aminobutyric acid

GDPs: Giant Depolarizing Potentials

HCO_3^-: bicarbonate

I_{KCa}: Ca-dependent K current

I_M: M current

IPSP: inhibitory postsynaptic potentials

LTP: long-term potentiation

Mx: muscarinic receptors subtype x

MCPG: (RS)-α-methyl-4-carboxyphenylglycine

mGluR: metabotrobic glutamate receptors

NBQX: 6-nitro-7-sulphamoylbenzo(f)-quinoxaline-2,3-dione

NGF: nerve growth factor

NMDA: N-methyl-D-Aspartate

NMDAR: NMDA receptor

P: postnatal day

PKC: protein kinase C

PLC: phospholipase C

PTX: Pertussis Toxin

SEM: standard error of the mean

TrkA: tyrosine kinase

TTX: tetrodotoxin

t-ACPD: *trans*-1-aminocyclopentane-1,3-dicarboxylic acid

VSCCs:: voltage sensitive calcium channels

Abstract

Giant Depolarizing Potentials (GDPs) .are network-driven oscillations occuring in the hippocampus during the two first postnatal weeks at the frequency of 1-7 GDPs/min. They consist in large depolarizations lasting 300-500 ms with superimposed fast action potentials, are $GABA_A$-mediated and are synchronous over the entire hippocampus. The present study has investigated firstly the mechanisms of GDPs generation in hippocampal slices during the first postnatal week and their modulation by acetylcholine acting on muscarinic receptors. Moreover, since the main source of acetylcholine (ACh) within the hippocampus derives from the septo-hippocampal pathway that originates from basal forebrain (BF) cholinergic neurons (that depend on nerve growth factor (NGF) for their survival and maintenance), in a second set of experiments, the role of NGF on the cholinergic function of hippocampal cells has been elucidated.

Whole cell patch clamp recordings from CA3 pyramidal cells under current clamp conditions revealed that GDPs originated from the interplay of γ-aminobutyric acid (GABA) acting on $GABA_A$ receptors and glutamate acting on ionotropic (*RS*)-α-amino-3-hydroxy-5-methyl-4-isoxadepropionate (AMPA) receptors. Bath application of D(-)2-amino-5-phosphovaleric acid (AP-5, 50 μM) or (+)-3-(2-carboxy-piperazin-4-yl)-propyl-1-phosphonic acid (CPP, 20 μM) produced only a transient reduction in GDPs frequency by 37 ± 9 % and 36 ± 11 %, respectively (mean ± SEM; n=10 and n=7). In contrast, superfusion of 6-cyano-7-nitroquinoxaline-2,3-dione (CNQX, 10-40 μM) completely blocked GDPs. However, in the presence of CNQX, it was still possible to re-induce the appearance of GDPs with GABA (20 μM), AMPA (5 μM) or KCl (6.5 mM). This effect was prevented by the more potent and selective AMPA receptor antagonist GYKI 53655 (50-100 μM). In the presence of GYKI 53655, both kainic and domoic acid (0.1-1

μM) were unable to induce GDPs. 6-chloro-3,4dihydro-3-[2-norbornen-5-yl]-2H-1,2-4benzothiadiazine-7- sulfonamide 1,1-dioxide (cyclothiazide, 20 μM), a selective blocker of AMPA receptor desensitization, increased GDPs frequency by 76 ± 14%. Experiments were also performed using an intracellular solution containing potassium fluoride (KF) to block $GABA_A$ receptor-mediated responses. In these conditions, a glutamatergic AMPA component of GDPs was revealed in the majority of the cells, at least 30 min after breaking into the whole cell configuration, as indicated by the change in GDPs reversal potential towards more positive values (from -40.8 ± 6.2 mV immediately after breaking into the whole cell configuration to -15.8 ± 13.1 mV after 30-40 min of cell dialysis with intracellular F^-), by the linearity of the amplitude-voltage relationship and by the sensitivity of the residual component of GDPs to CNQX. With a F^--containing solution, GDPs could still be recorded synchronous with those detected simultaneously with KCl-filled electrodes, although their amplitude was smaller. Similar results were found in pair recordings obtained from minislices containing only a small portion of the CA3 area, suggesting that GDPs generation requires activation of AMPA receptors by local release of glutamate from recurrent collaterals. GDPs were modulated by endogenous ACh acting on muscarinic receptors. Thus their frequency increased in the presence of the acetylcholinesterase inhibitor edrophonium (20 μM), in a developmentally regulated way from 17 ± 8 % at P3 to 102 ± 23 % at P6, suggesting an increase in cholinergic fibres and/or receptors with age. The effects of edrophonium were prevented by low concentration of pirenzepine, indicating the involvement of M1 receptor types. Exogenous application of carbachol produced both an up and down regulation of GABA release assessed as GDPs. These effects were mediated by M1 and non M1 (possibly M2) receptor subtypes since they were prevented by pirenzepine and methoctramine, respectively. The potentiating effect of carbachol on GDPs

frequency and membrane depolarization were blocked by GYKI 53665 (50 μM) and by bicuculline (10 μM) indicating that they were due to a muscarinic-dependent increase in the glutamatergic drive to interneurons. In GYKI 53665, carbachol was still able to increase the frequency of spontaneous GABA-mediated synaptic potentials, suggesting a direct action of carbachol on muscarinic receptors localised on interneurons.

Intracellular and extracellular recordings have been used to assess the cholinergic function in hippocampal slices from juvenile rats chronically deprived of NGF. NGF was neutralised by implanting into the lateral ventricle of postnatal (P) days 2 rats, αD11 hybridoma cells (secreting monoclonal antibodies specific for NGF). Parental myeloma cells (P3U) were used as controls. At P15-P18, slow cholinergic EPSPs could be elicited in cells from both αD11- and P3U-treated rats. However, slices from αD11-implanted rats exhibited a 50% reduction in acetylcholine release following electrical stimulation of cholinergic fibres. This effect was associated to a significant increase in the sensitivity of pyramidal cells to carbachol, as suggested by the shift to the left of the dose/response curve. This may reflect a compensatory mechanism for the reduced efficacy of cholinergic innervation in NGF-deprived rats. In both αD11 and P3U-treated rats, carbachol was able to induce a similar concentration-dependent depression of the field EPSPs, evoked by Schaffer collateral stimulation, suggesting that presynaptic muscarinic receptors were not altered. In rats implanted with αD11 cells at P2 and sacrificed one week later, a significant reduction in GDPs frequency was observed in the CA3 hippocampal area (from 3.3 ± 0.33 GDPs/min in controls to 1.7 ± 0.32 GDPs/min in αD11-treated animals). Probably this is in relation to the reduced levels of ACh in the hippocampus of NGF-deprived animals. In keeping with this, ACh released following electrical stimulation of hippocampal slices of αD11 treated rats was reduced with respect to control animal. Moreover, in αD11-treated animals it was

impossible to evoke slow cholinergic EPSP in the CA1 region. In rats implanted with αD11 cells at P15 and sacrificed at P21-P24, no changes in the sensitivity to carbachol were found. At this developmental stage, no differences in acetylcholine release were observed between P3U- and αD11-treated animals.

The present data clearly demonstrate that GDPs result from the interplay of GABA and glutamate acting mainly on AMPA receptor types. ACh by activating muscarinic receptors would further strenghten the action of GDPs, thus contributing to the fine tuning of hippocampal neuronal circuitry in a period when theta rhythm is not developed yet.

1 Introduction

1.1 The hippocampal formation

1.1.1 Functions of the hippocampus

The hippocampus is an elongated structure located on the medial wall of the lateral ventricle, whose longitudinal axis forms a semicircle around the thalamus. The hippocampus is among the best characterized cortical structures. Its layered organization (Andersen et al., 1971) is particularly suitable for anatomical and physiological investigations. The hippocampus is connected with several cortical and subcortical areas *via* the entorhinal cortex, the subiculum and the fimbria-fornix. It plays a crucial role in many physiological functions. Neuropsychological studies on patients with hippocampal damage have indicated that this structure is essential for learning and memory processes (Scoville and Milner, 1957). In particular, it has been suggested that in humans the hippocampus is fundamental for declarative memory: the memory for everyday facts and events that is subjected to conscious recollection and verbal or other explicit means of expression (for a review see Jaffard and Meunier, 1993). Another suggested function concerns the spatial memory that in rodents is associated to a cognitive map. This memory reflects the ability of the animal to recognize cues in the environment (a typical test consists to find a specific place such as a platform in opaque water). Experiments in rats indicate the presence of "place cells", whose firing rate appears to be related to the spatial position of the animal (Nadel, 1991). Furthermore, rats with hippocampal lesions typically exhibit an impairment in conventional radial arm maze tasks, even if some experiments demonstrate that other cortical structures could be involved in place learning (Eichenbaum, 1996).

Memory has been classified also as episodic and semantic. Episodic memory consists in a record of personal events while semantic is the memory of knowledge acquired in lifetime. In this scheme the hippocampus is critical for everyday episodic memory. Recent findings linking data from declarative, spatial and episodic memory, suggest that the principal function of the hippocampus is to promote flexible associations by recognizing relations among different items.

For example by measuring the activation of cortical areas with magnetic resonance imaging in human subjects, it has been observed that the subiculum is maximally activated when there is a recall of the word associated to a known corresponding object picture (retrieval task), whereas the parahippocampal cortex is maximally activated during acquisition of new information such as new words associated to new objects (encoding task, Gabrieli et al., 1997).

Defining exactly hippocampal functions is difficult, since most of the information is derived from hippocampal lesions which in humans are usually not restricted exclusively to the hippocampal formation but involve also surrounding areas.

The hippocampus is also involved in neurological disorders such as epilepsy, stroke and Alzheimer's disease.

1.1.2 Organization of the hippocampal formation

1.1.2.1 Internal circuit

The hippocampal formation includes the entorhinal cortex (EC), the subiculum, the dentate gyrus (DG) and the hippocampus proper. The hippocampus proper has been divided by Lorente de No' (Lorente de No',1934) in four different regions, named CA1, CA2, CA3 and CA4 (from Cornus Ammonis). The CA2 region is so small that it is often ignored and the CA4 usually refers to the

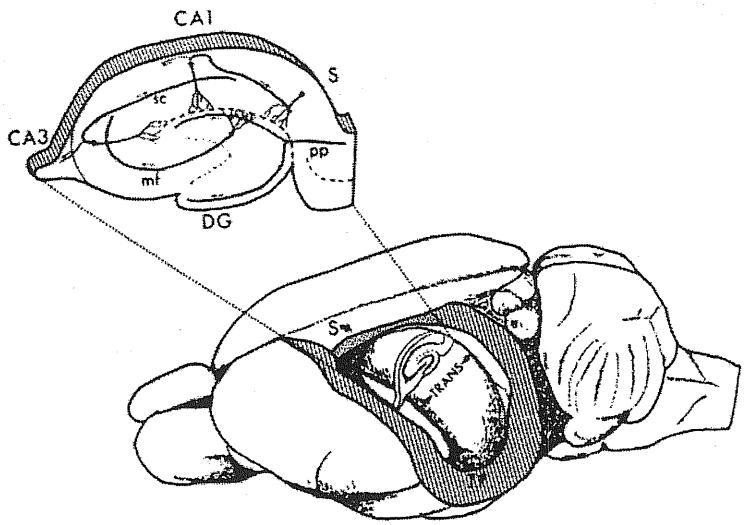

Figure 1.1 *Position of hippocampal formation in rat brain in which the cortical surface has been removed*
The hippocampus is an elongated structure with the septotemporal axis from the septal nuclei (s) to the temporal cortex (T). The *in vitro* experiments have been performed on transversal slices showed in the picture at the top. In this picture are shown the major neuronal elements and the 'three synaptic circuit' (see text). Dentate gyrus (DG), perforant path (PP), mossy fiber (mf), Shaffer collateral (sc). (Amaral and Witter, 1989)

terminal part of the CA3. As mentioned before the hippocampus presents a layered organization through its longitudinal axis. Thus, when the hippocampus is cut across its transverse axis (the septotemporal one), it is possible to indentify an intrinsic circuit that is preserved in all slices taken with this orientation (Skrede and Westgard, 1971). Fig. 1.1 shows a transverse slice of the hippocampal formation. The classical view of the 'three-synaptic circuit' is schematized in Fig. 1.1 (picture at the top). The dentate gyrus receives the main input from the perforant pathway, which originates in the entorhinal cortex (layer II). Then the granular cells of DG project to CA3 pyramidal neurons through their axons, the mossy fibers. CA3 cells make synaptic contacts with the dendrites of pyramidal cells located in the CA1 region through their axons, the Schaffer collaterals. In this classical picture, many connections are not considered (Amaral, 1993): EC sends direct projections also to neurons located in the CA1 and CA3 regions and in the subiculum; the subiculum receives a projection from the CA1 area; cells in the CA1 and subiculum project in turn to neurons localized in layer V/VI of the EC. We should consider in this circuit also the recurrent collaterals of principal cells (mostly in the CA3 region) and the interneurons. A simplified diagram of the circuitry of the hippocampal formation and its connections is shown in Fig. 1.2.

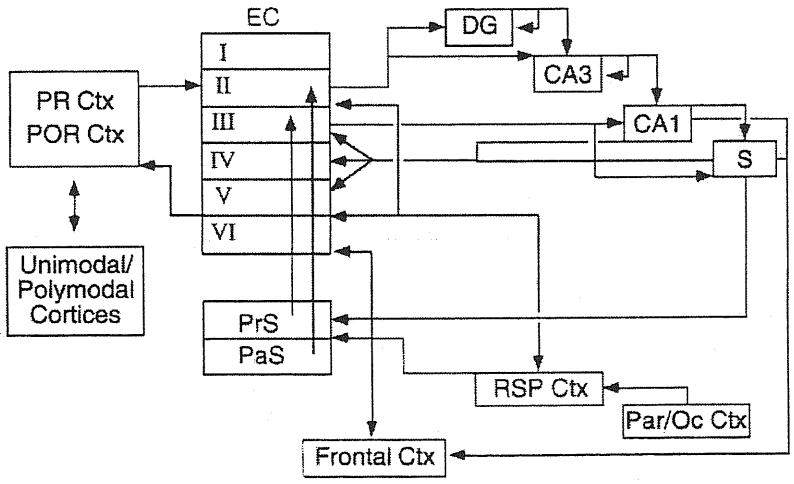

Figure 1.2 Diagram of the circuitry of the hippocampal formation and its fundamental connections. Abbreviations: DG dentate, gyrus; EC, entorinal cortex; S, subiculum; Par/Oc Ctx, parietal occipital cortex; RSP Ctx, retroeplenian cortex; PrS, presubiculum; PaS, parasubiculum; PR Ctx, perrinal cortex; POR Ctx, postrhinal cortex.

1.1.2.2 Input and output of the hippocampal formation

The hippocampus receives many input from several brain regions: the principal ones are from the EC, the septal region and the controlateral hippocampus. The input from the EC is the major sensory input, since the EC receives projections from olfactory, associative cortices, several thalamic nuclei, claustrum and the amygdala. The septohippocampal pathway (reviewed by Dutar et al., 1995) originates in the basal forebrain (BF) from the medial septal nucleus and the nucleus of the diagonal band of Broca and enter in the hippocampus mainly through the fimbria, the dorsal fornix and the supracallosal striae. Septal neurons project mainly to the ipsilateral hippocampus. The target areas are both the dentate gyrus and the hippocampus proper. The septohippocampal pathway provides most of the cholinergic innervation to the hippocampal formation: about 80% of septohippocampal pathway's fibers are cholinergic, while the remaining ones are GABAergic. This pathway should be considered bidirectional, therefore, it is also an output from the hippocampus. It plays a critical role in learning and memory processes, in the generation and maintenance of the theta rhythm (see pag. 24), and in neurodegenerative diseases such as Alzheimer's and Parkinson's diseases (Dutar et al., 1995). Other important neuromodulatory inputs are serotonergic fibers originating from the medial raphe nucleus (Azmitia and Segal, 1979) and noradrenergic projections from the locus coeruleus (Lindvall and Bjorkland, 1974).

The hippocampus projects back to the same regions from which its input originate, such as EC (layer V/VI), the septal complex via the fimbria-fornix (precommisural fibers), the controlateral hippocampus, again through the fimbria fornix. Moreover, the anterior thalamus and hypothalamus receive a projection from postcommisural fibers of the fornix, arising mainly from the subiculum.

1.1.3 Neuronal cells

Hippocampal neurons can be divided into two main groups: principal cells and interneurones. These two types of cells differ for their morphological and electrophysiological properties.

1.1.3.1 Morphological properties

Principal cells

In the dentate area, principal cells are the granule cells and the mossy cells. Granule cells are distributed along the DG and have only apical dendrites that arborize in the *stratum moleculare*. Their axons (mossy fibers) project to the hilus, where they give rise to several local collaterals, and to the *stratum lucidum* of the CA3 region. Mossy cells have densely spiny dendrites that are typically confined to the hilar region, and their postsynaptic targets are usually the dendrites of granule cells.

Principal neurons in the hippocampus proper are pyramidal cells, which have cell bodies arranged in a layer that forms the *stratum pyramidale* of CA1 and CA3 regions. They bear basal dendrites that arborize and form the stratum oriens and apical dendrites that are radially orientated in *stratum radiatum* and *lacunosum-moleculare*. Both basal and apical dendrites are covered with spines, where synaptic contacts occur. A characteristic of CA3 pyramidal neurons is the presence on their proximal dendrites of *thorny excrescences* where large boutons of mossy fibers make synapses *en passant*. Quantitative estimations indicate that each CA3 pyramidal neuron on average receives roughly 80 synaptic inputs from the mossy-fibers, 7700 from other CA3 pyramidal neurons and 4500 from the perforant path (Traub and Miles, 1991; Bernard and Wheal, 1994). Pyramidal cells project also to interneurons (a pyramidal cell innervates about 200 interneurons, Sik et al., 1993). In most of the cases they make only a single synaptic contact.

Principal cells in the DG, in the hilus and in hippocampus proper are excitatory and release glutamate as neurotransmitter.

Interneurons

Most non-pyramidal neurons are local interneurons. Some of them however, have an extrahippocampal or commissural projection. In contrast with the rather uniform population of principal cells, interneurons show a great variability in morphology and axonal arborization and they are distributed in the entire hippocampus. Interneurons are essential for synchronization of a large population of principal cells and therefore they play a crucial role in network oscillations,

plasticity and epileptic phenomena. They innervate both the soma and/or dendrites of pyramidal cells (Miles et al., 1996) or interneurons and are heavily interconnected (for an extensive review see Freund and Buzsaki, 1996). They mediate both feedback and feed-forward inhibition. In the feedback inhibition they receive excitatory inputs from collaterals of principal cells of the same hippocampal region, while in the feed-forward their activation is caused by extrahippocampal or intrahippocampal inputs. On the basis of their function four classes of interneurones can be distinguished: axo-axonic cells (or chandelier), basket cells, dendritic inhibitory cells, interneuron-selective cells (IS). Axo-axonic cells, whose soma is located within or immediately adjacent to stratum pyramidale and whose dendrites span all hippocampal layers, make synaptic contacts on the initial axonal segment of principal cells. Basket cells innervate the perisomatic region (cell body and proximal dendrites) of principal cells and are activated either in a feedback or in a feed-forward manner. They can also innervate interneurons. They are highly divergent making synaptic contacts with 1000-2000 pyramidal cells with 2-10 boutons in the same region and receive typically monosynaptic input from about 100-200 excitatory cells.

Dendritic inhibitory cells are extremely variable in their localization and pattern of axonal and dendritic arborizations. As the other types of interneurons they make synaptic contacts with 1000-2000 pyramidal neurons with 2-10 synapses but on different dendritic branches.

The last class of interneurons innervates exclusively other interneurons, both on the soma and on the dendrites. They receive excitatory input from the Schaffer collaterals and perhaps from the entorhinal cortex. A possible role for this class could be the control of population oscillations and/or disinhibition in hippocampal networks by inhibiting interneurons that innervate pyramidal cells.

Interneurons mediate the inhibition of principal cells and interneurons: they release γ-aminobutyric acid (GABA) as neurotransmitter. The common feature of highly convergent and divergent signals is responsible for the capability of interneurons to synchronize a large population of pyramidal cells.

1.1.3.2 Electrophysiological properties

Pyramidal cells and interneurons differ not only in their morphological aspect but also in their electrophysiological properties that reflect different distribution and/or type of receptor subunits and/or ion channels. Although different interneurons may have distinct electrophysiological characteristics, usually they differ from pyramidal cells in their higher membrane input resistance, faster membrane time constant, higher spontaneous firing rate, shorter-duration and smaller-amplitude action potential, larger amplitude of fast- and medium-afterhyperpolarization and weaker spike frequency accommodation in response to depolarizing current injection (Lacaille and Williams, 1990, Morin et al., 1996). Despite the variability in intrinsic membrane properties, pyramidal cells and interneurons have similar evoked inhibitory and excitatory postsynaptic currents (IPSCs and EPSCs respectively; Morin et al., 1996).

Different classes of interneurons mediate different responses in pyramidal cells. Dual recordings from interneurons and pyramidal cells indicate that basket and axo-axonic interneurons are the source of the prominent IPSPs of pyramidal neurons, whereas dendritic interneurons evoke slower IPSPs (measured in the soma). Also the function between perisomatic and dentritic interneurons is different: the first class limits the repetitive discharge of sodium-dependent spikes while the second one could suppress the generation of calcium-dependent action potentials (Miles et al., 1996).

Interneurons can synchronize a large population of pyramidal cells and a mechanism proposed to explain this synchronization is the interaction between synaptic events and intrinsic conductances. An action potential evoked in basket or axo-axonic cells induces an IPSP in the postsynaptic pyramidal neurons followed, if the post-synaptic element is sufficiently depolarized (<60 mV), by a rebound that is able to trigger action potential. The same mechanism could be responsible for the phase relationship between subthreshold oscillation in pyramidal cells and activity in these interneurons. Similar effects can be obtained by hyperpolarizing with brief current pulses the pyramidal cell, suggesting that the intrinsic membrane conductances are responsible for the events (Cobb et al., 1995). The postinhibitory rebound could be either to the

inactivation of an inward current or the deactivation of a persistent outward current.

1.2 Principal neurotransmitters within the hippocampus

Neurotransmitters act on two different types of receptors: ionotropic and metabotropic. Ionotropic receptors consist in proteins that gate ion channels and mediate fast synaptic transmission.

Metabotropic receptors are linked through G-protein to ionic channels, directly or by second messenger systems, and mediate slow synaptic transmission. They allow both divergence and convergence of signals. Activation of the same receptor can be linked to different metabolic pathways and/or channels. On the other hand, the same cellular process can be regulated by different neurotransmitters. The effects of the same neurotransmitter could vary between different cells but also in different regions of the same cell, according to the expression of different receptor subtypes.

GABA and glutamate are the principal neurotransmitters within the hippocampus. In the following paragraphs a brief description of these neurotransmitters and their receptors is given. Then the effects of acetylcholine mediated by muscarinic receptors, different subtypes of these receptors and the development of the cholinergic system in the hippocampus are described.

1.2.1 GABA

1.2.1.1 GABA in adult rats

GABA is the main inhibitory neurotransmitter in the adult hippocampus. It is released by GABAergic interneurons on both soma and dendrites of principal cells and on interneurons. Beside GABAergic terminals originating from local interneurons, the hippocampus receives GABAergic afferents from the entorhinal cortex *via* the perforant path and from the medial septal nuclei through the septohippocampal pathway whose GABAergic component innervates only interneurons (Freund and Antal, 1988).

GABA stabilizes the resting potential and so inhibits firing and of the cell by acting on two main classes of receptors: $GABA_A$ and $GABA_B$, coupled to an anionic and a cationic conductance, respectively.

$GABA_A$ receptors mediate fast synaptic responses and constitute an integral ion channel permeable to chloride (Cl^-). Other anions can flow through the channel, such as bicarbonate (HCO_3^-), Br^-, I^-, acetate (Borman et al., 1987). The channel is almost impermeable to F^-, the permeability ratio between F^- and Cl^- is 1:50. The action of GABA through these receptors is competitively antagonized by bicuculline and blocked by picrotoxin in a non-competitive way (Sivilotti and Nistri, 1991). Picrotoxin acts as a channel blocker and in some preparation it has been used to block $GABA_A$ receptors from inside the cell (Akaike et al. 1995). When the receptor is activated an inward or outward chloride current can be generated, depending on the electrochemical driving force. In pyramidal cells it has been shown that application of GABA in the dendritic layer induces a membrane depolarization, while in the soma a membrane hyperpolarization (Alger and Nicoll, 1979; Andersen et al., 1980). A difference in chloride equilibrium potential between soma and dendrites could account for these findings (Misgeld et al.,1986). The hyperpolarizing or depolarizing nature of GABA may depend on the amount of transmitter released. At higher doses of GABA (such as those achieved with high frequency stimulation) the electrochemical gradient for Cl^- is diminished and the efflux of bicarbonate anions could be responsible for the depolarizing response (Grover et al., 1993; Staley et al., 1995). Changes in the equilibrium potential for bicarbonate affect the depolarizing effect more than the hyperpolarizing one, while the latter effect is more sensitive to changes in Cl^- gradient (Perkins and Wong, 1996). In physiological conditions, the polarity of GABA responses could be due to the concentration of CO_2 and therefore could be dependent on the energy consumption of the locally active neurons. Recently the depolarizing action of GABA has been attributed to bicarbonate-dependent K^+ transient (Kaila et al., 1997).

$GABA_B$ receptors mediate the slow synaptic responses (Dutar and Nicoll, 1988a). They are selectively activated by baclofen and blocked by phaclofen, 2-hydroxy-saclofen, CGP 35348 or

CGP 55945A (Bowery, 1993). These receptors are linked to a pertussis toxin (PTX) sensitive G-protein and they induce an increase in K^+ conductance and/or decrease in voltage-dependent Ca^{2+} conductances (Bormann, 1988). $GABA_B$ autoreceptors are thought to downregulate GABA release (Thomson and Gahwiler, 1989; Misgeld et al., 1995; Jarolimek and Misgeld, 1997).

1.2.1.2 GABA in neonatal rats

The GABAergic system is completely developed at birth. A peculiar characteristic of GABA in neonatal rats is that its action through $GABA_A$ receptors is depolarizing. During the first postnatal week, GABA provides most of the excitatory drive to principal cells (Ben-Ari et al., 1989; Cherubini et al., 1991). Through its depolarizing action, GABA exerts a trophic function. In fact it ensures elevation of intracellular calcium $[Ca^{2+}]_i$ following calcium entry through the activation of voltage-dependent calcium channels (Leinekugel et al., 1995). These calcium signals are essential for consolidation of synaptic connections and development of the adult neuronal circuit (Shatz, 1990). The depolarizing effect of GABA could be attributed to a reversed chloride gradient (the reversal potential for Cl^- is about -50 mV in neonatal versus -70 mV in adults) following changes in the chloride homeostasis. This can be due to the deficiency of an outwardly directed Cl^- pump (Misgeld et al., 1986). Other reasons could be differences in permeability of GABA-gated Cl^- channel to other anions (HCO_3^-), or lack of an inward rectifying Cl^- channel (CIC-2) that in adult neurons contribute to maintain a low chloride concentration inside the cell (Stanley, 1994). The ClC-2 channel, which belongs to a large gene family including in mammals at least nine different members (Jentsch, 1996), is highly expressed in neuronal and non-neuronal tissues. Recently, in our laboratory a novel form of ClC-2 channel (ClC-2nh) has been cloned from a neonatal cDNA library (Mladinic, 1997). This channel, which as a result of alternating splicing, is truncated in the amino terminal region, is highly expressed in neonatal but not in the adult hippocampus. When expressed in *Xenopus* oocytes it induces currents that strongly rectify in the outward direction. Hence, channel opening by depolarization (as during burst of action potentials) leads to chloride accumulation inside the cell above the

equilibrium. Therefore, activation of $GABA_A$ receptors would produce an outwardly directed flux of chloride.

In neonatal hippocampal neurons another response to GABA probably mediated by a different receptor type has been recently characterized. Like $GABA_A$-mediated responses this novel response to GABA is chloride dependent but bicuculline and baclofen insensitive (Strata and Cherubini, 1994). It is blocked by picrotoxin and shows only a moderate desensitization and a very fast recovery from desensitization (Martina et al., 1995). For its similarity with GABA response obtained in the visual pathway and in the retina it is supposed to be mediated by $GABA_C$-like receptors (Cherubini and Strata, 1997).

1.2.2 Glutamate

Glutamate is the main excitatory neurotransmitter in the CNS. In the hippocampus it is released by pyramidal cells and by afferent fibers from EC and DG. It acts on ionotropic and metabotropic receptors localized in pyramidal cells and interneurons.

1.2.2.1 Ionotropic receptors

Ionotropic receptors can be divided according to their different electrophysiological and pharmacological properties in two main categories: N-methyl-D-aspartate (NMDA) and non-NMDA receptors. They mediate fast and slow component of EPSPs, respectively.

NMDA receptors are activated by NMDA and blocked by the channel blocker MK 801, by selective competitive receptors antagonists (+)-3-(2-carboxy-piperazin-4-yl)-propyl-1-phosphonic acid (CPP), D(-)2-amino-5-phosphovaleric acid (D-AP5) and by the broad spectrum ionotropic antagonist kynurenic acid. Five NMDA receptor (NMDAR) subunits have been cloned: the NMDAR1 and four types of NMDAR2 (2A, 2B, 2C, 2D). A functional receptor is composed by the NMDAR1 and one or more subunits of NMDAR2 type (Edmonds et al., 1995). They open predominantly large single conductance channels (40-50 pS) that show high permeability to calcium. They require glycine as a co-agonist (Johnson and Ascher, 1987). A

peculiar characteristic is their voltage-dependent block by extracellular magnesium (Mg^{2+}). The block can be removed upon cell depolarization. This characteristic confers a negative slope conductance in the current-voltage relationship between -40 and -80 mV and suggests a role of detector of coincident events: the depolarization of a postsynaptic cell and the release of glutamate. This is important in synaptic plasticity phenomena according to Hebb 's hypothesis. In fact Hebb (Hebb, 1949) proposed that

"When an axon of cell A is near enough to excite a cell B and repeatedly or persistently takes part in firing it, some growth process or metabolic change take place in one or both cells such as that A's efficiency, as one of the cells firing B, is increased"

As a consequence the efficacy of the synapses increases or decreases according to the synchronism of the activity of the two neurons. An example of phenomenon that follow this rule is the long term potentiation (LTP), that consists in a long-lasting increase in the amplitude of a synaptic response following brief, high frequency activity of a synapse. Since their function of coincidence detectors allows calcium entry, NMDA receptors play a crucial role in LTP in the CA1 area and a form of LTP in CA3 (when the stimulus involves the collateral fibers but not mossy fibers). Blocking these receptors prevents LTP.

Non-NMDA receptors have been classified as (*RS*)-α-amino-3-hydroxy-5-methyl-4-isoxadepropionate (AMPA) and kainate receptors on the basis of their pharmacological properties. Now they are classified according to the homology of cloned subunits. They are assembled from a family of subunits consisting of several different members: GluR1-4 comprise the AMPA receptor subunits, GluR5-7 with KA-1 and KA-2 the kainate receptors subunits (Edmonds et al., 1995). They open relative low conductance channels (<20 pS for AMPA and 4 pS for kainate). These channels are less permeable to calcium even if in interneurons Ca^{2+} permeability of AMPA receptors is higher that in pyramidal neurons (Jonas et al., 1994). This could be due to the lack of the GluR2 subunit that is not expressed in most AMPA receptors localised on interneurons (Leranth et al., 1996). The lack of this subunit would confer calcium permeability to AMPA receptors (Hollman et al., 1991; Burnashev et al., 1992). AMPA and

kainate receptors may coexist in the same neuron (Lerma et al., 1993). The lack of specific receptor agonists has precluded the differentiation between kainate- and AMPA- mediated responses. In fact kainic (or domoic) acid and AMPA activate both kind of receptors. Moreover antagonists such as 6-cyano-7-nitroquinoxaline-2,3-dione (CNQX), 6,7-dinitroquinoxaline-2,3(1H,4H)-dione (DNQX), 6-nitro-7-sulphamoylbenzo(f)-quinoxaline-2,3-dione (NBQX), kynurenic acid do not discriminate between these two receptor types and many responses thought to be mediated by kainate are in fact AMPA dependent. Recently a new compound has been synthesized (GYKI 53665, from Lilly Indianapolis) that selectively blocks AMPA receptors, thus allowing the isolation of kainate receptor-mediated responses (Paternain et al., 1995). Recent reports have shown that repetitive stimulation of the mossy fibers activate kainate receptors in the CA3 region (Castillo et al., 1997; Vignes and Collingridge, 1997). These receptors, probably extra synaptic, would be activated by spill-over of glutamate following a brief tetanus (Lerma, 1997). Using the less specific compound GYKI 52466, a presynaptic inhibitory action exerted by kainate receptors has been suggested: activation of kainate receptors inhibits glutamate release from synaptosomes and decrease NMDA evoked EPSP (Chittajallu et al., 1996) inhibiting Ca^{2+} influx into presynaptic terminals (Kamiya and Ozawa, 1998). Also a down-regulation of GABAergic inhibition in hippocampal CA1 pyramidal neurons induced by kainate or a selective agonist for GluR5 ((RS)-2-amino-3-(3-hydroxy-5-tert-butylisoxazol-4-yl)propanoic acid, ATPA) has been reported (Rodriguez-Moreno et al., 1997, Clarke et al., 1997). This may account for the increased cell excitability and epileptogenic properties of kainic acid.

1.2.2.2 Metabotropic receptors

There are different subtypes of metabotropic glutamate receptors (mGluR, at present 8) that differ in their pharmacological properties, signal transduction pathway and location. They can be divided into three groups according to their transduction mechanisms and pharmacology. Members of group I activate phospholipase C (PLC), while those of groups II and III inhibits

adenylyl cyclase, even if the exact transduction mechanisms can be more complex (Pin and Bockaert, 1995). The most used agonist and antagonist are the *trans*-1-aminocyclopentane-1,3-dicarboxylic acid (*t*-ACPD) and (RS)-α-methyl-4-carboxyphenylglycine (MCPG) respectively, even if the potency of the drugs varies between different groups (Pin and Bockaert, 1995). The high variability in the subtypes and second messenger systems involved is reflected by the broad spectrum of electrophysiological responses (for a review see Schoepp and Conn, 1993; Pin and Bockaert, 1995). These receptors are located pre- and postsynaptically. At the post-synaptic level they modulate ionotropic AMPA and NMDA receptors activity and many membrane currents such as I_{AHP}, I_M and I_{Ca}. At pre-synaptic level these receptors may potentiate the release process by activating the protein kinase C (PKC) or potentiating the activity of Ca^{2+} channels: they may also inhibit release by blocking N-type voltage sensitive calcium channels (VSCCs). Of particular interest are mGluR 2/3 that are localized on the mossy fibers where they inhibit transmitter release. They can be selectively activated by 2-(2,3-dicarboxycyclopropyl) glycine (DCG-IV).

1.2.2.3 Glutamate in the neonatal hippocampus

The glutamatergic system, in contrast to GABAergic one, is not completely developed at birth. In the immediate postnatal period, granule cells in the DG are still postmitotic and their axons, the mossy fibers, even if they start to make synaptic contacts with CA3 pyramidal neurons already at P1, reach a complete development towards the end of the second postnatal week (Amaral and Dent, 1981). The thorny excrescences can not be observed before P9. Moreover, in the CA3 region, spontaneous glutamatergic synaptic potentials are difficult to detect before the end of the first postnatal week (Hosokawa et al. 1994). It has been suggested that at birth, in the CA1 region, only NMDA receptors are functional while AMPA-mediated responses are silent (Isaac et al., 1995; Liao et al., 1995). The percentage of silent synapses decreases from postnatal day (P) 2 to P5 (Durand et al., 1996). Silent synapses can be converted into functional ones by various pattern of electrical stimulation of afferent fibers (Isaac et al., 1995; Durand et al., 1996).

This process requires activation of NMDA receptors, intracellular calcium and, according to Hebb's rule, coincident activity of pre- and post-synaptic site since it is input specific. A study of the development of the excitatory circuit revealed that the association between CA3 and CA1 cells strengthens over development by increasing the number of functional synaptic contacts between CA3-CA1 cell pairs, rather than by changing the reliability or efficacy of individual synapses (Hsia et al., 1998).

1.2.3 Acetylcholine

As mentioned before the hippocampus receives a large cholinergic innervation from the septo-hippocampal pathway that originates from the medial septal nucleus and the diagonal band of Broca in the basal forebrain. Cholinergic fibers innervate in a laminar fashion both the soma and the dendrites of pyramidal cells and interneurones. In contrast to GABAergic fibers, cholinergic fibers do not have a preferred postsynaptic target, since they innervate pyramidal cells and interneurons in the same proportion as occur in the neuropil (Frotscher and Leranth, 1983; Freund and Buzsaki, 1996). Acetylcholine (ACh) released from cholinergic terminals acts on both muscarinic and nicotinic receptor types.

Here only muscarinic receptors and their responses will be considered. Muscarinic receptors are metabotropic receptors distributed both post-and pre-synaptically where they exert different type of effects (Krnjevic, 1993).

1.2.3.1 Postsynaptic effects in pyramidal neurons

In the hippocampus, acetylcholine decreases several membrane K^+ conductances. This effect can be mimicked by muscarine and blocked by atropine. This modulation can strongly affect the excitability of a cell, since K^+ currents contribute to the resting membrane potential, spike repolarization, spike frequency adaptation and after-hyperpolarization (Storm, 1990). The decrease in K^+ conductance may involve block of I_M (Halliwell and Adams, 1982), I_{AHP} (Bernardo and Prince, 1982; Cole and Nicoll, 1984; Figenschou et al., 1996), I_{Kleak} (Madison et

al., 1987; Benson et al. 1988). Also a block of I_A has been reported in cultured hippocampal neurons (Nakajima et al., 1986). The blocking effect of ACh on I_{AHP} can be due to a direct effect of this neurotransmitter on calcium-dependent potassium channels or to a reduction in calcium entry through voltage-dependent calcium channels. However, since carbachol affects neither spike repolarization nor the fast AHP, its effect may occur at some step after calcium entry (Lancaster and Nicoll, 1986). Other effects associated to muscarinic activation are: activation of a Ca^{2+}-dependent inward current (Caeser et al., 1993; Gahwiler and Brown, 1987), modulation of the delayed rectifier K^+ current I_K (Zhang et al., 1992), I_Q (Colino and Halliwell, 1993) and sodium current (Cantrell et al., 1996). An increase in K^+ conductance by muscarinic agonists, although present in central neurones (McCormick and Prince, 1986; Egan and North, 1986; McCormick and Pape, 1988), has not been described in the hippocampus.

Moreover, ACh modulates NMDA responses. It has been shown that, after an initial suppression, ionophoretic application of acetylcholine produces a long-lasting facilitation of the slow NMDA-mediated component of the EPSP. The effect of ACh is postsynaptic since this neurotransmitter enhances the responses evoked by puff application of NMDA in the presence of tetrodotoxin, without affecting the responses induced by application of kainate or quisqualate (Markram and Segal, 1990).

1.2.3.2 *Effects presynaptic to pyramidal neurons*

Effects of acetylcholine at presynaptic level have been also demonstrated. Local application of ACh on the apical dendrites of principal cells reduces the amplitude of the field EPSP and somatic population spike. It also reduces the amplitude of intracellularly recorded EPSPs and IPSPs without affecting the kinetics of the responses and membrane conductance (Hounsgard, 1978). When applied to the pyramidal layer, ACh exerts a disinhibitory role: facilitate population spike (Krnjevic et al., 1981; Ben-Ari et al., 1981) and reduces the amplitude of IPSPs (Valentino and Dingledine, 1981). Similar results can be produced by electrical stimulation of the medial septum (Krnjevic et al., 1988; Rovira et al., 1983). In this case however, a direct inhibitory effect

on GABAergic interneurons, the target of the GABAergic septohippocampal projection, can not be ruled out (Toth et al., 1997). Experiments on synaptosomes demonstrate that ACh acting through muscarinic receptors inhibits release of ACh (autoreceptors) and other neurotransmitters (heteroreceptors) (Raiteri et al., 1984; Marchi and Raiteri, 1989). Recently it has been demonstrated that carbachol increases the frequency of spontaneous and miniature (m) EPSPs, recorded in the presence of tetrodotoxin (TTX, Bouron and Reuter, 1997). The mechanism underlying the presynaptic effect of ACh on muscarinic receptors is not clearly understood. A reduction in calcium conductance, an increase in K^+ conductance and/or a modulation of intracellular calcium can account for a decrease in transmitter release. The contribution of nicotinic receptors in controlling transmitter release cannot be neglected. In particular in the CA1 region, it has been shown that nicotinic agents enhance the population spike when applied in the somatic region and enhance the field EPSP when applied in the dendritic region (Rovira et al. 1983). The enhancement of population spike has been interpreted has a disinhibitory effect. However more recently a direct excitatory effect of nicotine on interneurons has been reported (Jones and Yakel, 1997).

1.2.3.3 Effects on interneurons

All the muscarinic effects described have been studied in pyramidal neurons in hippocampal slices. The action of ACh on interneurons has not been deeply investigated. Direct evidence for an excitatory action of ACh on identified interneurons has been found by Recce and Schwartzkroin, 1991. Thus, the application of carbachol induces a rapid membrane depolarization, an effect that is antagonized by muscarinic antagonists and persists when synaptic transmission is blocked. Some indirect evidence for this action has been obtained measuring inhibitory post-synaptic potentials in pyramidal neurons (Pitler and Alger, 1992; Behrends and ten Bruggencate, 1993). Carbachol exerts mainly three actions: depression of the evoked IPSP or EPSC, enhancement in frequency and amplitude of spontaneous action potential dependent $GABA_A$-mediated IPSPs and reduction in frequency of mIPSCs. These contradictory

effects (enhance of spontaneous events and decrease in miniature and evoked ones) could be explained by different actions of carbachol. Receptors localized on terminals where neurotransmitters (GABA or glutammate) are released would decreased the release, while other subtypes localized on dendrite and soma would increase the excitability of cells and so the action potential dependent activity.

1.2.3.4 Muscarinic receptor subtypes: pharmacology, distribution and intracellular pathways

There are five distinct subtypes of muscarinic receptors named M1-M5 and codified by the five genes m1-m5. They show different pharmacology and distribution within the hippocampus. Furthermore they present different electrophysiological characteristics and are linked to different second messenger systems.

Pharmacology of muscarinic receptors

The muscarinic receptor subtypes show different affinity to acetylcholine. M1, the most abundant within the hippocampus have a lower affinity than the other muscarinic receptor subtypes (McKinney, 1993). Many compounds have been used to study and identify different subtypes of muscarinic receptors. As a general antagonist atropine is used, while the most used muscarinic agonist is carbachol that activates all subtype of receptors, although it is not selective since it can activate also nicotinic receptors. Selective agonists for the different subtypes of muscarinic receptors are not available, and even if some drugs bind preferentially certain

Tab. 1.1: Antagonist affinity constant for mammalian muscarinic receptors.

	M1	M2	M3	M4	M5
Atropine	9.0-9.7	9.0-9.3	8.9-9.8	9.1-9.6	8.9-9.7
Pirenzepine	7.8-8.5	6.3-6.7	6.7-7.1	7.1-8.1	6.2-7.1
Methoctramine	7.1-8.5	7.8-8.3	6.3-6.9	7.4-8.1	6.9-7.2
4-DAMP	8.6-9.2	7.8-8.4	8.9-9.3	8.4-9.4	8.9-9.0

Log affinity constant (pK_B values) for the most common antagonist for the 5 muscarinic receptor subtypes. Data are from a variety of mammalian species and include information from binding and functional studies (From Caufield and Birdsall, 1998).

subtypes their affinity constants are very close to one another. The selectivity for the antagonists is higher, but far from giving good pharmacological tools that allow to distinguish without ambiguity between different receptor subtypes. For example pirenzepine, the most used antagonist, allows one to distinguish M1 from M2, but the affinity constants for M4 and M1 are not sufficiently distant to separate responses mediated by these two receptor subtypes. Since cells usually coexpress more than one receptor subtype, to study the affinity of various compounds for different receptor subtypes, cloned M1-5 receptors can be expressed in cell lines. In these cases only one receptor subtype is expressed and so the binding properties can be determined without ambiguity. Although the situation in neuronal cells may be different, affinity constant obtained with these experiments have been remarkably comparable with apparent affinity constants determined in functional experiments using Arunlakshana-Schild analysis (Caufield and Birdsall, 1998). Table 1.1 summarizes the Log affinity constant for the most used antagonists.

Distribution of muscarinic receptors within the hippocampus

To study the localization of different receptor subtypes many different methods can be used. *In situ hybridization* allows one to identify and to localize the mRNA encoding for different genes, but does not permit a quantitative study. Receptor autoradiography identifies binding sites of different agonists/antagonists and thus distinguishes different receptors on the basis of their pharmacological properties. This method however, has the limitation that the selectivity of different compounds for distinct muscarinic receptor sub-types is quite poor. A third method consists in using specific antibodies against different receptor subtypes to detect the immunoreactivity or to do immunoprecipitation analysis to quantify the data.

Recently, Levey et al. (1995), using specific antibodies against different muscarinic receptors, mapped their location within the rat hippocampus. M1 subtypes were found in the soma of pyramidal cells in all regions (more abundant in the CA1 region) and in the apical and basal dendrites of stratum radiatum and stratum oriens, respectively. M2 were present especially in non-pyramidal neurons with higher levels in the CA3 region. M3 were observed in pyramidal

neurons of the CA3 subfield. M4 were distributed on commissural pathway fibers. Due to low levels of M5 protein, these receptors were not considered. The same approach was used to identify muscarinic receptor subtypes expressed on afferent fibers (Rouse and Levey, 1996). These authors found that M2, M3 and, to a lesser extent, M1 receptors are expressed in septohippocampal pathway fibers; M1, M3 and M4 in commissural/associative pathway; M1 and M3 subtypes were expressed in the perforant path (also few M2 and M4); finally M1 subtype was found to be expressed in raphe-hippocampal terminals. The M2 receptor subtype is a typical presynaptic autoreceptor localized on presynaptic terminals: its activation down regulates the release of acetylcholine and other neurotransmitters (Raiteri et al., 1984; Marchi and Raiteri, 1989). Mc Kinney et al., (1993) have proposed that in the hippocampus presynaptic receptors are a mixture of M2 and M4, with a dominance of M4.

The discrepancy between different studies could be explained by the low selectivity of muscarinic agonists and antagonists for different receptors.

Intracellular pathways and electrophysiological responses

The multiple pre and postsynaptic effects of achetylcholine described can be attributed to distinct muscarinic receptor subtypes (McKinney, 1993). Most of the work in slices has been done when only two receptor subtypes were known and various effects were classified as pirenzepine sensitive or insensitive, mediated by M1 and M2 receptor subtypes, respectively. Carbachol-induced membrane depolarization and block of AHP were associated to M1 receptors, while block of the M current and reduction of EPSPs amplitude to M2 (Dutar and Nicoll, 1988b). Subsequently, the block of K^+_{LEAK} conductance was associated to M3 receptors (Pitler and Alger, 1990). It can be concluded that M1, M3, and M5 mediate mainly postsynaptic responses, while M2 and M4 mediate the presynaptic ones, although this classification can not be consider absolute. For example, carbachol-induced LTP has been considered a postsynaptic effect mediated by M2 receptors (Auerbach and Segal, 1996). On the other hand, carbachol-induced decrease in amplitude of the field EPSPs, a typical presynaptic effect, has been associated to M1

(Sheridan and Sutor, 1990). Even in these cases the poor selectivity of agonists and antagonists could account for different interpretations.

All receptor subtypes are coupled with a G-protein but, as for the electrophysiological responses, the identification of the intracellular pathways associated with the activation of distinct receptor subtypes is not trivial. For this purpose different muscarinic receptors were expressed in NG108-15 neuroblastoma glioma hybrid cells (Brown et al., 1993). Although the situation in native neuronal receptors may be very different, cells that expressed M1 or M3 receptors responded to application of ACh (or ACh agonists) with an increased production of inositol phosphate and intracellular Ca^{2+} concentration (with consequent activation of a Ca-dependent K current (I_{KCa}), and inhibition of the voltage-gated K current I_M). These effects are resistant to Pertussis Toxin (PTX). Cells that expressed M2 or M4 responded with a reduced production of cyclic AMP (with consequent inhibition of a voltage-gated Ca-current, an effect totally prevented by PTX).

1.2.3.5 Cholinergic system in neonatal rat hippocampus

The septo-hippocampal pathway is not completely developed at birth. Biochemical and immunoistochemical methods have been used to study the ontogenetic development of acetylcholine esterase (AChE) and choline acetyl transferase (ChAT), the two enzymes responsible for degradation and synthesis of ACh, respectively (Matthews et al., 1974; Nadler et al., 1974; Milner et al., 1983). It has been found in mice that acetylcholine esterase (AChE) and ChAT positive fibers enter in the hippocampus at P2 (Hohmann and Ebner, 1985). These fibers start to reach their targets during the first postnatal weak (Rami et al., 1989). In this period the two cholinergic markers increase dramatically and only towards the end of the third postnatal week the system can be consider almost completely developed (Nyakas et al, 1994). Binding studies have revealed that muscarinic receptor are present at about one-third of the adult level (Rotter et al., 1979). There is a first increase in number of muscarinic receptors at P4 and then a sharp increase between P7 and P10 (Ben-Barak and Duday, 1979). The increase in binding sites

continues until the age of 4-6 weeks. At P16 all receptor subtypes are present in the same percentage as in adulthood (Tice et al., 1996).

In spite of changes in cholinergic innervation and receptors, during the first postnatal week electrophysiological responses to ACh or carbachol are similar to those found in the adult (Recce and Schwartzkroin, 1991).

1.2.3.6 Role of Nerve Growth Factor (NGF) in the maintenance and survival of cholinergic neurons

The nerve growth factor (NGF) is a member of the neurotrophin family, which acts on a tyrosine kinase (TrkA) and on the low affinity P75 receptors (Chao, 92). Neurotrophins exert a trophic action in the nervous system (Barde, 1989). In particular several studies have demonstrated a specific action of NGF on the maintenance and survival of basal forebrain (BF) cholinergic neurons. NGF and NGF mRNA are highly expressed in hippocampal neurons innervated by cholinergic fibres (Korshing et al, 1985; Shelton and Reichardt, 1986). The NGF receptors TrkA and P75 are expressed on BF cholinergic neurons; NGF injected into the hippocampus is taken up by cholinergic nerve terminals and retrogradely transported (Auberger et al, 1987). Transection of the septo-hippocampal pathway results in retrograde degeneration of neurons in the medial septum and in the diagonal band of Broca. This causes a decrease in both choline acetyltransferase (ChAT) and acetylcholine esterase (AChE) activities in the hippocampus (Gage et al., 1986). This lesion leads also to an impairment of various behavioral tasks. All these effects could be prevented by local application of NGF (Hefti, 1986), suggesting that neuronal death depends on the lack of retrograde transport of NGF and not on the absence of contact between afferent fibers and their targets (Hefti, 1986).

1.3 Oscillations and rhythmic activities

The ability to generate synchronized oscillatory activities appears to be a particular feature of mammalian central nervous system. Many kinds of oscillations can be detected from several neural structures by means of different recording techniques. Persistent fluctuating potentials were discovered in 1875 by Caton who described them as "feeble current of the brain" (Brazier, 1968). With the development of the electroencephalogram, applied for the first to humans by Berger in 1924, rhythmic waves were identified. These waves arise from the collective activity of a large number of neurons. This electrical activity changes according to different brain regions from which it is detected, age and behavioural state of the subject. The improvement of technology has allowed the recordings of activity from a more limited number of neurons (with intratissue extracellular electrodes) or from a single neuron (intracellular electrode). These techniques have been extensively used *in vivo* and *in vitro* to detect the activity of many brain areas. In particular the introduction of intracellular recordings has revealed that the single-neuron correlate of electroencephalographic waves are constituted by membrane potential oscillations comprising periodic pattern of action potentials (Steriade et al. 1994).

In general, oscillations can be generated by a network of neurons or by the intrinsic properties of single neurons. Network-driven activity is induced by means of functional contacts between the elements of the network, even if these elements are not intrinsically able to produce a similar behavior when synaptically isolated. Intrinsic oscillations are due to membrane properties of single cells, in particular to voltage-dependent conductances.

Oscillations constitute the basic form of communication between different cell assemblies at cortical or subcortical level. They can synchronize the activity of anatomically distributed

populations of neurons in different structures (Klimesch, 1996; Buzsaki and Chrobak, 1995). This cooperation has been hypothesized to play a fundamental role in information encoding. It has been suggested that oscillations do not contain information, but provide the temporal structure for correlated neurons that do encode specific information (Gray et al., 1989; Koning et al., 1996). It has been also proposed that oscillatory activity may provide a timing reference for a neronal code based on the phase relationship of individual neurons to the reference oscillation (O'Keefe and Recce 1993; Hopfield, 1995).

How information is encoded and transmitted within the central nervous system is one of the most challenging question in neuroscience. Pyramidal cells and interneurons in the cortex have been initially viewed as elements that integrate and fire. Then it has been demonstrated that the highly irregular firing of cortical cells can not be simply explained by the temporal integration of random EPSPs (Softky and Koch, 1993). The precise timing of action potentials depends on a particular combination of presynaptic inputs, suggesting that neurons act as coincidence detectors. In this case the information is carried by the precise timing of action potentials (Softky, 1995; Mainen and Sejnowski, 1995). An alternative theory emphasizes the role of firing rate in information processing. In this view the membrane potential is assumed to undergo a random walk between the resting membrane potential and spike threshold, hence the timing of action potential is irrelevant (Shadlen and Newsome, 1994; Zohary et al., 1994). Recently it has been suggested that the information is better transmitted by brief (<25 ms) bursts of action potentials (Lismann, 1997). Central synapses are very unreliable and therefore they do not propagate the information relative to a single action potential that, at least in some cortical structures, can be considered just noise. In contrast, when two or more stimuli occur within 10-20 ms, if a single synapse does not respond to the first stimulus, its probability of responding to

the second is almost 1, hence the information is propagated. When the synapse responds to the first stimulus its probability of responding also to the second is very low (Stevens and Wang, 1995).

Whatever are the mechanisms for encoding information, oscillations seem to play a fundamental role in this important function.

1.3.1 Oscillations in the hippocampus

Many types of oscillations occurring at different frequency are present in the hippocampus. These include the theta rhythm (4-10 Hz), gamma oscillations (20-80 Hz) and high frequency (150-200 Hz) oscillations.

1.3.1.1 Theta rhythm

The most studied oscillatory activity in the hippocampus is the theta rhythm. It can be observed in juvenile and adult animals both in pyramidal cells and interneurons at a frequency ranging from 4 to 12 Hz. Since the septum is crucial for the expression of the theta rhythm, this rhythmic activity can not be observed in hippocampal slices, and until now it can be clearly recorded only *in vivo*. Recently two novel kinds of preparation *in vitro* that contain both the hippocampus and the septum have been developed: slices including septum and hippocampus (Toth et al., 1997) and the intact hippocampal formation (Khalilov et al., 1997).

There are two kinds of theta rhythm classified by their pharmacological properties.

The type I theta (7-10 Hz) is associated with arousal and exploration in the intact animal. It is atropine-resistant and can not be detected during anesthesia. The type II can be observed under

anesthesia and sometimes during immobility; it is atropine-sensitive and the oscillation frequency is 4-6 Hz.

Since the description of the theta rhythm by Green and Arduini (1954), one of the most intriguing controversies is whether this activity is generated intrinsically to the hippocampal formation or whether it requires an extrinsic pacemaker, such as the medial septum. Many experimental observations suggest that the cholinergic system within the septum is responsible for the type II theta rhythm generation (reviewed by Bland, 1986). The septohippocampal pathway is mainly cholinergic and lesion of septal nuclei could abolish the hippocampal theta rhythm while septal electrical stimulation at the theta frequency could induce it. Furthermore application of atropine to the septum abolishes the theta rhythm while acetylcholine agonists or the anticholinesterase eserine elicited it. Then, the finding that in hippocampal slices acetylcholine or its agonists are able to induce rhythmic pyramidal cell oscillations at 4-8 Hz (Bland et al., 1988;MacVicar and Tse, 1989) lead to the hypothesis that pyramidal neurons can generate theta rhythm. As an alternative interpretation, based mostly on anatomical evidence that the cholinergic septohippocampal projection mainly terminates on interneurons, a role of interneurons in the theta rhythm generation has been suggested (Buzsaki, 1984).

In the last years the role of GABA in theta rhythm generation has been put forward. It has been found that the septohippocampal projection contains a GABAergic component that selectively innervates interneurons (Freund and Antal, 1988). Furthermore it was observed that, selective lesions of septal cholinergic cells reduce but do not abolish hippocampal theta activity (Lee et al., 1994). Recently it has been observed that stimulation at 5 Hz of the septohippocampal pathway, through disinhibition of GABAergic interneurons by GABA released from GABAergic

fibers (after blockade of AMPA/kainate, NMDA and muscarinic receptors) may reproduce a theta-like activity (Toth et al., 1997).

1.3.1.2 Gamma oscillations

Gamma rhythms range from 20 to 80 Hz and have been identified in several cortical areas. In the hippocampus they tend to occur during theta rhythm. Pyramidal cells and interneurons fire in phase (Bragin et al., 1995). Several models have been proposed for gamma oscillations. These include: network of excitatory-inhibitory neurons, recurrent inhibitory loops, mutual excitation, intrinsic oscillator in a network and network of inhibitory neurons (Jefferys et al., 1996). Recently it has been suggested that the inhibitory network excited by glutamate acting on metabotropic receptors (without fast EPSPs) may sustain gamma oscillations (Whittington et al., 1995).

1.3.1.3 High frequency oscillations

High frequency network oscillations (150-200 Hz) are present in hippocampal slices *in vitro* where they can be detected at the principal cell layers level as brief series of repetitive population spikes. It has been recently demonstrated that, in contrast to other types of synchronized activity (theta or gamma rhythms) which are mediated by chemical synaptic transmission, they are probably due to direct electrotonic coupling between neurons, most likely through gap-junctional connections (Draguhn et al., 1998).

1.3.2 Oscillations during development

Spontaneous forms of correlated activity constitute a particular feature of CNS development. During development, neuronal oscillations have been shown to regulate patterning of connections (Shatz, 1990), to direct neuronal differentiation (Spitzer, 1994) and to regulate the rate of cell migration (Komuro and Rakic, 1996). In the visual system, in absence of any stimulus, highly correlated activity occurs in ganglion cells and resembles waves that propagate across the retina. This activity occurs in clusters of retinal ganglion cells and requires synaptic activity (Meister et al., 1991; Wong et al., 1993) and cholinergic input (Feller et al., 1996). The mechanism responsible for this synchronous activation seems to be electrical coupling between retinal ganglion cells (Penn et al., 1994; Kandler and Katz, 1995). Another example of patterned spontaneous activity during development is present in the rat neocortex, where spontaneous increase in cytosolic calcium can be detected in subpopulation of cells, the so called electrical domains. Within each domain the cells are coupled with gap junctions, but in contrast to the activity detected in the retina, these oscillations are not blocked by TTX (Yuste et al., 1992).
Also in the hippocampus in early postnatal life a highly correlated activity can be detected in the form of giant depolarizing potentials (GDPs). These will constitute the main object of this thesis.

1.3.3 Giant depolarizing potentials (GDPs)

A peculiar characteristic of the hippocampus of neonatal rats is the presence of spontaneous events called Giant Depolarizing Potentials (GDPs, Ben Ari et al., 1989; Xie et al., 1994). GDPs can be recorded in hippocampal slices as well as in the intact hippocampal formation (Khalilov et al., 1997). GDPs consist in large (25-50 mV) depolarizations lasting 300-500 ms with superimposed fast action potentials and followed by an afterhyperpolarization. Their frequency

varies from slice to slice, but usually it ranges from 0.05 to 0.2 Hz. GDPs are network driven events since: i) they are synchronous in extracellular and intracellular recordings; ii) they are synchronous within the entire hippocampus as shown by pair of intracellular recordings (Strata et al., 1997, Menendez de la Prida et al., 1998); iii) their frequency is independent of membrane potential; iv) they are abolished either by TTX or by superfusion with a solution containing a high concentration of divalent cations, known to preferentially block polysynaptic activity.

The large depolarization induced by GDPs triggers an elevation of $[Ca^{2+}]_i$ following calcium entry through activation of voltage-dependent calcium channels (Leinekugel et al., 1995). Thus, calcium fluctuations co-active with GDPs can be detected by optical recordings with Ca^{2+}-sensitive dyes in groups of neighboring cells, both pyramidal neurons and interneurons (Garaschuk et al., 1998).

GDPs are events mediated by GABA acting on $GABA_A$ receptors: they reverse at the same potential of the responses induced by exogenous applications of GABA or the $GABA_A$ agonist isoguvacine and they are reversibly blocked by bicuculline or picrotoxin. As already mentioned, GABA acting through $GABA_A$ receptors, at this developmental stage, is depolarizing. Towards the end of the first postnatal week, a shift from the depolarizing to the hyperpolarizing direction of GABA responses occurs without any significant change in resting membrane potential. In concomitance with this circumstance, GDPs, can be recorded as spontaneous hyperpolarizing events (Ben-Ari et al, 1989, Gaiarsa et al., 1991). Then, they disappear towards the end of the second postnatal week. Until P5 bicuculline suppresses all synaptic activity, whereas after this age it starts to induce spontaneous synchronized interictal discharges (Ben-Ari et al., 1989), similar to those observed in the disinhibited adult hippocampus. Bicuculline-insensitive spontaneous EPSPs can be recorded only after P6 (Hosokawa et al., 1994). In contrast to the

CA3 area, in the CA1 subfield, bicuculline does not induce any interictal activity until P13 (Garaschuk et al., 1998). It should be mentioned that while GDPs are synchronous within the entire hippocampus (Khazipov et al., 1997; Menendez de la Prida et al., 1998; Garaschuk et al., 1998), interictal discharges recorded in disinhibited juvenile or adult hippocampal slices are generated in the CA3 area and then propagate to the CA1.

GDPs need a glutamatergic drive for their expression. In previous studies (Ben Ari et al., 1989; Gaiarsa et al., 1991; Strata et al., 1995) it has been shown that GDPs can be modulated by activation of both ionotropic and metabotropic glutamate receptors. Antagonists of NMDA receptors reduce GDPs frequency or sometimes block them, whereas the AMPA/kainate receptors antagonist CNQX always blocks GDPs. GDPs are also blocked by the broad spectrum ionotropic glutamatergic antagonist kynurenic acid. The application of any ionotropic glutamatergic agonist increases their frequency (Gaiarsa et al., 1991). Also metabotropic receptors play a modulatory role. Bath perfusion of the metabotropic glutamatergic receptor (mGluR) agonist or antagonist (RS)-α-methyl-4-carboxyphenylglycine (MCPG) increases or reduces GDPs frequency, respectively. *t*-ACPD as well as the electrical stimulation of the hilus are able to trigger GDPs in the presence of kynurenic acid an effect that is antagonized by MCPG or bicuculline (Strata et al. 1995). This suggests that, in early postnatal life, glutamate through mGluR enhances the synchronous release of GABA, responsible for GDPs. This effect seems to be mediated by protein kinase A (PKA): the effect of t-ACPD is in fact mimicked by 8-Br-cAMP, forskolin or IBMX and it is prevented by the PKA inhibitor Rp-cAMPS (Strata et al., 1995). GDPs frequency is also increased by application of micromolar concentrations of glycine, an effect that is mimicked by D-serine and is antagonized by the NMDA receptor antagonist D-APV (Gaiarsa et al., 1990). The effect of glycine is insensitive to strychnine, indicating that

occurs on the glycine site of presynaptically located NMDA receptors. GDPs can be also modulated by GABA. Application of GABA increases the frequency of GDPs and induces their appearance when they are blocked by kynurenic acid. Similar effects can be obtained by applying the competitive inhibitor of the GABA transporter nipecotic acid (Strata, 1996). GDPs can be also evoked by stimulation of the hilus. They are strongly reduced by AP-5 and, as spontaneous GDPs, they are completely abolished by bicuculline (Ben-Ari et al., 1989).

The mechanisms underlying neuronal synchronization and GDPs disappearance are still a matter of speculation. It has been suggested that gap junctions play a crucial role in GDPs generation. In the hilar region interneurons are electrically coupled and the number of dye coupled cells decreases during the first two postnatal weeks (Strata et al., 1997). In this hippocampal region, oscillations would be paced by an inward rectifier cationic current with properties similar to I_h. In favour of this hypothesis is the observation that GDPs disappear when extracellular Cs+ or gap junction blockers are present in the bath (Strata et al., 1997).

Recently it has been suggested that synchronization could be determined by the interplay of excitatory GABAergic connections between interneurons and glutamatergic connections presumably from pyramidal cells to interneurons (Khazipov et al., 1997). Hence, in interneurons a glutamatergic component of the GDP could be revealed after intracellular blockade of $GABA_A$ receptors with an internal solution containing fluoride (Khazipov et al., 1997). In particular, it has been suggested that the main contribution to GDP generation may be provided by NMDA receptors that would be activated following GABA-induced depolarization, while AMPA receptors would play only a minor role (McLean et al. 1995; Leinekugel et al. 1997; Ben Ari et al., 1997).

Although the function of GDPs in synaptogenesis is still not fully understood, a recent report underlines the importance of spontaneous network oscillations in promoting the maturation of glutamatergic synapses in the developing hippocampus through a mechanism similar to long-term potentiation (Konnerth et al, 1998). Thus, an active recruitment of new synapses rather than an active elimination of redundant connections would be the principal mechanism underlying activity-dependent synaptic reorganization in the immature hippocampus.

2 Aim of the work

Aim of this thesis was to investigate: i. the role of the glutamatergic drive in GDPs induction; ii. the role of ACh on GDPs modulation; iii. the effects of NGF deprivation of the cholinergic function in the hippocampus.

As already mentioned, GDPs constitute a peculiar feature of hippocampal development. They are generated by GABA acting on $GABA_A$ receptors and are modulated by glutamate acting on both ionotropic and metabotropic receptor subtypes. However, it is not clear whether a glutamatergic drive is necessary for GDPs induction and if this is true, through which type of ionotropic glutamate receptors glutamate exerts its effect. According to previous work from this laboratory (Strata, 1996) GABA itself would be able to synchronize the entire network as suggested by the experiments in which GDPs could be re-induce by GABA in the presence of the broad spectrum ionotropic glutamate receptors antagonist kynurenic acid. On the other hand, it has been recently proposed that GDPs result from the synergistic action of GABA and glutamate that would preferentially activate NMDA receptors (Ben Ari et al., 1997). In this thesis the role of glutamate on AMPA/kainate receptors has been further investigated, taking advantage of new pharmacological tools selective for AMPA receptor subtype. Furthermore the question whether GDPs bear a glutamatergic component has been addressed by blocking at the level of single pyramidal cell the GABAergic response with intracellular fluoride. Pair recordings using different anions in the patch pipettes (KF or KCl) have been used to study the depolarizing action of GABA in network synchronization and to identify the source of glutamatergic drive in minislices disconnected from the rest of the hippocampus.

The hippocampus receives a large cholinergic input from the septohippocampal pathway and this pathway is of fundamental importance in maintaining higher cognitive functions. In view of the

developmental profile of the cholinergic fibers and the role played by GDPs in synaptogenesis the modulation of GDPs by ACh has been investigated. In particular, this study has been aimed at clarifying how ACh regulates GDPs, which subtype of muscarinic receptors is involved and the mechanisms underlying network synchronization.

As already described in the introduction the basal forebrain cholinergic neurons, from which the septohippocampal pathway originates, depend on NGF for their survival and maintenance. The following experiments have been therefore undertaken to assess the effects of NGF deprivation on the cholinergic function on hippocampal neurons, the target of the cholinergic projection. NGF was neutralized by specific monoclonal antibodies, released by hybridoma cells implanted in the lateral ventricle of rats. To see whether the effects of endogenous NGF on the cholinergic function are age-dependent, rats were implanted at three different postnatal ages: P2, P8 and P15 and the experiments were performed one or two weeks later.

All these aims were pursued with electrophysiological experiments on hippocampal slices, using standard intracellular technique or the patch clamp technique in the whole cell configuration.

3 Methods

3.1 Slice preparation

Hippocampal slices were prepared from postnatal day P1-P24 old Wistar rats (P0 is the day of birth). Animals were decapitated after being anaesthetized with intraperitoneal injection of urethane (2 g Kg^{-1}). The brain was quickly removed from the skull and immersed in oxygenated (95% O_2 and 5% CO_2) cold artificial cerebrospinal fluid (ACSF). The hippocampi were dissected free. Transverse 500-600 μm thick slices were cut with a McIlwain tissue chopper and maintained at room temperature (22-24 °C) in artificial cerebrospinal fluid (ACSF) containing (in mM): NaCl 126, KCl 3.5, NaH_2PO_4 1.2, $MgCl_2$ 1.3, $CaCl_2$ 2, $NaHCO_3$ 25, glucose 11, (when oxygenated the pH was 7.3-7.4). After incubation for at least one hour, an individual slice was transferred to a submerged recording chamber, continuously superfused at 33-34°C with oxygenated ACSF at a rate of 3ml/min. In some experiments minislices were prepared by isolating by a knife cut a small portion of the CA3 region from the rest of the hippocampus.
In the cases of animals treated with hybridoma or myeloma cells, slices were obtained only from the hippocampus controlateral to the injection side, while the ipsilateral one was quickly frozen in dry ice for ELISA experiments.

3.2 Solutions and drugs

In patch clamp experiments, the intracellular solution contained (in mM): KCl or KF 140, $MgCl_2$ 1, NaCl 1, EGTA 1, HEPES 5, K_2ATP 2; the pH was adjusted to 7.3 with KOH; the osmolarity was adjusted to 280 mOsm with sucrose. In a few experiments in order to differentiate glutamatergic from GABAergic synaptic events, a mix of K-gluconate (90 mM) and KCl (40

mM) was used. In these cases, the Cl^- equilibrium potential was at about -30 mV. At this potential GDPs could be clearly recognized from the synaptic noise. In *intracellular experiments* the solution used in the electrode was KCl 3M or K-methylsulphate 2M.

Drugs were dissolved in ACSF and applied in the bath by changing the superfusion solution to one which differed only in its content of drug(s). The ratio of flow rate to bath volume ensured complete exchange within 1 min. Drugs used were:

(*RS*)-α-amino-3-hydroxy-5-methyl-4-isoxadepropionate (AMPA), domoic acid, kainic acid, N-methyl-D-Aspartate (NMDA), (+)-3-(2-carboxy-piperazin-4-yl)-propyl-1-phosphonic acid (CPP), D(-)-2-amino-5-phosphonopentanoic acid (D-AP5), 6-cyano-7-nitroquinoxaline-2,3-dione (CNQX) or CNQX disodium, 6,7-dinitroquinoxaline-2,3(1H,4H)-dione (DNQX), γ-aminobutyric acid (GABA), bicuculline, all puchased from Tocris; kynurenic acid, tetrodotoxin (TTX), carbachol, 6-chloro-3,4dihydro-3-[2-norbornen-5-yl]-2H-1,2-4benzothiadiazine-7-sulfonamide 1,1-dioxide (cyclothiazide), physostigmine (eserine), ethyl[m-hydroxyphenil]-dimethylammonium (edrophonium) chloride, atropine sulfate salt, 5,11Dihydro-11[(4-methyl-1-piperazinyl)acetyl]-6H-pyrido-[2,3-b][1,4]benzodiazepin-6one (pirenzepine) dihychloride from SIGMA; GYKI 52466, N,N'-bis[6-[[(2-Methoxyphenyl)methyl]amino]hexyl]-1,8-octane diamine (methoctramine) tetrahydrochloride from RBI; GYKI 53655, from Lilly; echothiophate, gift of Prof. Andrea Nistri.

Stock solution of CNQX, DNQX, cyclothiazide were solved in DMSO at concentrations at least 1000 times lower than those used for the experiments; kynurenic acid was solved at a concentration of 100mM in NaOH equimolar solution. A solution containing DMSO at 1/1000 was tested in some experiments and did not change GDPs frequency or membrane potential.

3.3 Electrophysiological recordings

3.3.1 Patch clamp whole cell recordings

To study GDPs and their modulation by glutamate and ACh during the first postnatal week, patch clamp whole cell recordings (in current clamp configuration) were performed from CA3 and CA1 pyramidal cells. The patch was blind and neurons were identified mainly from their electrophysiological properties (i.e. accomodation). According to the blind technique, a patch pipette is advanced through the slice and positive pressure is continuously applied to it. A current pulse of 1 nA lasting 100 ms is continuously applied. When a voltage variation during the current injection occurs, presumably the pipette tip is touching the cell membrane. At this point the amplitude and duration of current pulse are reduced to 0.5 nA and 50 ms respectively and the positive pressure is released usually causing an increase in amplitude of the voltage step. Then, a negative pressure is applied and a high resistance seal is established. The amplitude and duration of the current pulse are reduced to 0.01 nA and 20 ms and further negative pressure breaks the patched membrane to establish a whole-cell configuration. Current was injected through the recording electrode by means of a standard amplifier (Axoclamp 2B, Axon Instruments, Foster City, CA). Patch pipettes were pulled from borosilicate glass capillaries (1.5 mm od) and had a resistance ranging from 3 to 6 MΩ when filled with the intracellular solution. When the electrode was placed in the bath, its resistance was balanced in bridge mode, and capacitative transients were minimized by negative capacity compensation. The bridge balance was further adjusted and checked repeatedly during the experiments, usually it had a value ranging from 20 to 50 MΩ. A low positive pressure to the pipette applied just after breaking into the whole-cell configuration helped to keep the electrode resistance low. Cell input resistance was measured from the amplitude of hyperpolarizing potentials evoked by injecting a steady current through the

recording electrode and usually ranged from 200 to 500 MΩ. Single spikes were evoked by injecting depolarizing current pulses of 0.1-0.4 nA for 10 ms through the recording electrode. Accommodation was checked injecting current pulses of different amplitude (0.1- 0.3 nA) for 800 ms.

3.3.2 Intracellular recordings

To investigate the effects caused by NGF deprivation on the cholinergic function in the hippocampus, intracellular recordings were performed on CA1 pyramidal neurons using conventional microelectrodes. The CA1 area was chosen because this region receives a large innervation from the septohippocampal pathway. Cholinergic fibers are rather compact in stratum oriens and therefore easy to stimulate. Pipettes were pulled from borosilicate glass capillaries (Clark 1.2 mm od) and had a resistance ranging from 40 to 120 MΩ when filled with KCl and from 70 to 140 MΩ when filled with K-methylsulphate. The recording methods were similar to those described for the blind patch. Also the measurements of input resistance, spike accommodation, etc. were similar.

3.3.3 Extracellular recordings

The presynaptic effects of carbachol on the release of glutamate in NFG deprived animals was studied using extracellular field potentials (fEPSP). fEPSPs, evoked in the CA1 region by stimulation of the Schaffer collaterals (at 0.05 Hz using bipolar twisted NiCr insulated electrodes) were recorded with 2 M NaCl-filled electrodes (resistance 2-5 MΩ) positioned in the stratum radiatum. The stimulation intensity was set so that the amplitude of the fEPSP was about half of the maximal response. fEPSPs were recorded with a Dam 80 Differential Amplifier (WPI,

Inc., USA) and acquired and analyzed with the 'LTP' software package (courtesy of Dr. W.W. Anderson, Bristol University, UK).

3.3.4 Electrical stimulation

GDPs recorded with a patch pipette in CA3 region were evoked with stimulating electrodes (twisted NiCr insulated wire, 50 μm o.d.) placed in the hilus or in the stratum radiatum. Usually the stimulation intensity was increased until it reached the threshold for GDPs, and then fixed to a value 20-30% higher. Clusters of GDPs could be elicited by a train of stimuli (20-50 at 10-30 Hz) delivered by stimulating electrodes placed in the hilus, stratum radiatum or in the fimbria. The stimulation intensity was 2-3 times that required to induced single GDPs. Slow cholinergic EPSPs were evoked in the CA1 region by stimulation of cholinergic fibers in stratum oriens. Parameters of stimulation consisted in 30-50 pulses (40 μs duration each), at 15-25 Hz.

3.3.5 Data acquisition and analysis

During the experiments, the sampled voltages and currents were simultaneously recorded on a pen recorder and displayed on a digital oscilloscope. They were also stored on a magnetic tape after digitization with an A/D converter (Digidata 1200). The program pCLAMP (Axon Instruments, Foster City, CA) was used to inject current pulses, to trigger evoked events and to acquire data on line. Signals acquired from the computer were amplified 5 times and filtered at 10 kHz. Sampling time was different between events. Input resistance, accommodation and I/V curve were measured acquiring data at a frequency of 1.25 kHz. The frequency used to record GDPs was 3 kHz, while that used to acquire a spike was 10 kHz. The amplitude and frequency of GDPs were analyzed off-line with Axoscope (Axon Instruments, Foster City, CA) after a

reacquisition of data from tape. Even in this case data were amplified 5 times, filtered at 100 kHz and the frequency of acquisition was 1 or 2 kHz.

The amplitude, rising phase, half width of GDPs were analyzed in some cells. Events were detected and analyzed with AxoGraph 3.5.5 program (Axon Instrument). To identify the events, the program uses a detection algorithm based on threshold in amplitude or on a sliding template. The template did not induced any bias in the sampling of the events since it was moved along the data trace one point at a time and was optimally scaled to fit the data at each position. Data traces were sampled at a frequency of 5 kHz and then filtered at 10 Hz in order to eliminate spikes. The detection criterion was calculated from the scaling factor of template and from how closely the scaled template fitted the data. The threshold for detection was set at 5 times the standard deviation of the baseline noise. If an appropriate template is used, the program can detect all GDPs present in the analyzed trace. GDPs are usually clearly distinguishable from other events. The program marks all detected events on the trace analyzed and it allows one to verify them in an expanded scale.

If not otherwise stated, data are expressed as mean ± S.E.M. Student's unpaired t-test was used for comparison of unpaired data.

3.4 Cell culture and intraventricular injection of anti-NGF antibodies *in vivo*

To study the role of endogenous NGF on the cholinergic function in the hippocampus, hybridoma cells secreting αD11 monoclonal antibodies selective for NGF (Cattaneo et al., 1988), were injected into the right lateral ventricle of Wistar rats at P2 or P15. This antibody neutralises NGF action by inhibiting its binding to TrkA receptor and is specific for NGF, as it

does not cross-react with other neurotrophins in an *in vitro* bioassay (Gonfloni, 1995). Parental myeloma cells (cells line P3-X63Ag8, briefly P3U) were injected as a control. Hybridoma and myeloma cells were grown in Dulbecco's modified Eagle's medium supplemented with 10% fetal bovine serum. Cells were washed four times in Hank's balanced salt solution and finally resuspended at $2x10^5$ cells/µl and implanted into the right ventricle at postnatal (P) day P2 (1 µl) or P15 (2). Animals were sacrificed one or two weeks after the injection. For the injection, animals were anaesthetized with ether at P2 or with chloral hydrate (4 ml/kg, 0.9% of saline sterile solution) at P15. Cells were injected with a 17 gauge needle connected to a 25 µl Hamilton by a polyethylene cannula, 1.5 mm lateral to the median suture and 0.5 mm posterior to Bregma at P2 and 1,5 lateral 0.5 anterior to Bregma at P15. After injection, animals were treated with cyclosporin A (Sandoz, 15 mg/kg) every other day in order to prevent implant rejection. In previous work it was demonstrated that hybridoma cells are present in the host brain up to one month after injection (Domenici et al., 1994).

3.5 Antibody detection

In animals injected with hybridoma cells, levels of αD11 antibodies were detected in the hippocampus by means of ELISA. Cortices and hippocampi of injected rats were collected and rapidly frozen on dry ice. On these samples, proteic extracts were perfomed. Hippocampi and cortices were homogenized (1:5 weight/volume) in extraction buffer (0.125 M NaCl, 0.05 M Tris pH 7.6, 2 mM EGTA, 2 mM EDTA, aprotinin 100 µg/ml, leupeptin 2 µg/ml and phenylmethansulfonyl fluoride 0.2 M). The homogenized tissue was centrifuged at 44.000 rpm for 30 minutes at 4^0C. The soluble fraction collected was centrifuged again at 12.000 rpm for 15 minutes at 4^0C. NUNC Maxi Sorp plates (Applied Scientific, San Francisco, CA) were coated

with NGF (5µg/ml, 50µl per well). Plates were then washed 5 times in 0.05 % Tween 20 in PBS followed by 5 washes with PBS, and then blocked with 100 µl of 10% of 10mM PBS containing 2% milk for 2 hours at room temperature. αD11 standards were prepared by serial dilution with PBS 2% milk from 250 ng to 0.125 ng of αD11 antibody. For the CSF samples, the standards were diluted in PBS 2% milk. For the tissue samples, standards were diluted in 50 µl of PBS/2% milk, containing proteic extracts from cortices and hippocampi of normal rats, diluted 1:10. Tissue samples were prepared by diluting the extracts 1:10 in 50 µl PBS 2% milk and incubated with solid phase NGF overnight at 4°C. The plates were then washed as above, and incubated 2 hours at room temperature with 50 µl per well of biotinylated rabbit anti rat IgG (AMITY) in PBS/2% milk. After washing, the peroxidase reaction was developed by adding to each well 50 µl of 1-step TMB Turbo ELISA (PIERCE) and this reaction was stopped by adding 50 µl of 2 M sulphuric acid. Standards and samples were analyzed with an ELISA-reader at 450 nm.

3.6 Determination of acetylcholine release following stimulation of hippocampal slices

For releasing experiments, hippocampal slices (400 µm thick) were obtained from 29 Wistar rats (implanted with P3U or αD11 cells at P2 or P15, see Table 4.5 in the Results). Slices prepared according to a previously described technique (Vannucchi et al., 1990) were kept at room temperature in oxygenated ACSF for 30 min and then for an additional 20 min in ACSF containing physostigmine sulphate (3.8 µM, Sigma). They were then transferred to Perspex superfusion chambers of 0.9 ml volume and superfused at 37°C with oxygenated ACSF containing 3.8 µM physostigmine sulphate (at the rate of 0.2 ml min^{-1}). Following 60 min of

washing, 5 min fractions were collected from each chamber. After collection of two 5 min samples, slices were electrically field-stimulated at 2 Hz for 5 min with rectangular pulses of alternating polarity (current strength: 30 mA cm^{-2}, pulse duration: 5 ms). One cycle of stimulation was followed by a 10 min period of rest. At the end of the experiments, slices were weighed. 1 ml samples of superfusate added to 50 µl of 0.25 µM ethylhomocholine (EHC) as internal standard were purified over Sephadex G-10 columns (Vannucchi et al., 1990). ACh was eluted from columns with 2 ml of formic acid (10 mM). The eluate was then dried in a vacuum centrifuge, resuspended in 100 µl of bidistilled water, filtered over Whatman GF/C paper in a blue Gilson tip, and centrifuged for 5 min at 2,000 g. ACh release was quantified by HPLC according to the method described (Casamenti et al., 1993). In brief, ACh was separated in a cation exchange column prepared by loading a reverse-phase Chromspher Cartridge C18 column (Chrompack, Middleburg, The Netherlands) with sodium lauryl sulphate. An enzymatic post-column reactor (10 X 2.1 mm, Chrompack) containing acetylcholinesterase (EC 3.1.1.7, type VI-S) and choline (Ch) oxidase (EC 1.1.3.7), obtained from Sigma Chemical (St. Louis, MO, USA), covalently attached to Hypersil APS-2, activated with glutaraldehyde was used. In the enzymatic reactor, ACh is hydrolyzed to acetate and Ch; Ch is subsequently oxidized enzymatically to produce hydrogen peroxide. The latter compound was electrochemically detected by a platinum electrode at +500 mV. The mobile phase consisted of 0.2 M potassium phosphate (pH 8) containing 5 mM KCl, 1 mM tetramethylammonium chloride and 0.3 mM EDTA. The flow rate was 0.7 ml min^{-1}. To evaluate the amount of ACh in the perfusate, standard calibration curves were constructed by spiking 1 ml of ACSF solution, containing 0.5 µM EHC as internal standard, with known amounts of ACh. All the standards were then passed through the Sephadex G-10 columns described above. The peak height ratios of standard ACh to the internal standard

were then plotted against their concentrations, and the concentration of ACh estimated by regression analysis.

3.7 Immunohistochemistry

Brains were collected from animals injected at P2, P8 or P15, one, two or three weeks after the injection. All animals were deeply anaesthetized and perfused through the left cardiac ventricle with saline solution followed by 4% paraformaldehyde (PFA) in 0.1 M phosphate buffer pH 7.4 (PB: 1ml/gr of body weight). Brains were postfixed in this solution for 4 hours, and then cryoprotected with 25% sucrose in PB 0.1 M pH 7.4. Coronal brain sections were cut with a sliding microtome at a thickness of 40 μm (P2 and P8) or 30 μm (P15) and collected in 0.1 M PB pH 7.4.

Cholinergic neurons of the basal forebrain were labeled with a monoclonal antibody directed to cholinacetyltransferase (ChAT) (Umbriaco et al., 1994). Brain sections were washed in 0.1 M PB, and incubated overnight at 4°C in the primary antibody diluted in 0.1 M PB pH 7.4 containing 0.3% TritonX-100 and 10% normal goat serum (NGS), at a final concentration of 2.5 μg/ml. Section were washed in 0.1 M PB and incubated in biotinylated goat anti-mouse IgG (Sigma, ST. Louis, MO) at a dilution of 1: 200 in 0.1 M PB containing 0.3% Triton-X 100 and 10% NGS, for 1 hour at room temperature. Following washes in 0.1 M PB, sections were incubated in an avidin-biotin-peroxidase mixture (Vectastain ABC Kit, Vector Laboratories, Belmont, CA) diluted in 0.1 M PB containing 0.3% TritonX-100, for a further hour at room temperature. The peroxidase reaction was revealed with a nickel intensified method. Sections were washed in 0.1 M PB followed by washes in 0.1 M sodium citrate (Na citrate) pH 6, and then incubated in a developing solution for 5 to 10 minutes [0.04% 3,3'-diaminobenzidine

tetrahydrochloride (Sigma), 0.2% nickel ammonium sulphate, 0.2% D(+)-glucose, 0.002% glucose oxidase (Sigma) in Na citrate 0.1 M pH 6]. Sections were then washed in Na citrate pH 6, followed by washes in 0.1 M PB pH 7.4, mounted on 2% gelatin coated slides, dehydrated and mounted with DPX.

3.7.1 Quantitative analysis

To evaluate the density of ChAT positive cells, cell counts were made at 200x magnification using an ocular grid mounted on a Zeiss Axiophot microscope. ChAT positive cells were counted at 4 representative levels through the whole rostrocaudal extention of the medial septum (MS) and diagonal band (DB) regions. MS was demarcated against DB by an horizontal line paralleling the anterior commisure. For each age, 3 controls and 3 experimental animals were analyzed. For each group the mean of density was calculated (cell/mm^2), and un-paired t-test was performed on the mean density to evaluate the statistical significance. Furthermore, in the same areas the cell body size was measured with the MicroComputerImagingDevice software (IMAGING Research Incorporation, Ontario, Canada). Only cells with the nucleus on the focus plan were selected. The statistical significance was evaluated applying the man whitney rank sum test. In order to have a quantitative indication of the cell soma reduction, shrinkage index was calculated on the data obtained from the soma size measurements. It is defined as the difference between the mean of the median of P3U injected rats and the mean of the median of αD11 injected animals.

4. Results

4.1 Role of ionotropic glutamate and muscarinic receptors in GDPs modulation

As already described in the introduction, GDPs are modulated by both NMDA and non-NMDA ionotropic glutamatergic receptors (Ben-Ari et al., 1989, Gaiarsa et al., 1991). However, the different role played by these receptors in GDPs regulation has not been completely elucidated. Therefore, in a first set of experiments, the role of ionotropic glutamate receptors in GDPs generation was re-examined, taking advantage of new and more selective pharmacological tools. Moreover, the conductances activated during GDPs were studied in pyramidal cells after the block of $GABA_A$-receptor mediated inward current with an intracellular solution containing fluoride. Then, in a second series of experiments, the capability of endogenous ACh or carbachol, to modulate GDPs *via* muscarinic receptors was studied. The rationale behind these experiments is in the relatively late postnatal development of the septo -hippocampal pathway. This projection consists of cholinergic and GABAergic fibers (about 80% and 20%, respectively); the cholinergic projection plays a fundamental role in maintaining higher cognitive functions. Cholinergic fibers start to reach their target in the hippocampus at P1-P3 but attain an adult pattern only towards the end of the second postnatal week.

Stable whole cell recordings (in current clamp configuration) lasting more than 30 min were obtained from 250 CA3 pyramidal cells in slices from P1-P6 old rats which exhibited spontaneous GDPs. GDPs consisted of large (30-50 mV) depolarizing potentials lasting 400-700 ms, which triggered action potentials, followed by an afterhyperpolarization and occurred at the

frequency of 4.3 ± 0.4 GDPs/min. Analysis of the frequency of GDPs at different ages did not show any significant difference.

4.1.1 AMPA receptor activation is necessary for GDPs induction

To test the role of AMPA receptors in GDPs induction, the selective AMPA/kainate receptor antagonist CNQX (10-40 μM) was applied (n=4). As reported earlier (Gaiarsa et al., 1991), this compound completely blocked spontaneous GDPs (Figure 4.1), even in slices from rats as young as P2. A full recovery was obtained 10-15 min after wash. The effects of CNQX were not due to

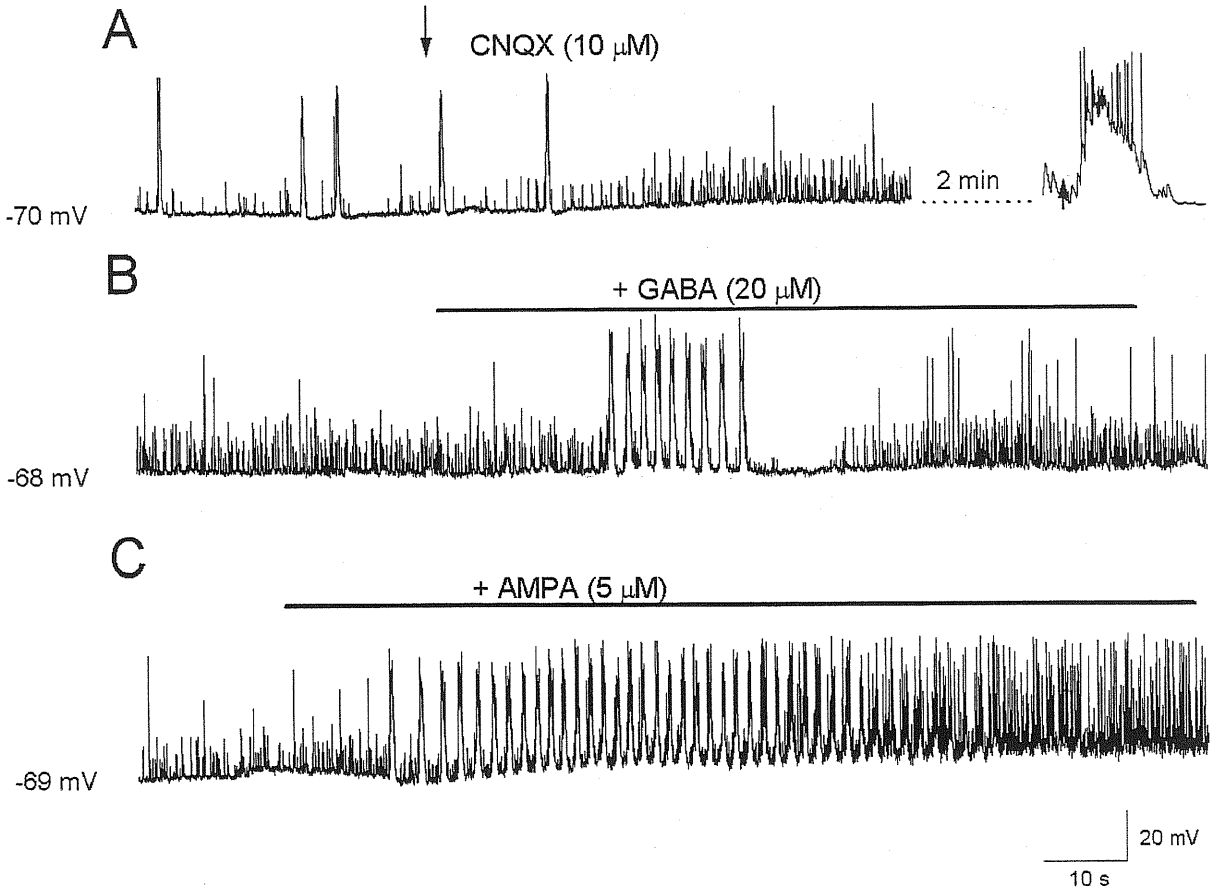

Figure 4.1 10 μM CNQX only partially blocks AMPA receptors.
A, B, C are recordings from the same CA3 pyramidal neurons recorded at P5. A Bath application of CNQX (arrow) blocked the spontaneous but not the evoked GDP (shown on the right on an expanded time scale). This effect was associated to an increase in frequency and amplitude of spontaneous synaptic events. In the presence of CNQX, bath application of GABA (20 μM, B) or AMPA (5 μM, C) was able to restore GDPs.

the solvent (DMSO) in which CNQX was dissolved, since the same concentration of DMSO did not produce any effect. Moreover in some experiments (n=6) CNQX disodium salt was used, and similar results were obtained. Mc Bain et al. (1992) have reported that bath application of CNQX to CA3 pyramidal neurons induced an increase in GABA-mediated synaptic noise. This effect was peculiar to CNQX and it was not mimicked by DNQX or kynurenic acid. The authors suggest a direct depolarizing action of CNQX on a small population of local interneurons. To avoid this problem, other AMPA receptors antagonists was tested. Similarly to CNQX, DNQX (20 μM, n=5), GYKI 52466 (20-100 μM, n=6) and kynurenic acid (2 mM, n=8) blocked GDPs. However, in the presence of these antagonists, it was still possible to evoke GDPs by focal stimulation (Figure 4.1) or to re-induce the appearance of spontaneous GDPs by bath application of GABA (20 μM), AMPA (5 μM) or NMDA (1 μM), although NMDA was ineffective in the presence of kynurenic acid. In the presence of kynurenic acid (2mM), increasing concentrations

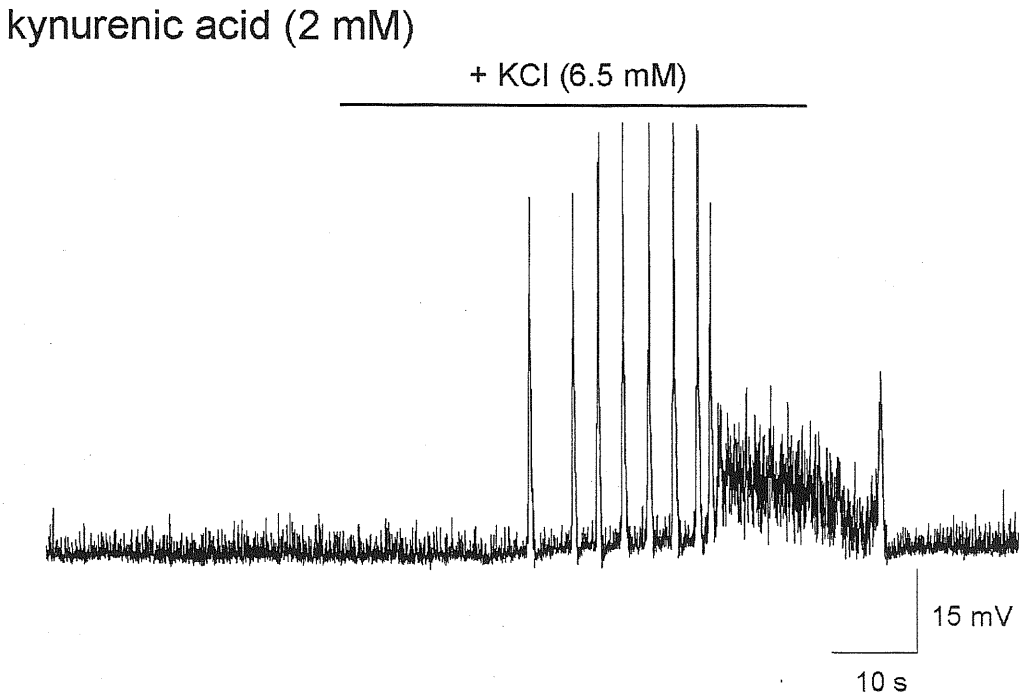

Figure 4.2 Bath application of 6.5 mM potassium in the presence of kynurenic acid induces the appearance of GDPs.
In slice from a P6 rat bath perfusion of kynurenic acid blocked GDPs. Increasing the extracellular potassium concentration from 3.5 to 6.5 (bar) induced the re-appearance of GDPs followed by a membrane depolarization associated to an increase in synaptic noise.

of external potassium (from 3.5 to 6.5 mM) were also able to induce the re-appearance of GDPs (Figure4.2) suggesting that a general increase in cell excitability and/or a depolarization of the terminals was sufficient to release neurotransmitters (including glutamate) able to synchronize the entire network.

AMPA-induced GDPs were usually associated to a 5-12 mV membrane depolarization. Both GDPs as well as the membrane depolarization were prevented (in the presence of kynurenic acid) by bicuculline (10 μM), suggesting that both phenomena were due to the release of GABA (Figure 4.3). The possibility to synchronize again the network with AMPA suggests that the

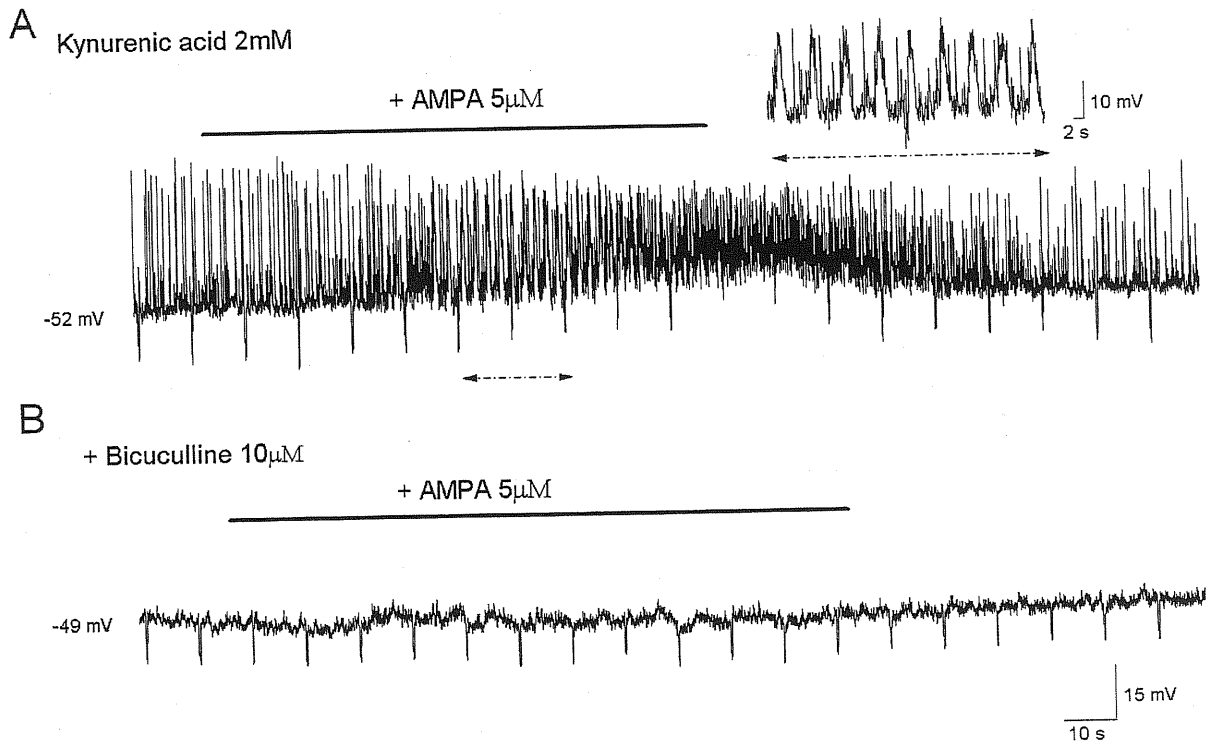

Figure 4.3 The AMPA-induced depolarization observed in the presence of kynurenic acid is prevented by bicuculline (P4)
A in the presence of kynurenic acid, AMPA (5 μM) induced the re-appearance of GDPs followed a membrane depolarization and an increase in synaptic noise. **B** The effects of AMPA were prevented by bicuculline (10 μM). Downward deflection in A and B are electrotonic potentials evoked by injection of rectangular current pulses (250 ms duration) through the recording electrode

concentrations of the competitive antagonists used were not sufficient to block AMPA receptors. To check whether this hypothesis was correct, a more potent, selective and non competitive AMPA receptor antagonist, GYKI 53655 (Paternain et al., 1995) was tested. GYKI 53655 (50-100 μM) blocked spontaneous GDPs, but in this case neither electrical stimulation nor AMPA (5 μM) or GABA (20 μM) application could induce evoked or spontaneous GDPs (Figure 4.4). These data suggest that the glutamatergic drive via AMPA receptors is essential for GDPs generation.

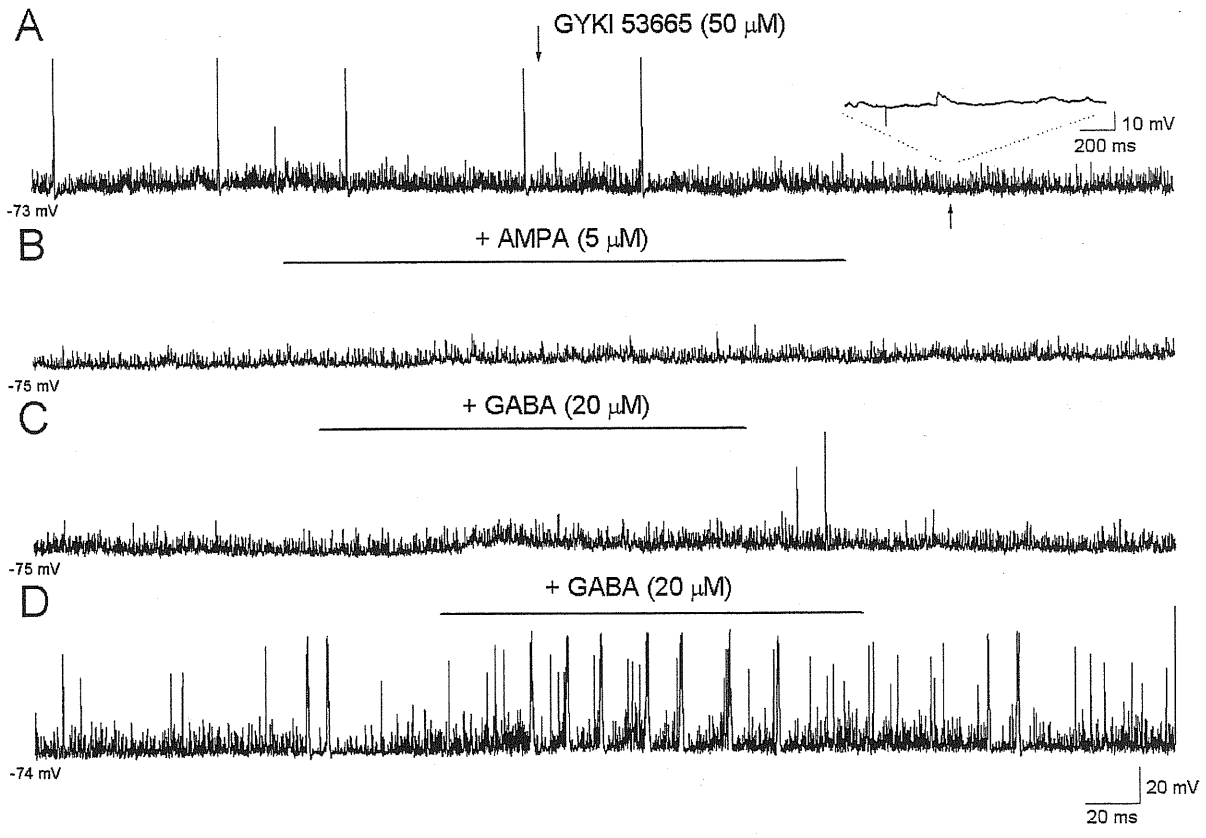

Figure 4.4 AMPA receptor activation is essential for GDPs induction
A, B, C and D are tracings from the same cell (recorded at P5). **A** Bath application of the selective AMPA receptor antagonist GYKI 53655 (arrow) readily blocked spontaneous and evoked GDPs. In the presence of GYKI 53655, electrical stimulation failed to evoke a GDP (in the inset above the trace on an expanded time scale). **B,C** n the presence of GYKY 53655, both AMPA (bar, B) and GABA (bar, C) failed to re-induce GDPs. **D** 30 minutes after washing GYKI, spontaneous GDPs reappeared. Bath application of GABA (20 μM, bar) was able to increase their frequency.

To further examine the role of AMPA receptors in GDPs induction, experiments were performed in the presence of cyclothiazide, a selective blocker of AMPA receptor desensitization (Partin et al., 1993). In the presence of cyclothiazide (20 μM) GDPs frequency increased by 76 ± 14% (n=6, Figure 4.5). In three of these experiments slices were obtained from rats as young as P1-P2. Although in these cases the effects of cyclothiazide were less pronounced (only a 50% increase in GDPs frequency was observed) these findings suggest that functional AMPA receptors are already present at very early stages of postnatal development.

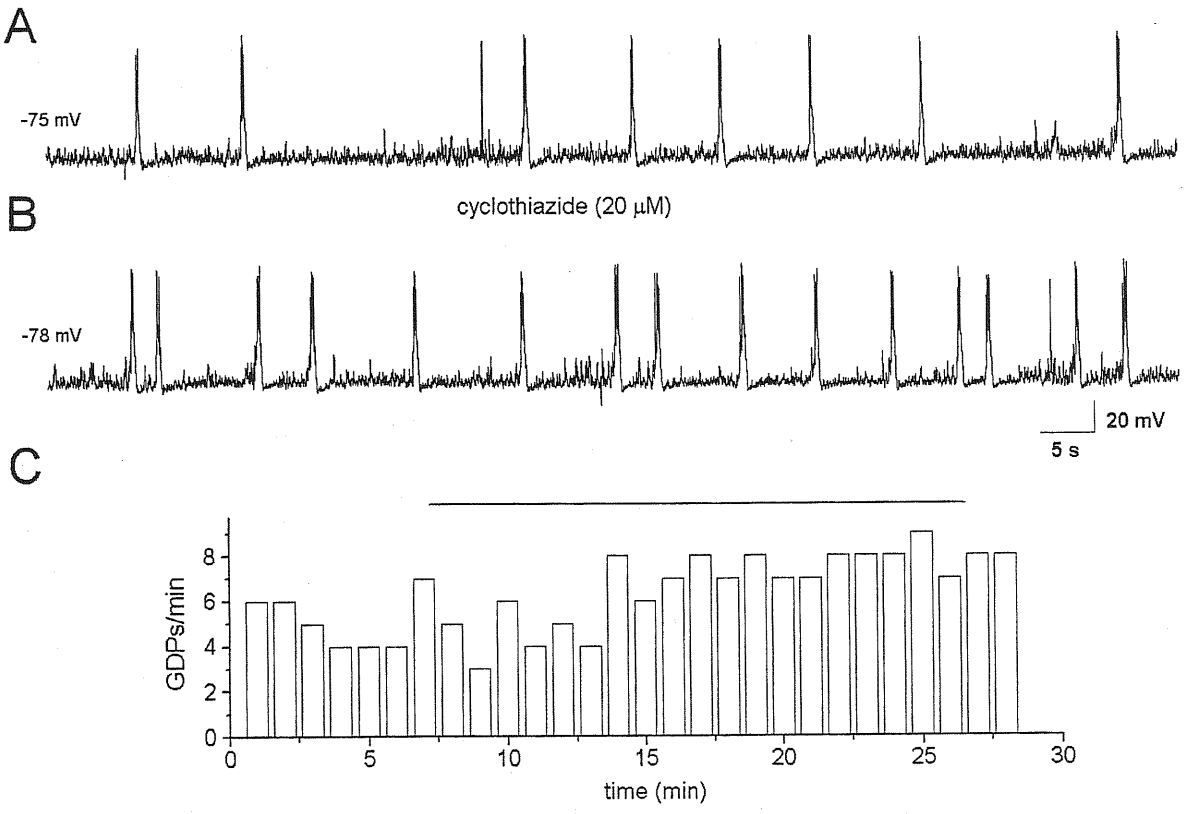

Figure 4.5 Cyclothiazide increases the frequency of GDPs.
A, B Representative tracing from a CA3 pyramidal cell recorded at P4 in control condition (A) and during bath application of cyclothiazide (B). **C** GDPs frequency of the cell shown in A and B is plotted against time. Each column represents the number of GDPs recorded in one min.

Kainate receptors were not apparently involved in GDPs induction, since in the presence of GYKI 53655 both kainate and domoic acid (0.1-1 μM) failed to induce GDPs (n=3, Figure 4.6). They increased synaptic noise without altering the membrane potential. In the absence of GYKI 53655, kainate and domoic acid increased GDPs frequency and synaptic noise and induce a membrane depolarization of 36 ± 4 mV (n=5, Figure 4.6).

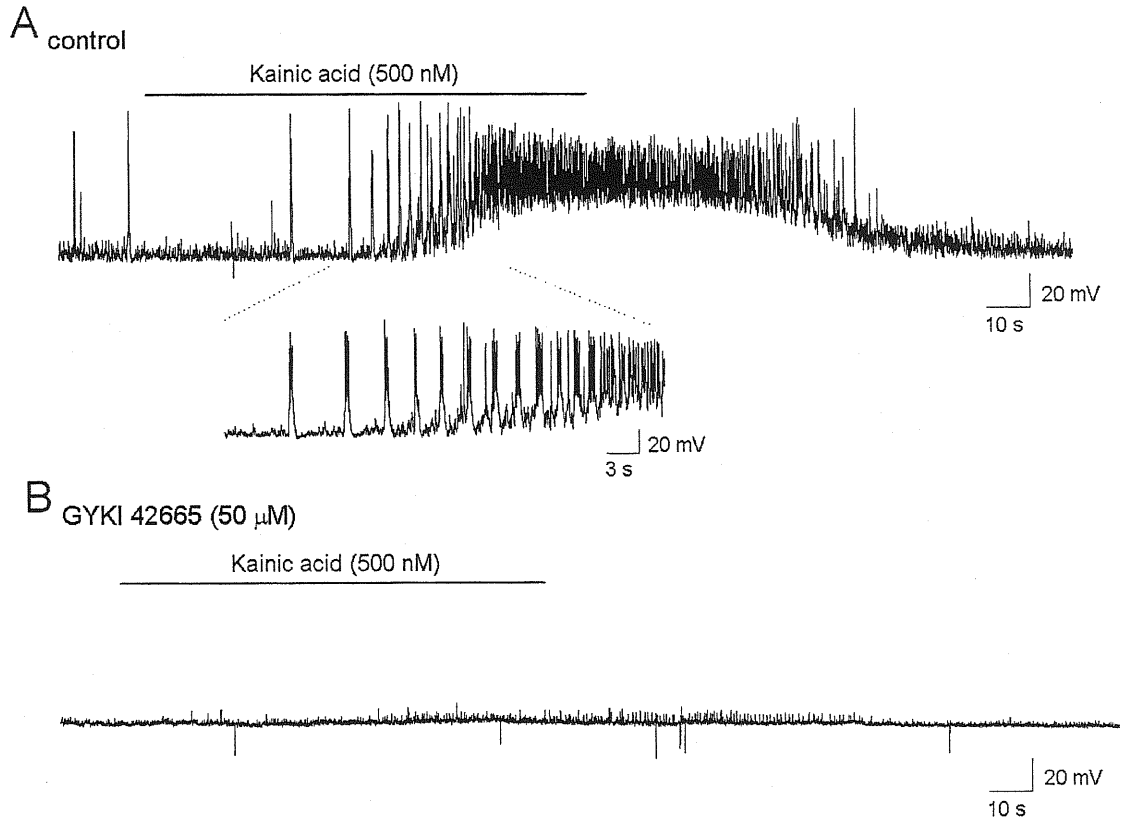

Figure 4.6 GYKI 53665 blocks the depolarization and increase in GDPs frequency induced by kainic acid. A and B are recording from the same cell (at P5). **A** Bath application of kainic acid induced an increase in GDPs frequency associated with a membrane depolarization and to an increase of synaptic noise. **B** Both GDPs and membrane depolarization were prevented by GYKI 53665. Downward deflection in A and B are electrotonic potentials evoked by injection of steady current through the recording electrode

4.1.2 NMDA receptors contribute to GDPs generation

To assess if NMDA receptors were necessary for GDPs generation, the selective NMDA receptor antagonists D-AP5 and CPP were applied in the bath. As shown in Figure 4.7, D-AP5 (50 μM) applied for 10-15 min produced a reduction of GDPs frequency that was not maintained throughout the period of drug application but slowly tended to recover towards control values.

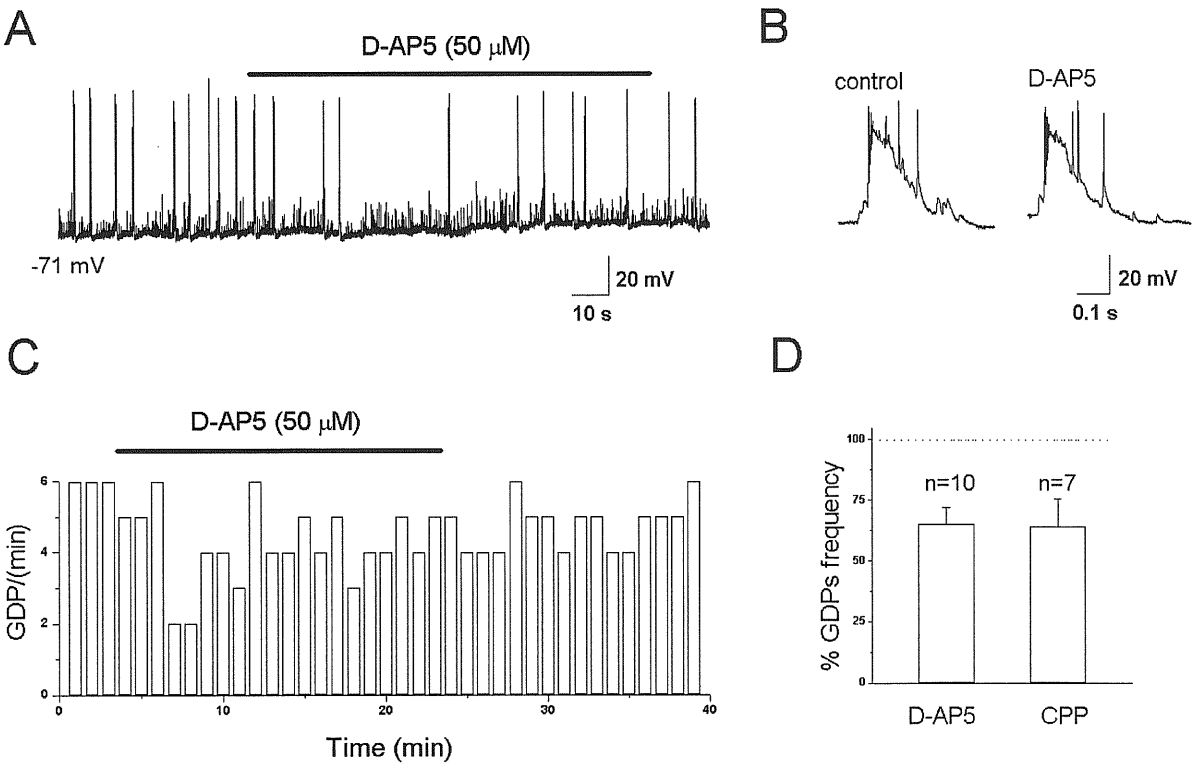

Figure 4.7. NMDA receptor activation is not essential for GDPs generation.
A Representative tracing from a CA3 pyramidal cell recorded at P4 in control condition and during bath application of D-AP5 (bar). **B** Two GDPs from the recording in A, are shown on an expanded time scale. **C** GDPs frequency for the cell shown in A is plotted against time. Each column represents the number of GDPs recorded in one min. **D** Normalized GDPs frequency recorded during application of D-AP5 (50 μM) and CPP (20 μM) respect to pre-drug treatment (100%, dotted line). Bars indicate standard error of the mean; n refers to the number of experiments

During D-AP5 applications, the GDPs frequency was reduced by an average of 35 ± 7 % (n=10). Similar results were obtained with CPP (20 μM, n=7; Figure 4.7 D). In two cases (out of seventeen) a complete blockade was observed during the first minutes of NMDA antagonist application, but also in this case after few minutes GDPs reappeared (Figure 4.8). Usually no

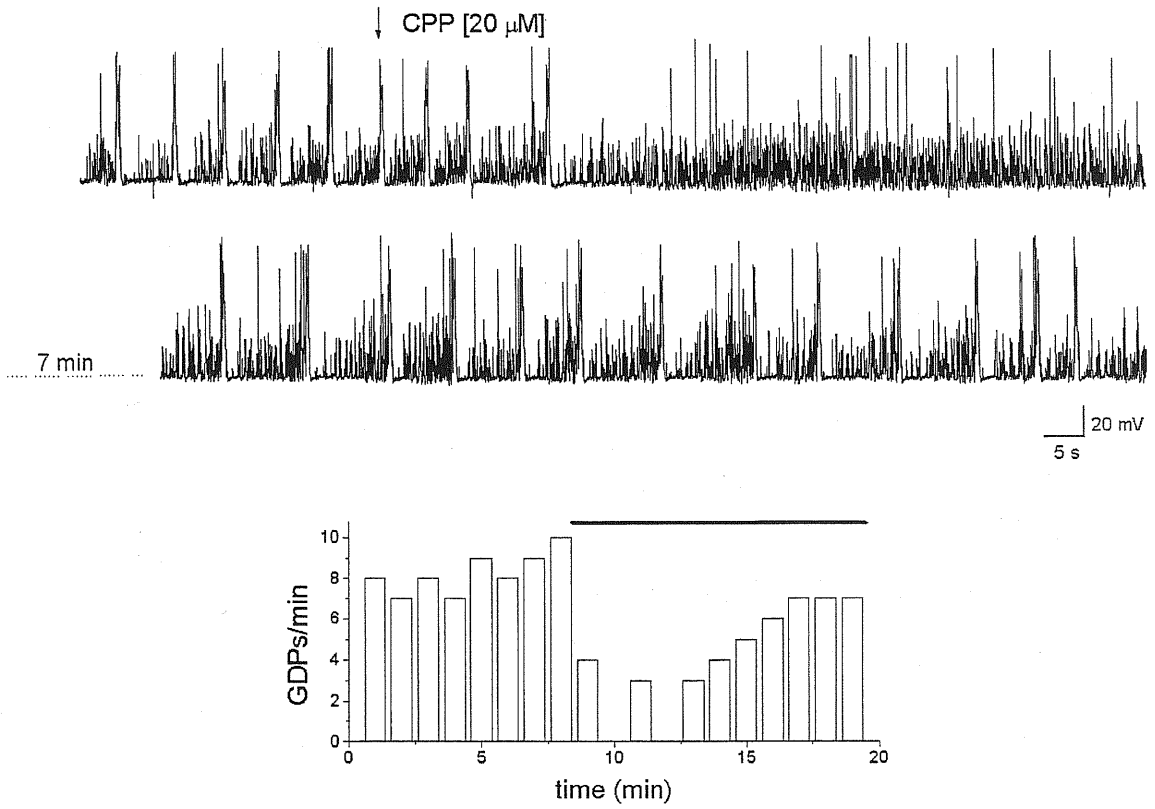

Figure 4.8 CPP induces a transient block of GDPs
A Representative tracing from a CA3 pyramidal cell recorded at P5. Bath perfusion of CPP (arrow) induced a transient block of GDPs whose frequency 7 min after CPP application was close to the pre-drug value. **B** GDPs frequency of the cell shown in A is plotted against time. Each column represents the number of GDPs recorded in one min.

changes in the shape of GDPs were observed during application of NMDA antagonists. These data suggest that while NMDA receptors may contribute to GDPs expression they are not essential for their induction. It is worthwhile noticing that, in the presence of CNQX (10-40 μM), DNQX (10-20 μM) or GYKI 52466 (the less specific one) GDPs re-induction by GABA or AMPA could be prevented by adding to the perfusate D-APV (30 μM) or CPP (20 μM) (Figure 4.9). In these experimental conditions also evoked GDPs could not be elicited. These observations indicate that the contribution of NMDA receptors to network synchronization is essential after partial block of AMPA/kainate receptors.

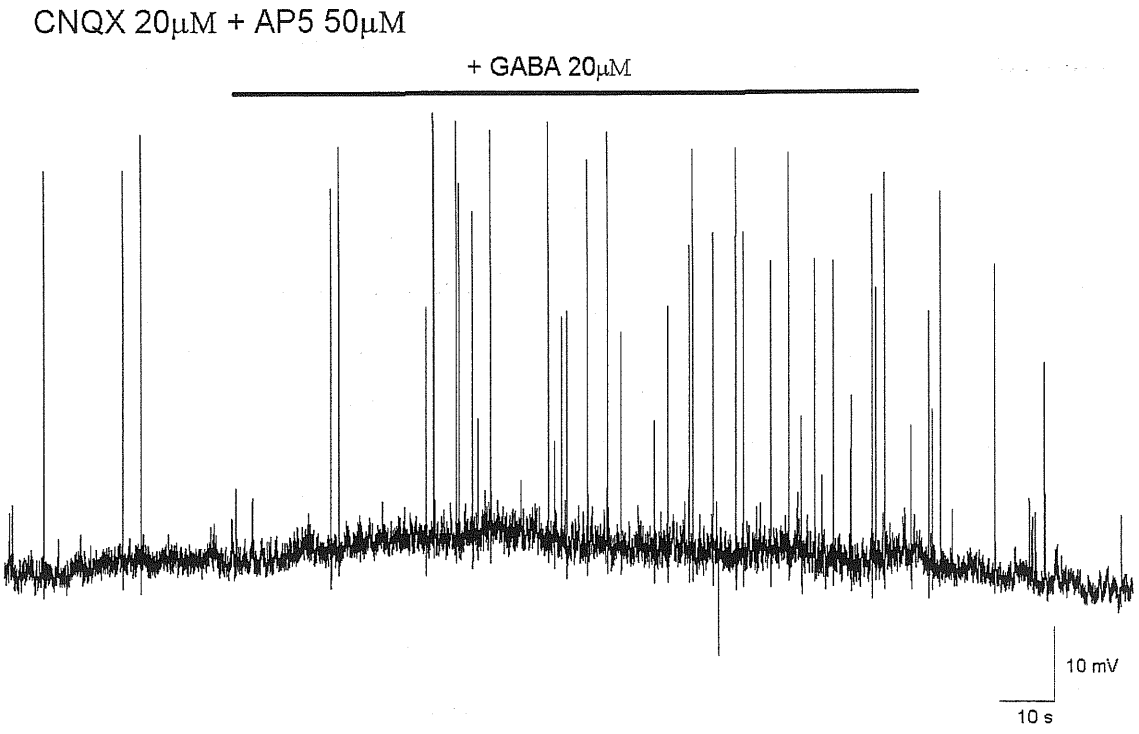

Figure 4.9 Co-application of CNQX plus AP-5 prevented re-induction of GDPs by GABA
Tracing of a CA3 cell at P4. Bath application of CNQX and AP-5 cmpletely abolished GDPs. These were not re-induced by application of GABA (bar). GABAproduced only a slight membrane depolarization associated with an increase in firing (upward deflection)

4.1.3 Intracellular blockade of $GABA_A$-receptor with fluoride reveals an AMPA-mediated component of GDPs

In a previous work aimed at understanding synchronization of interneuronal network (Khazipov et al. 1997), whole cell recordings were made from interneurons dialyzed with the poorly permeable anion F^- which suppresses GABA inward current (Bormann et al. 1987). We have used a similar approach to see whether also in pyramidal cells, glutamate receptors are activated during GDPs. To this purpose we have tested: i. GDPs reversal potential immediately and 30-40 min after a full whole-cell access was achieved with a F^- containing solution; ii. the pharmacological sensitivity of GDPs to ionotropic NMDA and non NMDA glutamatergic receptor antagonists. Furthermore we have tested whether GABA-induced responses were really blocked in the recorded cell and if NMDA and AMPA responses were altered using F-containing solution.

Immediately (3 to 5 min) after breaking into whole cell configuration, the reversal of evoked and spontaneous GDPs was -45.7 ± 6.1 mV (n=28) and -40.8 ± 6.2 mV (n=11), respectively. Plots of amplitude/voltage relationships were always linear. The slope of the regression lines through different data points was -0.58 ± 0.19 (n=28) for evoked (Figure 4.10) and -0.67 ± 0.14 (n=11) for spontaneous GDPs. After 30-40 minutes of dialysis with an intracellular F^- containing solution, a complete block of GABA-evoked responses in the presence of TTX (1 μM) was observed (Figure 4.11). The $GABA_A$ inward current suppression was associated to a significant shift of the reversal of GDPs towards more positive values and to a reduction in the slope of the regression lines, indicating a reduction of GDPs amplitude (Figure 4.10).

The reversal of the evoked and spontaneous GDPs was -14.1 ± 11.4 mV (n=17) and -15.8 ± 13.1 mV (n=6), respectively, while the slope of regression line was -0.29 ± 0.12, n=17 for evoked and

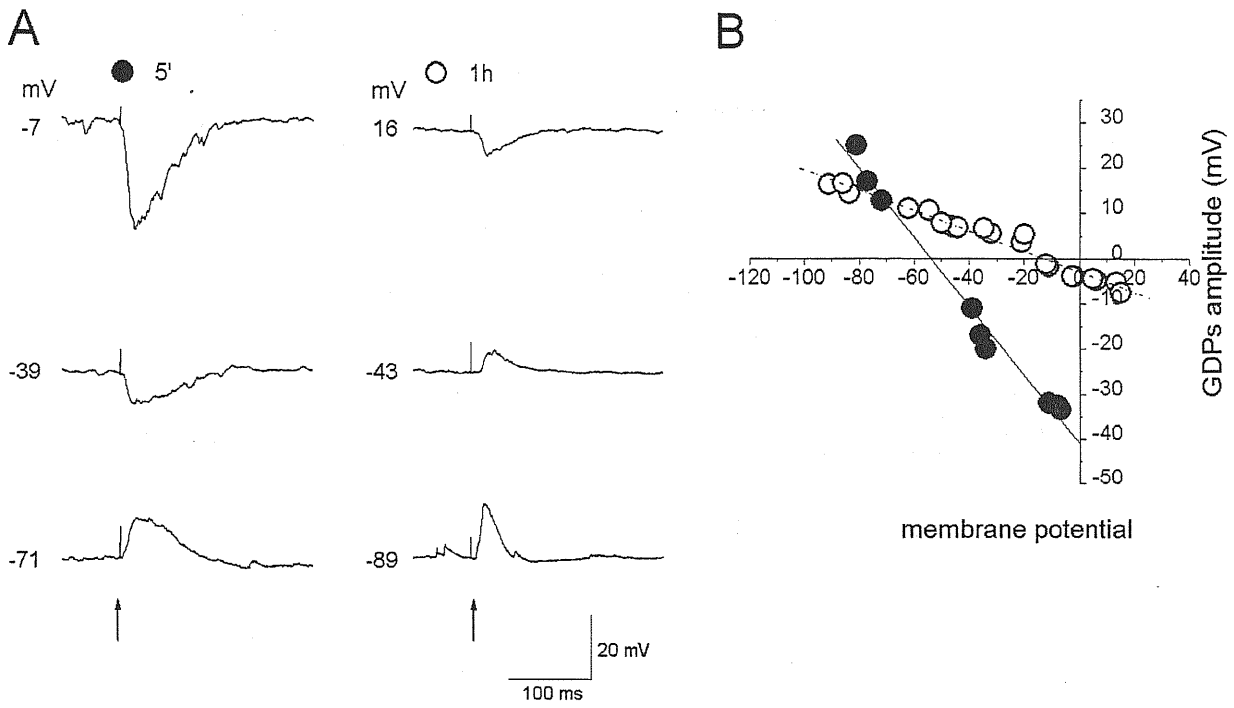

Figure 4.10 Intracellular blockade of GABA receptors with fluoride reveals a novel component of evoked GDP. **A** Evoked GDPs (arrows) recorded at different membrane potentials (at P4) with a patch pipette containing KF, 1 min (left) and 40 min (right) after breaking into the whole cell configuration. **B** Plot of GDPs (shown in A) amplitude versus membrane potentials. Note the shift to the right of the reversal potential and the change in the slope of the amplitude-voltage plot, 40 min after dialyzing the cell with fluoride.

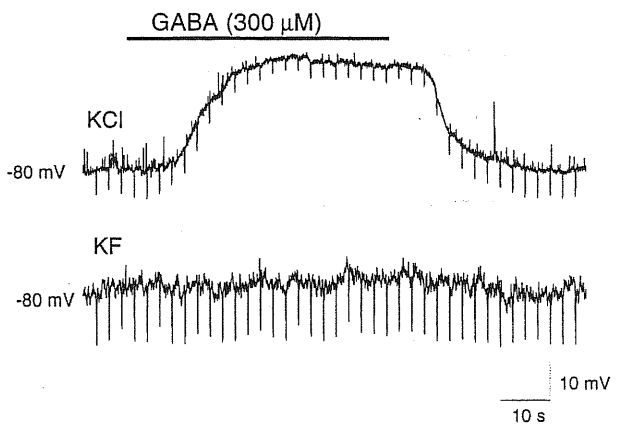

Figure 4.11. Intracellular fluoride blocks $GABA_A$ receptors.
Pairs of recordings from adjacent CA3 pyramidal cells patched with pipettes containing KCl and KF. Application of GABA (bar) in the presence of TTX (1µM) induced a membrane depolarization associated to an increase in membrane conductance only in the cell recorded with KCl. Downwards deflections are electrotonic potentials evoked by injection of steady current pulses of the same amplitude (250 ms duration).

-0.31 ± 0.13, n=6 for spontaneous. In the majority of cells the amplitude/voltage relationship was linear, while in four cases a rectification at more negative potentials was observed. The shift of the reversal potential towards more positive values as well as the reduction of the slope in the amplitude/voltage relationship suggest the presence of a different component unmasked after intracellular blockade of $GABA_A$ inward current with F^-. To understand the nature of this residual component, spontaneous and evoked GDPs were recorded at different membrane potentials in the presence of AMPA and NMDA receptor antagonists (Figure 4.12). Bath application of CNQX (10-20 μM) completely abolished the residual component of spontaneous GDPs and in 8/11 cases completely blocked the evoked GDPs. In 3/11 cells, D-APV (50 μM),

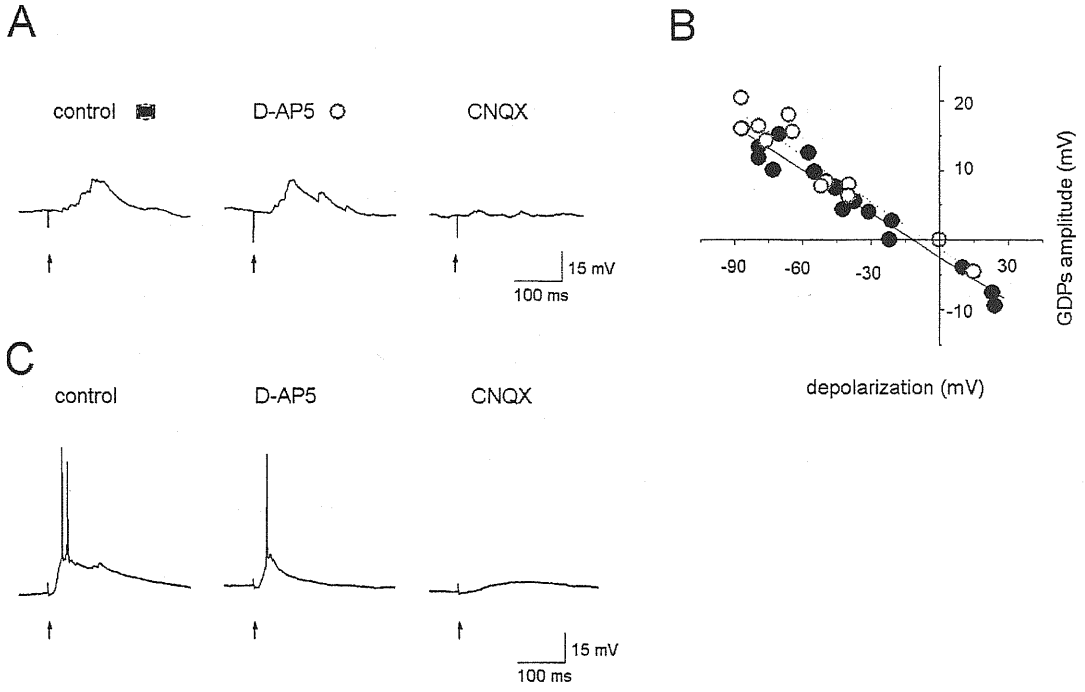

Figure 4.12. NMDA and non-NMDA glutamatergic component of the evoked GDP revealed after blocking GABA with intracellular fluoride.
A GDP evoked after 30 min breaking into whole-cell configuration, in control condition and in the presence of D-AP5 (50 μM) and CNQX (20 μM). Membrane potential –80 mV. **B** Plot of GDPs amplitude versus membrane potential in control conditions (closed circles) and in the presence of D-AP5 (open circles). **C** GDP evoked in another neuron in the same experimental conditions as in A. Note the presence of D-AP5 sensitive component. Arrows indicate the time of stimulation; membrane potential ranges from –77 mV to –65 mV.

reduced the amplitude and duration of GDPs. In the presence of D-AP5 and CNQX, GDPs could not be evoked.

It could be that the glutamatergic component of GDPs, which remains after blockade of $GABA_A$ inward current, is amplified as the result of the interference of intracellular F^- with phosphatases (Andrews and Babior, 1984), enzymes that regulate receptor desensitization (Yakel, 1997). To test this hypothesis, the amplitude of AMPA responses recorded in TTX (1 μM) with a F^- containing intrapipette solution was compared with that of responses recorded with a KCl solution. As shown in Figure 4.13, in F^-, AMPA responses were not significantly ($p>0.08$) different from those recorded in KCl.

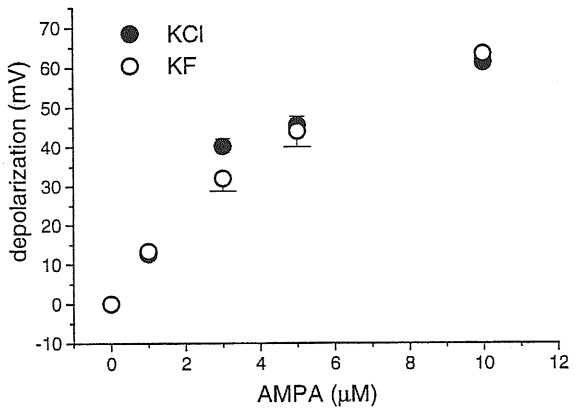

Figure 4.13. Intracellular fluoride does not affect AMPA responses.
Responses to increasing concentrations of AMPA recorded in the presence of TTX (1 μM) with KCl (open circles) or KF (closed circles) electrodes. Each symbol is the mean of 3-7 responses obtained at P3-P6. Bars represent the S.E.M. When not visible they are within the symbols.

Paired recordings performed from adjacent CA3 pyramidal cells (n=21), using two different intrapipette solutions showed that GDPs recorded with KF and KCl were still synchronous in the two cells confirming their combined glutamatergic and GABAergic nature (Figure 4.14). However, a clear difference in the shape of GDPs recorded with KF or KCl was observed. As depicted in Figure 4.14, in KF GDPs were smaller and exhibited a slower rising phase that often did not reach the threshold for action potential generation. When GABA (20 μM) or AMPA (5μM) were applied in the presence of kynurenic acid (1 mM), they were able to re-induce GDPs

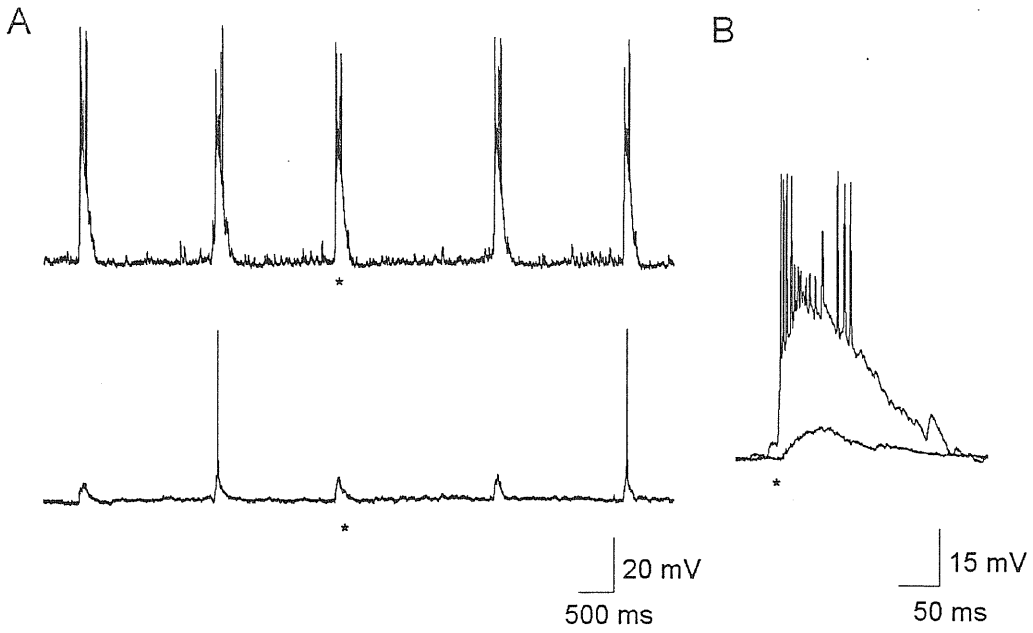

Figure 4.14 GDPs recorded with KCl or KF are synchronous but have different size
A. Pairs of recordings from adjacent pyramidal cells (at P5) patched with intrapipette solutions containing either KCl (top) or KF (bottom). Note that GDPs are synchronous in the two recordings. **B** Two GDPs (marked with an asterisk) are superimposed shown on an expanded time scale. GDPs recorded with KF are smaller in amplitude and exhibit slower kinetics.

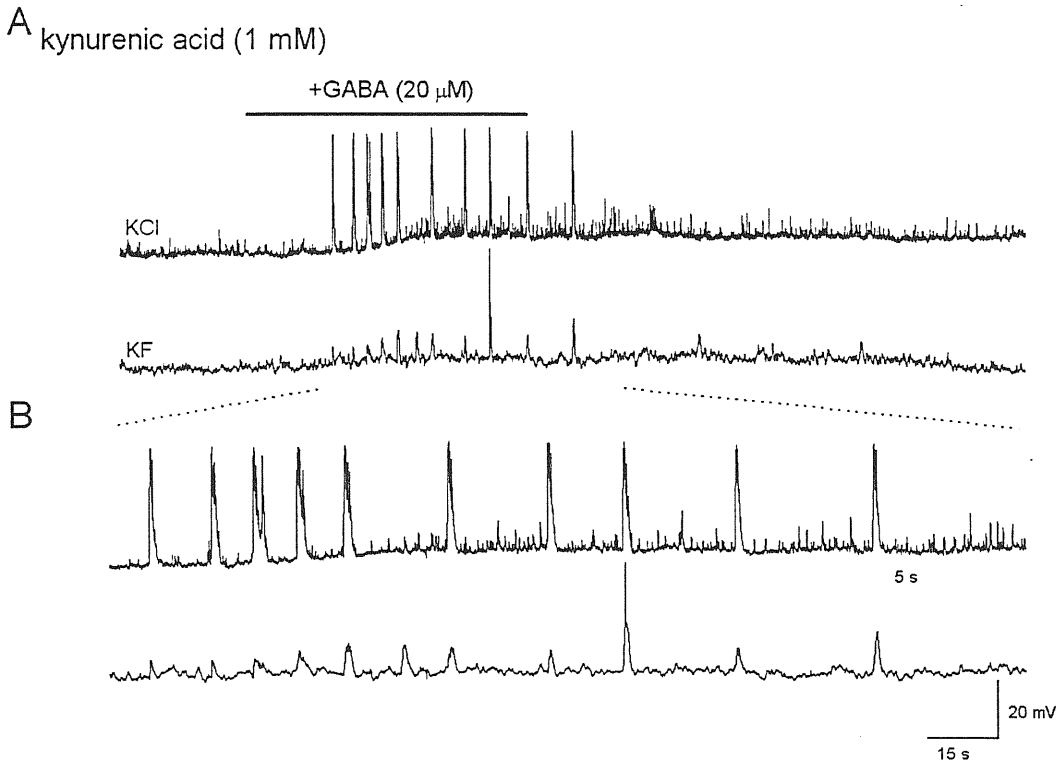

Figure 4.15 Kynurenic acid 1mM does not completely abolish the glutamatergic component of GDPs
A Pair recordings from the same cells of Figure 4.14. Bath application of the broad spectrum NMDA and non-NMDA ionotropic glutamatergic antagonist kynurenic acid abolished GDPs, that could be re-induced by bath application of GABA (bar) on the cell patched with KCl containing electrode (top trace). Note that a small component of GDPs coul be still detected in the cell patched with KF containing pipette (bottom trace). **B** Traces during GABA application are shown in an expanded time scale.

in the cell recorded with KCl electrode (Figure 4.15), but only a small response could be detected with the KF containing pipette synchronous with the GDPs recorded with the KCl electrode. In contrast when the antagonist concentration was increased to 2 mM no signals could be detected with the KF pipette though GABA still had a small depolarizing effect (Figure 4.16).

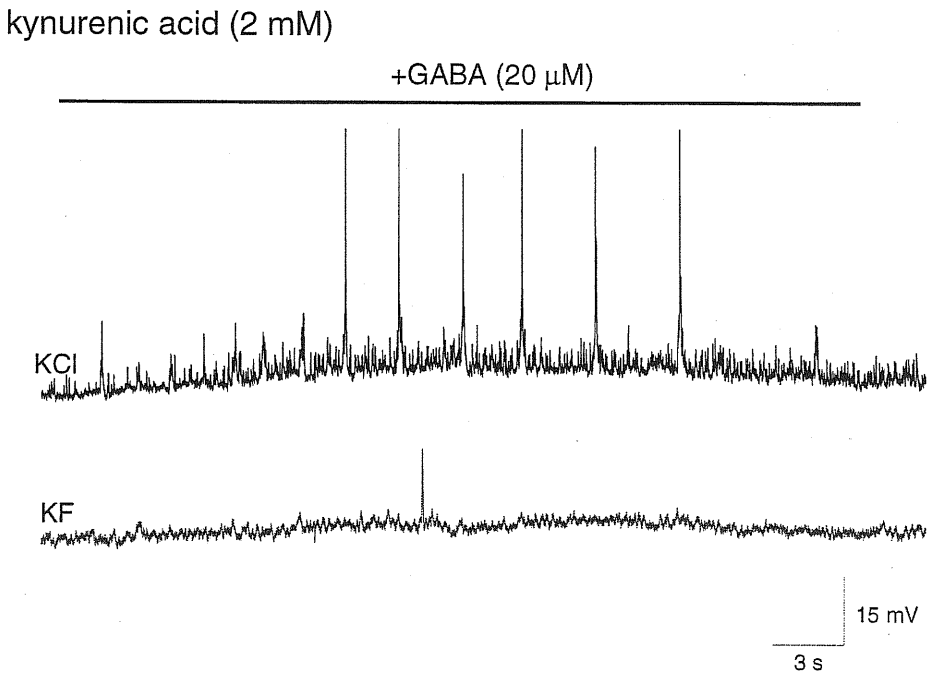

Figure 4.16 Kynurenic acid 2 mM completely abolishes the glutamatergic component of GDPs.
Pairs of recordings from the same cells of Figure 4.14 and 4.15. In the presence of kynurenic acid 2 mM, bath application of GABA could re-induced GDPs only in the cell patched with KCl. containing electrode.

4.1.4 Source of glutamatergic drive needed to synchronize GABAergic interneurons

Glutamate may be released from mossy fibers, known to make synaptic contacts with the proximal dendrites of CA3 pyramidal neurons and with GABAergic interneurons (Acsády et al., 1998). In early postnatal days, when the present experiments have been performed, mossy fibers are not completely developed (Gaarskjaer, 1986) and therefore their contribution to GDPs

induction is expected to be modest. On the contrary, associative-commisural fibers from the controlateral hippocampus as well as collaterals of CA3 pyramidal cells may be a good candidate for the source of this glutamatergic drive. In order to examine this hypothesis, in 3 slices, a small portion of the CA3 region was isolated with a knife cut from the rest of the hippocampus and paired recordings were performed from two adjacent CA3 pyramidal cells using two intrapipette solutions containing KF and KCl, respectively. In these conditions GDPs with characteristic similar to those reported above could be still recorded synchronously in the two cells (Figure 4.17). This suggests that a local population of pyramidal cells and interneurons is sufficient to generate GDPs and that collaterals of principal cells are probably the main source of glutamatergic drive.

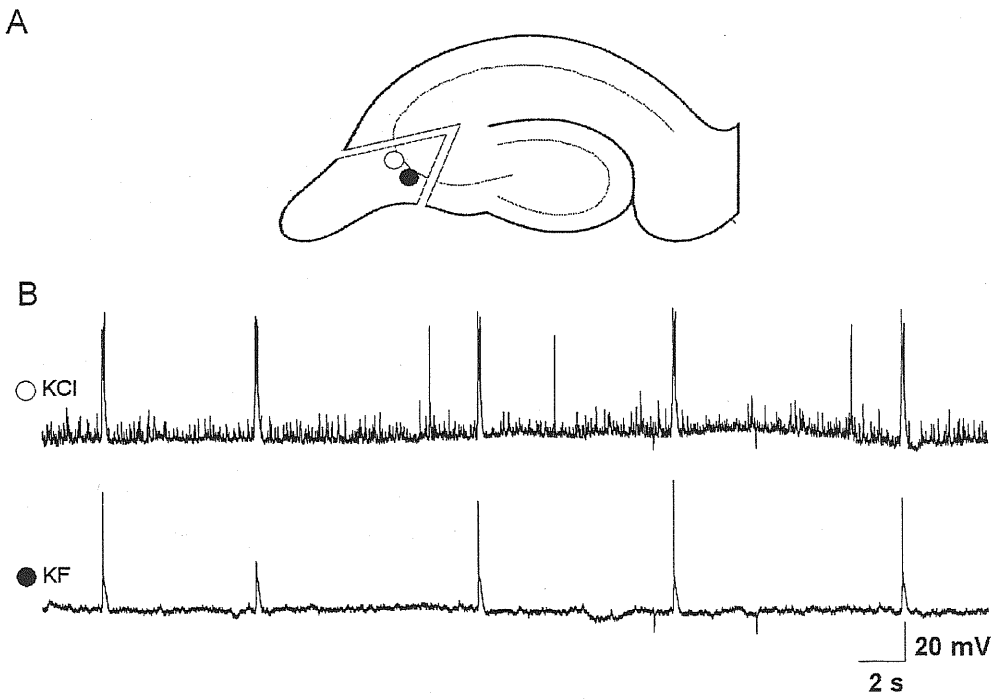

Figure 4.17 GDPs are still present in minislices of the CA3 region.
A Schematic diagram showing a minislice of the CA3 region disconnected with a knife cut from the rest of the hippocampus at P5. **B** Pairs of recordings from adjacent pyramidal cells (patched with KCl and KF intrapipette solutions) are still synchronous. In this case, the glutamatergic component of the GDP detected with KF can originate only from a local circuit.

4.1.5 Endogenous acetylcholine increases the frequency of GDPs

In order to see whether endogenous ACh was able to modulate GDPs, the muscarinic receptor antagonist atropine (2 μM) was applied in 5 slices from P3 to P6 old rats. In three cases, atropine rapidly (2-3 min) induced a decrease in the frequency of GDPs of 71 ± 8.5 % without changing their shape. This effect was concentration-dependent. In two cells the effect of atropine was

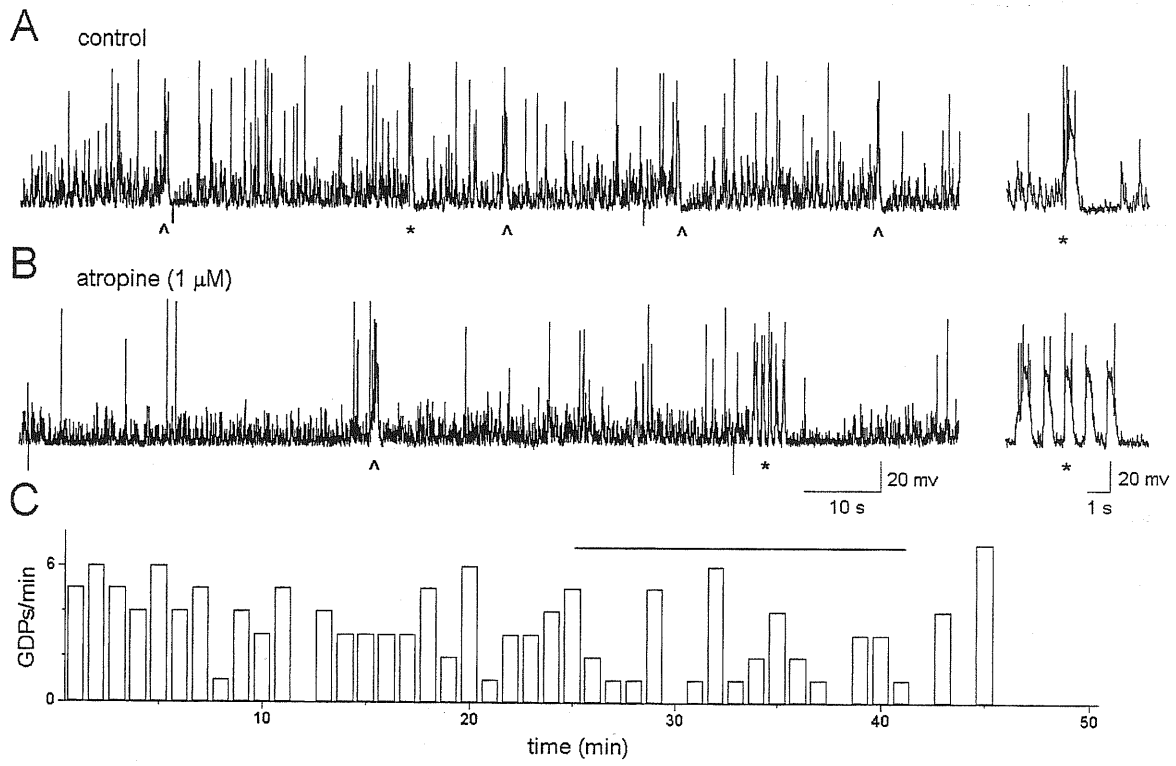

Figure 4.18 Atropine causes a reduction in GDPs frequency
A and **B** are continuous recording from a P4 pyramidal cell in control condition (A) and during application of atropine (1 μM, B). Note that in atropine the frequency of GDPs (marked with ^ or *) decreased. On the right, a single GDP and a cluster of GDPs (asterisks), occuring in control and in atropine application, are shown in an expanded time scale. **C** GDPs frequency of the cell shown in A and B is plotted against time. Each column represents the number of GDPs recorded in 1 min

transient: it lasted for 4-7 min and then GDPs frequency returned to control values in presence of the antagonist. In the remaining two cases atropine was ineffective. In Figure 4.18 the cell in which the inhibitory effect of atropine was maintained throughout the period of drug application is shown. Interestingly, in this case during atropine application GDPs started to appear grouped in clusters of 3-5 GDPs (in the histogram each peak during atropine superfusion corresponds to a cluster of GDPs) and within the cluster they also changed their shape (they showed a faster rising time 288 ± 23 ms versus 152 ± 14 ms and a reduced half width 54 ± 10 ms versus 21 ± 1 ms, in control and atropine, respectively). However overall, no significant ($p>0.5$) differences were observed in the rising time and half width of single GDPs in control and during atropine application.

Superfusion of the M1 or M2 receptor antagonists pirenzepine or methoctramine induced in some cases a transient effect similar to those of atropine. In 3 out of 7 cells, pirenzepine (1 – 3 μM) induced a reduction in GDPs frequency of 40 ± 18 %, while methoctramine (1 μM) induced a reduction of 50% in one out of three neurons. Since ACh is rapidly hydrolyzed by acetylcholinesterase, the following experiments were done in the presence of the acetylcholinesterase inhibitor edrophonium (20 μM). This compound caused an increase in the frequency of GDPs in almost all neurons tested (50/57, Figure 4.19). The mean frequency was 3.42 ± 0.24 GDPs/min in control and 5.76 ± 0.42 GDPs/min in the presence of edrophonium. These values were significantly different ($p< 10^{-5}$). The effect was rapid in onset (2 or 3 min) and was not associated to changes in membrane potential or membrane input resistance. In two cells (out of three analyzed) edrophonium changed the shape of GDPs, increasing their rise time by 10%. As shown in the graph of Figure 4.19, a transient block or a reduction of GDPs frequency occurred upon wash out of the drug. This effect was observed in 7 out of 8 cases, and it may due

to receptor desensitization following accumulation of ACh in the tissue induced by the block of AChE. To see whether this hypothesis was correct, edrophonium was applied in the bath for 12-18 min. In these cases the increase in frequency of GDPs was maintained for the entire period of drug application, ruling out the possibility that the observed block or reduction in GDPs frequency was due to an effect caused by the increased ACh concentration in the tissue. The effect of edrophonium was reproducible since two applications of this drug, separated by 15 min

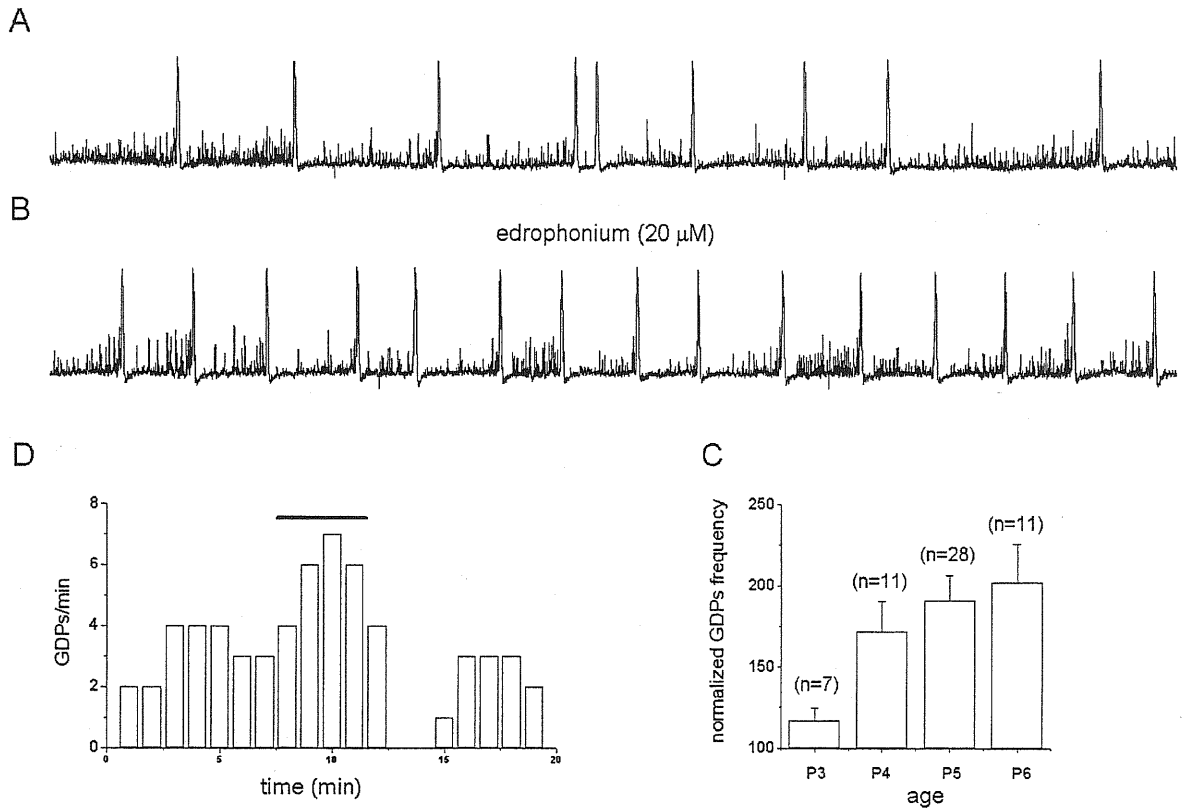

Figure 4.19 Edrophonium enhances GDPs frequency in a developmentally regulated way.
A, B Representative traces from a P5 old CA3 pyramidal cell in control condition (A) and during bath application of edrophonium (B). **C** GDPs frequency of the cell shown in A and B is plotted against time. Each column represents the number of GDPs recorded in 1 min. **D** Mean of normalized GDPs frequency at different postnatal ages. Bars are SEM; n, number of cell tested in each group.

of wash, induced similar effects. When the second application was made in presence of atropine the potentiating effect of edrophonium was prevented (n=2, data not shown).

The effect of endogenous ACh on GDPs frequency was developmentally regulated as shown by the fact that, in edrophonium, the percentage increase in frequency of GDPs varied from 17 ± 8 % at P3 to 102 ± 23 % at P6 (Figure 4.19). This suggests that an increase in cholinergic fibers and/or muscarinic receptors occurs with age.

In another set of experiments the effect of atropine, pirenzepine and methoctramine in antagonizing the action of edrophonium was investigated. Atropine (2 μM) induced a reduction in GDPs frequency of 64 ± 10 % (n=3). This reduction was only transient since after 7-15 minutes GDPs frequency increased again, although it never reached the value measured before atropine application (on average a 15% reduction of GDPs frequency was attained). Like atropine, pirenzepine and methoctramine, in the presence of edrophonium, reduced the frequency of GDPs up to about 50%. The concentrations of pirenzepine and methoctramine that gave 50% of maximum effect (EC_{50}) were 30 and 430 nM, respectively (Figure 4.20). The higher potency

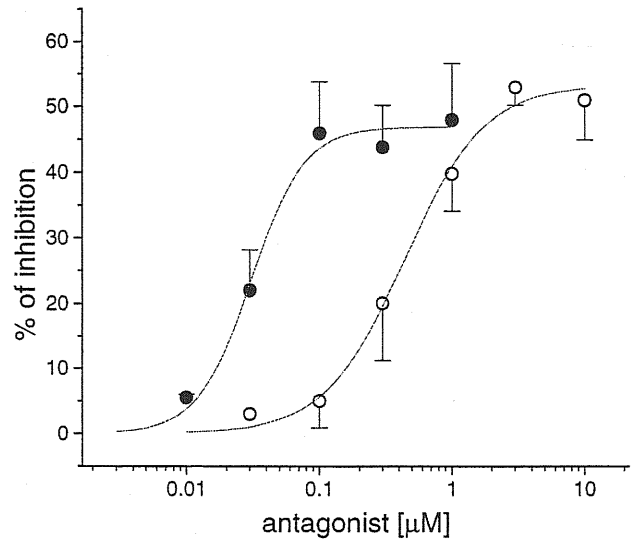

Figure 4.20 The effect of edrophonium is mediated by M1 muscarinic receptor subtype. Percentage of inhibition of GDPs frequency (in edrophonium) induced by increasing concentration of pirenzepine (closed circle) and methoctramine (open) circle. Each point represent the mean of 3-6 experiments, bars are SEM. Data point are fitted with Hill equation: $I(c) = I_{max}/[1+(EC_{50}/c)^n]$, where I is the percentage inhibition, c is the antagonist concentration, I_{max} is the maximal inhibition, EC_{50} is the effective concentration producing half maximum inhibition and n is the Hill coefficient.

of pirenzepine in antagonizing the effects of edrophonium on GDPs frequency in comparison to methoctramine, strongly suggests that M1 subtype of muscarinic receptors are involved in edrophonium action. As for atropine, also the effect of pirenzepine and methoctramine was transient. However, the duration of the effect increased with the concentration of the antagonist used.

4.1.6 Carbachol enhances GDPs frequency

In Figure 4.21 a representative example of the effect of carbachol in a CA3 pyramidal cell at P5 is shown. Carbachol enhanced GDPs frequency in a concentration dependent way. Usually this

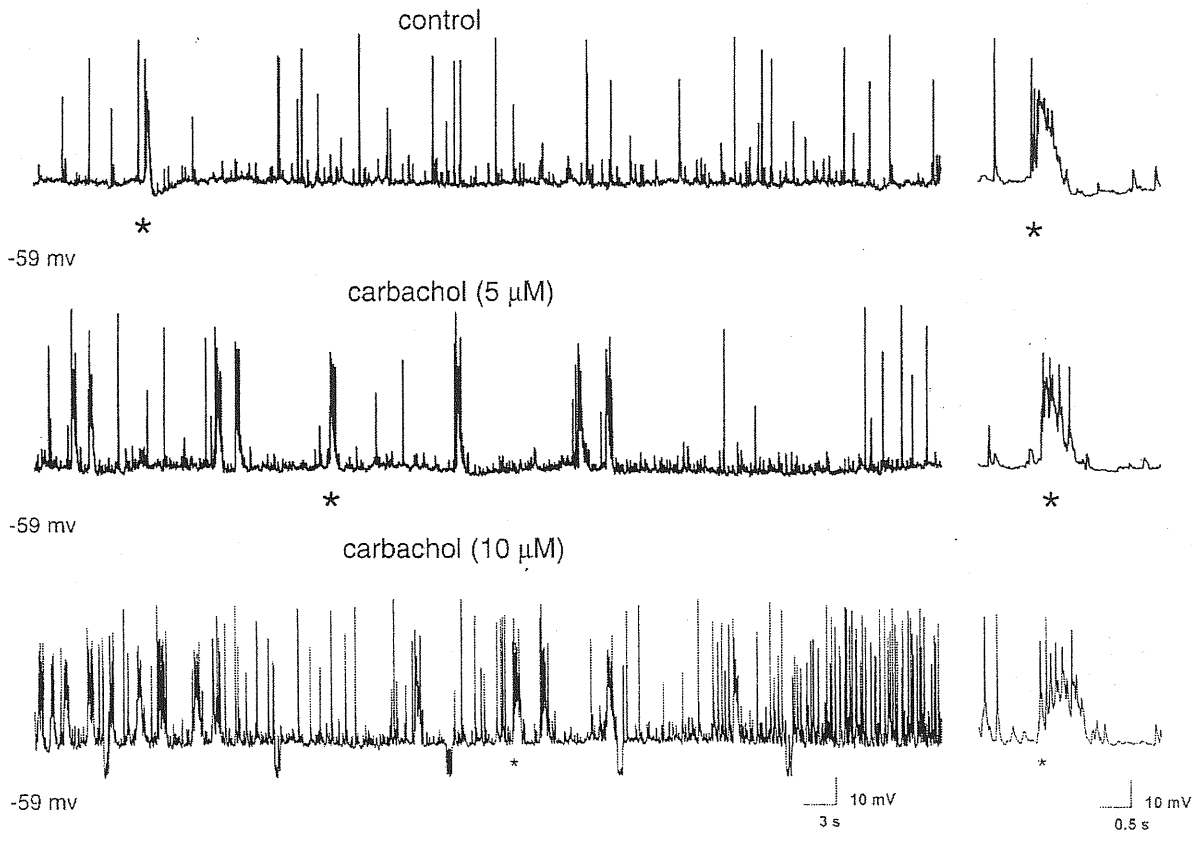

Figura 4.21 Carbachol increases GDPs frequency and changes their shape in concentration dependent way. Example of traces recorded from a CA3 pyramidal neuron at P5 in control condition (top trace) and during application of carbachol 5 μM (midle trace) and 10 μM (bottom trace). GDPs marked with an asterisk are shown on the right in expanded scale. Down deflections are electrotonic potential evoked by injection of steady current through recording electrode

effect was not associated to any change in membrane input resistance. Carbachol (10 μM), induced a transient increase in GDPs followed by an increase in synaptic noise. Carbachol modified also the shape of GDPs that became wider: their amplitude was slightly reduced and the following AHP was abolished (see Figure 4.21).

Since the effect of edrophonium was age dependent, the same concentration of carbachol (3 μM) was applied in slices obtained from P3-P6 old animals (for 2-3 minutes at a membrane potential ranging from -65 to -75 mV). As for edrophonium, the effects of this drug changed markedly during development. At P3-P4, carbachol produced an increase in frequency of GDPs with small (about 2-4 mV) or no changes in membrane potential (Figure 4.22 A). The effect was rapid in

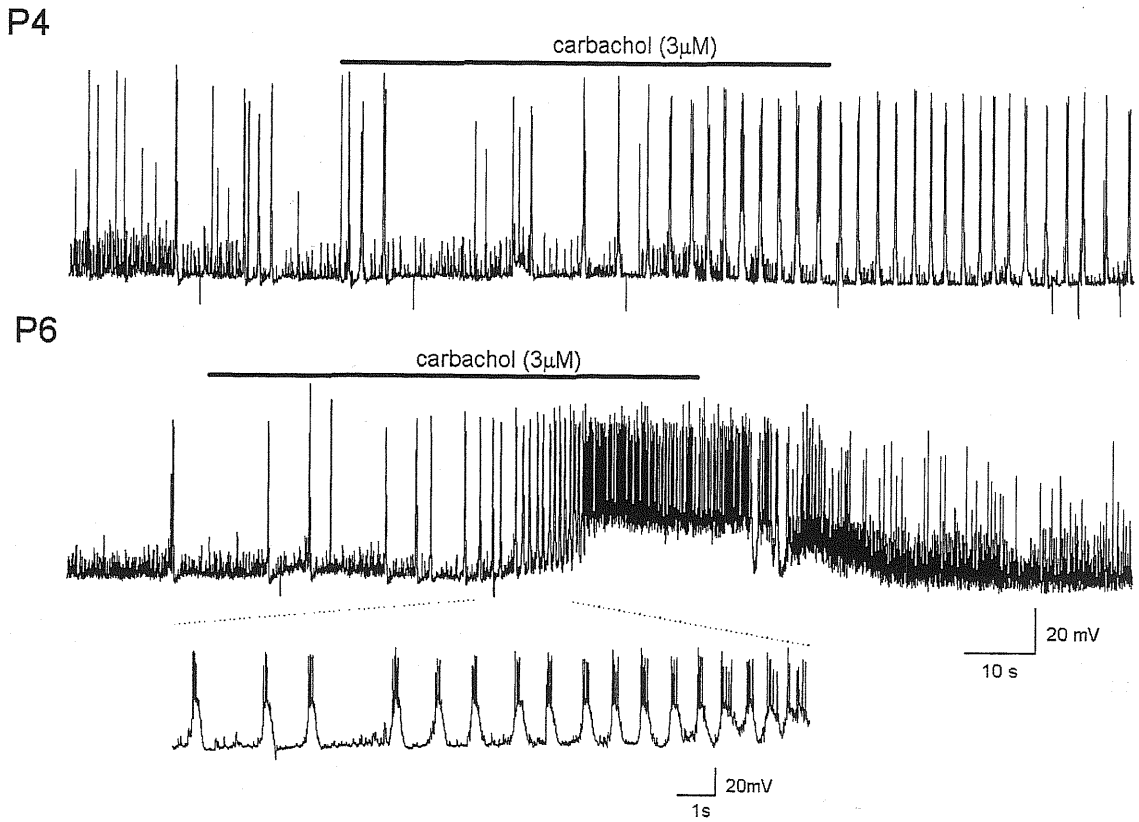

Figure 4.22 Effect of carbachol at different postnatal ages
A Recording from CA3 pyramidal neuron at P4. Bath application of carbachol (bar) induced an increase of GDPs frequency, in the absence of any change in membrane potential. **B** The same concentration of carbachol applied to a CA3 pyramidal cell at P6 induced a transient increase in GDPs frequency followed by a membrane depolarization and an increase in synaptic noise

onset (about one-two minutes after carbachol reached the tissue) and lasted for several minutes after wash out of the drug. After P5, carbachol caused only a transient but elevated increase in GDPs frequency followed, in the majority of the cases, by a membrane depolarization and an increase in synaptic noise. This often gave rise to high frequency action potentials (Figure 4.22 B). Upon wash out of the drug, the membrane potential came back to the resting value, but the increase in synaptic noise persisted for a prolonged period of time (from 1 to 4 minutes). During this period GDPs were usually absent, they started reappearing several minutes after wash. In Table 4.1 the parameters that described carbachol effects at different postnatal ages (ratio between maximum GDPs frequency, during at least 10 s, in the presence of carbachol and mean GDPs frequency in control, membrane depolarization and duration of the period during which GDPs were absent) are quantified. The effects of carbachol were prevented by application of atropine 2 μM (data not shown).

Table 4.1 Parameters describing carbachol effect at different post-natal ages.

	frequency increase	membrane depolarization (mV)	inhibitory period (min)
P3	5.1 ± 0.4 (n=4)	2 ± 2 (n=5)	0 ± 0 (n=6)
P4	6.1 ± 1.1 (n=15)	1.5 ± 1.1 (n=11)	1.7 ± 0.5 (n=11)
P5	8.2 ± 4.3 (n=10)	12.2 ± 3.1 (n=12)	3.5 ± 0.6 (n=9)
P6	10.7 ± 4.8 (n=8)	19.3 ± 2.4 (n=9)	4.7 ± 0.6 (n=8)

Frequency increase expressed as a ration between the maximum frequency during carbachol application and mean frequency during control, membrane depolarization and the period during which GDPs are absent increase with postnatal age. Data are expressed as mean ± SE; n number of experiments

4.1.7 The effects of carbachol on GABA release are mediated by at least two different muscarinic receptor subtypes.

To see whether the effect of carbachol on GDPs frequency were mediated by distinct muscarinic receptors, additional experiments were performed using the selective muscarinic receptor antagonists pirenzepine and methoctramine known to act on M1 and M2 receptors, respectively (Auerbach & Segal, 1996). As shown in the representative example of Figure 4.23, application of pirenzepine (3 μM), prevented the effects of carbachol on GDPs frequency, synaptic noise and membrane depolarization. In contrast, in the same cell, carbachol applied in the presence of the M2 antagonist methoctramine (3 μM) caused an increase in GDPs frequency, which appeared

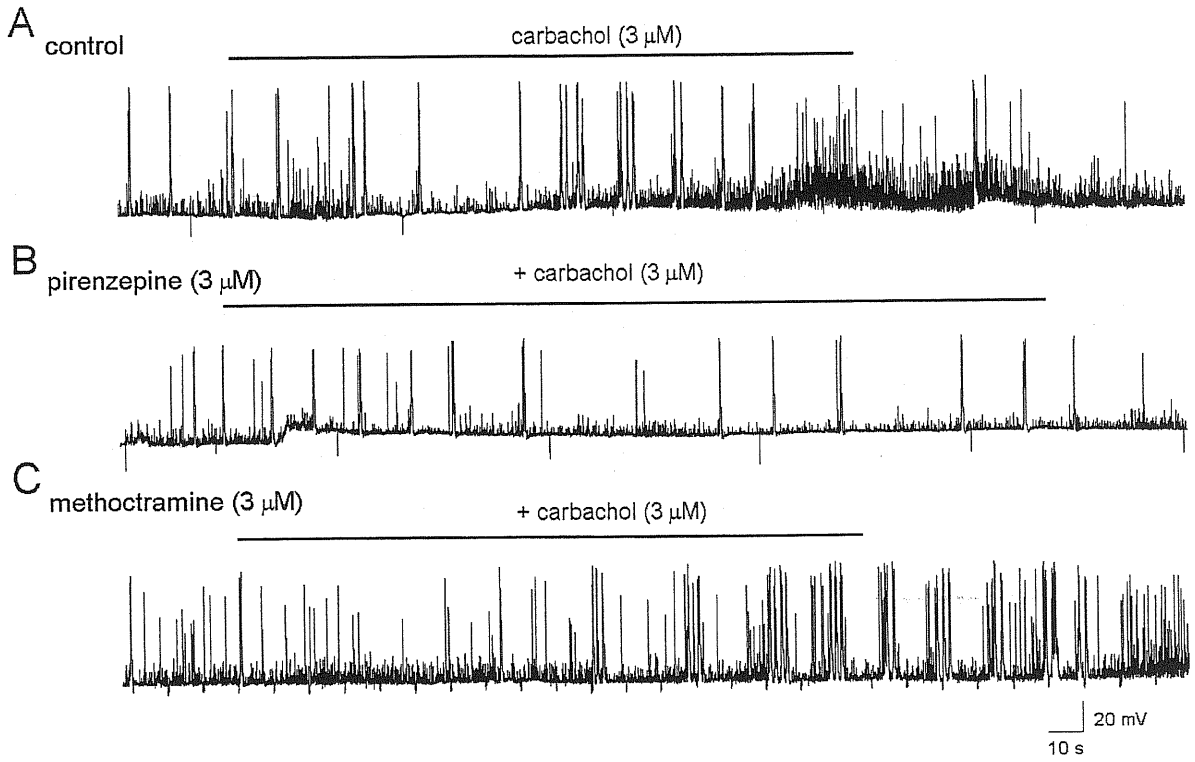

Figure 4.23 Pirenzepine and methoctramine depresses and enhances the action of carbachol respectively. Recordings from the same cell at P4. **A** Application of carbachol (bar) in control conditions induced an increase in GDPs frequency, that often occurred in cluster followed by increase of synaptic noise. **B** Bath perfusion of pirenzepine (3 μM) prevented the effects of carbachol observed in control. In this case carbachol induced a decrease in GDPs frequency. **C** Methoctramine (3 μM) potentiated the effect of carbachol on GDPs frequency. Note that GDPs occurred in clusters.

often grouped in clusters (Figure 4.23). A complete recovery was obtained after wash out of these drugs. Both the effects of pirenzepine and methoctramine were very consistent and could be reproduced in all cells tested (n=4). Pirenzepine always prevented the effects of carbachol. In 3 out of 4 cells this drug reduced the effects of carbachol on GDPs frequency by 50 ± 4%. In contrast during application of methoctramine (3 μM), the effect of carbachol was potentiated. The effect of carbachol was measured as the ratio between the GDPs frequency during application of this drug over that obtained in the absence of carbachol. This ratio in the presence of methoctramine was enhanced (117 ± 4 %). Since the effects of carbachol were quite variable at different postnatal ages and between cells from different slices of the same age, it was impossible to determine the relative EC_{50} values for these drugs. These experiments indicate that carbachol exerts two different effects on GDPs: it increases their frequency through a M1 receptor subtype, while it exerts an inhibitory action *via* a non M1, presumably a M2 receptor subtype.

4.1.8 Carbachol enhances the release of GABA from GABAergic interneurones either directly or indirectly through an action on glutamatergic cells

As already mentioned GDPs appear to be generated by the synergistic action of GABA and glutamate acting mainly on AMPA type of receptors. To see whether the increase in GABA release by carbachol was triggered by glutamate acting on ionotropic types of receptors, carbachol was applied either in the presence of NMDA or non NMDA receptor antagonists.

Superfusion of the NMDA receptor antagonist CPP (20 μM) did not modify the effects of carbachol on GDPs, membrane depolarization and increase in synaptic noise (n=4, Figure 4.24). When carbachol was applied in the presence of kynurenic acid (1mM) or DNQX (10-20 μM), it

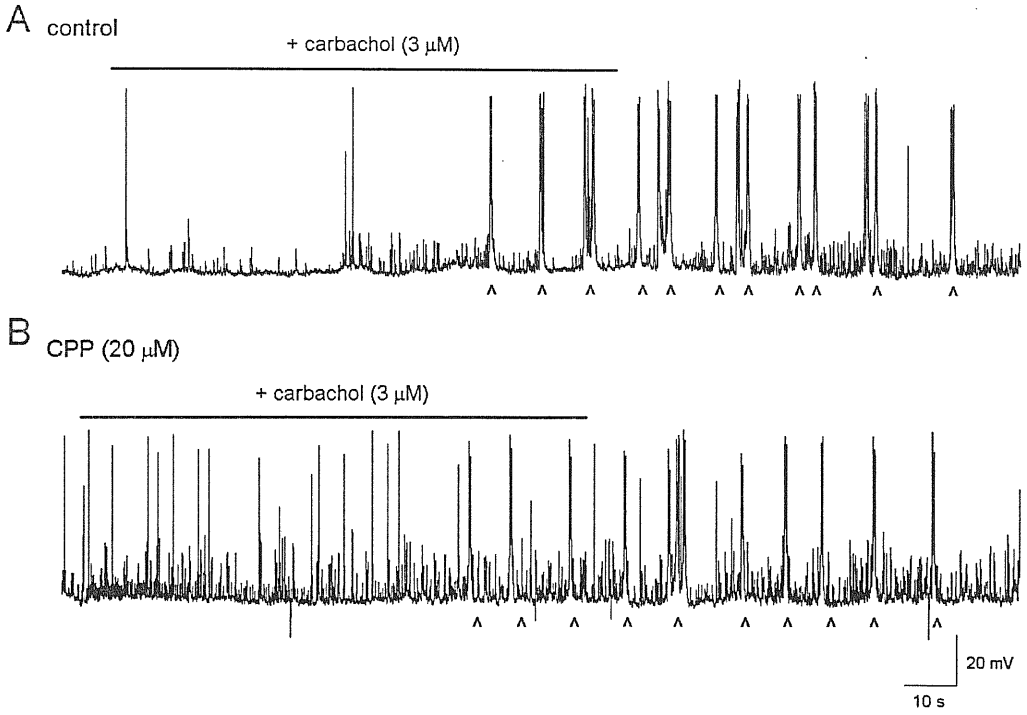

Figure 4.24 CPP does not affect the action of carbachol on GDPs
Recordings from the same cell at P4. Carbachol applied in the bath (bar) induced a similar increase in GDPs (^) frequency in control condition (A) and in the presence of the NMDA receptor antagonist CPP (B).

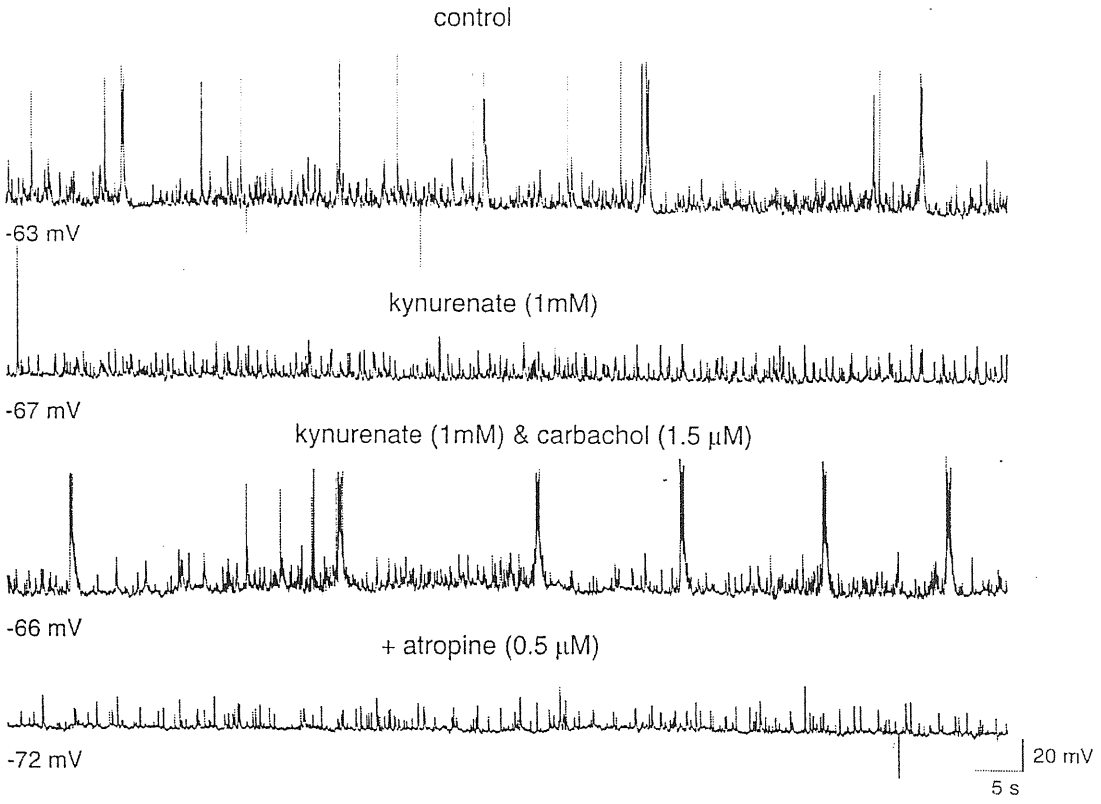

Figure 4.25 Bath application of carbachol in the presence of kynurenic acid induces the appearance of GDPs.
In a P5 old rat bath perfusion of kynurenic acid blocked GDPs. GDPs reappeared after addition of a low concentration of carbachol (1.5 μM, third trace). Bath application of atropine (0.5 μM) prevented the effect of carbachol (bottom trace).

always increased the synaptic noise and in the majority of the cells (6/8) it induced the reappearance of GDPs (Figure 4.25). Atropine (0.5-2 μM) and bicuculline (10 μM) prevented this effect. However, as for AMPA and GABA, carbachol failed to re-induce GDPs when applied in the presence of CNQX (10 μM) or DNQX (20 μM) plus CPP (20 μM) or in the presence of GYKI 53665 (50 μM). An increase in synaptic noise, that often reached the threshold for action potential generation, was observed when carbachol was applied in the presence of GYKI 53665 (Figure 4.26). These data suggest that carbachol control GABA release

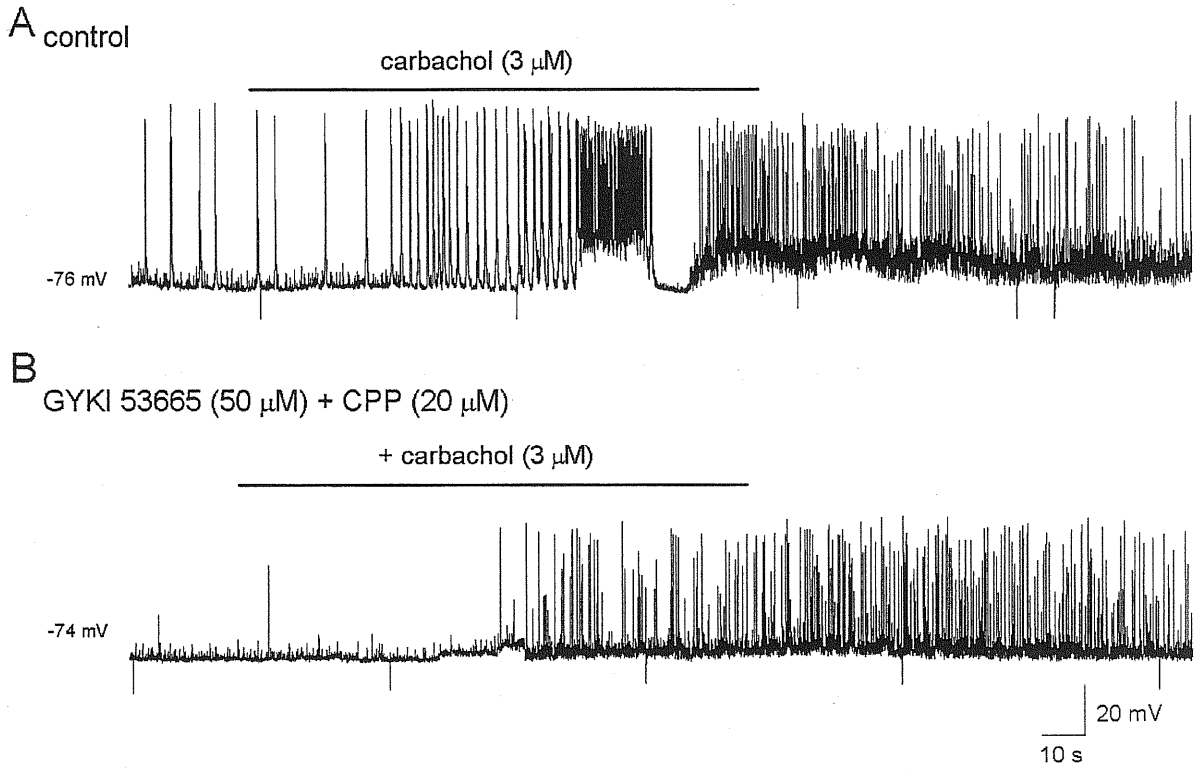

Figure 4.26 The effects of carbachol on GDPs and mebrane depolarization are prevented by GYKI 53655 and CPP.
Effect of carbachol applied in the bath (bars) at P5 in control condition (A) and during superfusion of GYKI 53665 plus CPP (B). Note that in the presence of glutamate ionotropic receptor antagonists carbacholwas still able to increase spontaneous GABAergic synaptic noise and firing rate.

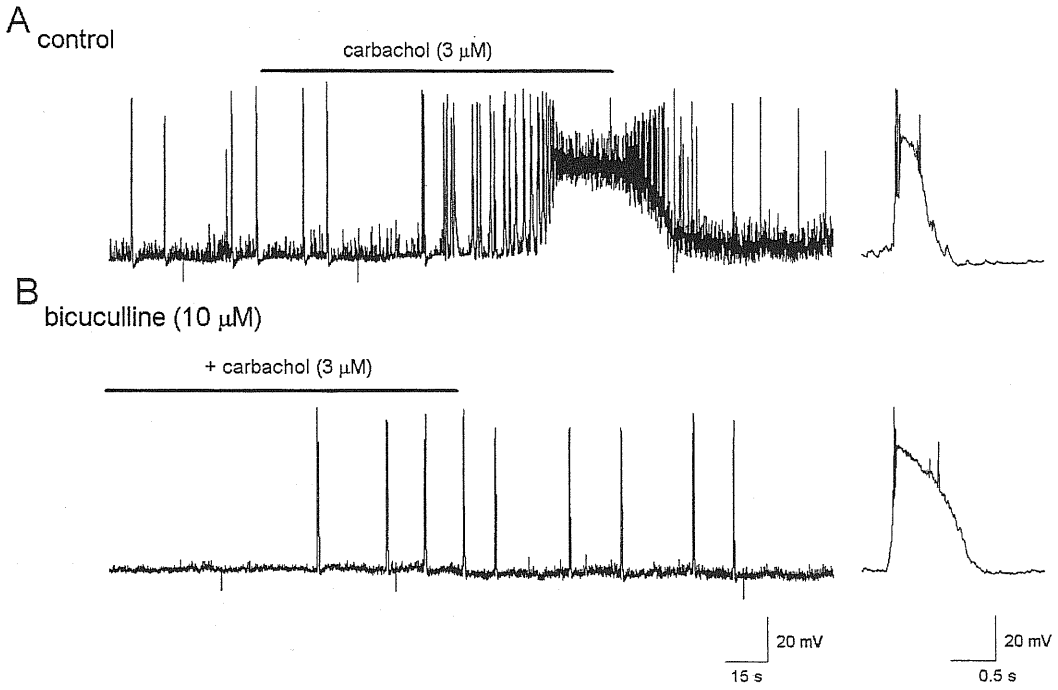

Figure 4.27 The effect of carbachol on GDPs and membrane depolarization are prevented by bicuculline. Effect of carbachol applied in the bath (bars, at P6) in control condition (A) and during superfusion of bicuculline (B). Note that in bicuculline carbachol induced interictal-like discharges whose shape (shown in the right at an expanded time scale) was different from GDPs

either indirectly through an action on the glutamatergic drive to interneurons (GDPs frequency and membrane depolarization) or directly through an action on GABAergic cells (spontaneous synaptic noise).

Carbachol-induced increase in frequency of GDPs, spontaneous ongoing synaptic noise as well as membrane depolarization were prevented by bath application of bicuculline (10 μM, Figure 4.27). When bicuculline was applied in P4-P6 slices for more that 5 minutes, often (n=5/7), induced the appearance of interictal bursts. These occurred at the frequency of 0.06-0.72 events/min. In contrast to GDPs that reversed near the reversal potential for Cl^-, they changed polarity at around 0 mV, independently from the chloride concentration in the pipette solution,

indicating that they were due to ionotropic glutamate receptors activation. In agreement with previous reports (Psarropoulou & Dallaire, 1998) carbachol increased the frequency of interictal bursts in a dose dependent manner (Figure 4.28) and it reduced their amplitude. Interictal bursts were blocked by CNQX (10 μM), indicating that they were due to the action of glutamate on AMPA/kainate receptor types. As already reported (Psarropoulou & Dallaire, 1998) the potentiating effects of carbachol on interictal bursts triggered at P5-P8 by bicuculline, was prevented by pirenzepine, indicating an action on M1 receptor subtypes (Figure 4.28).

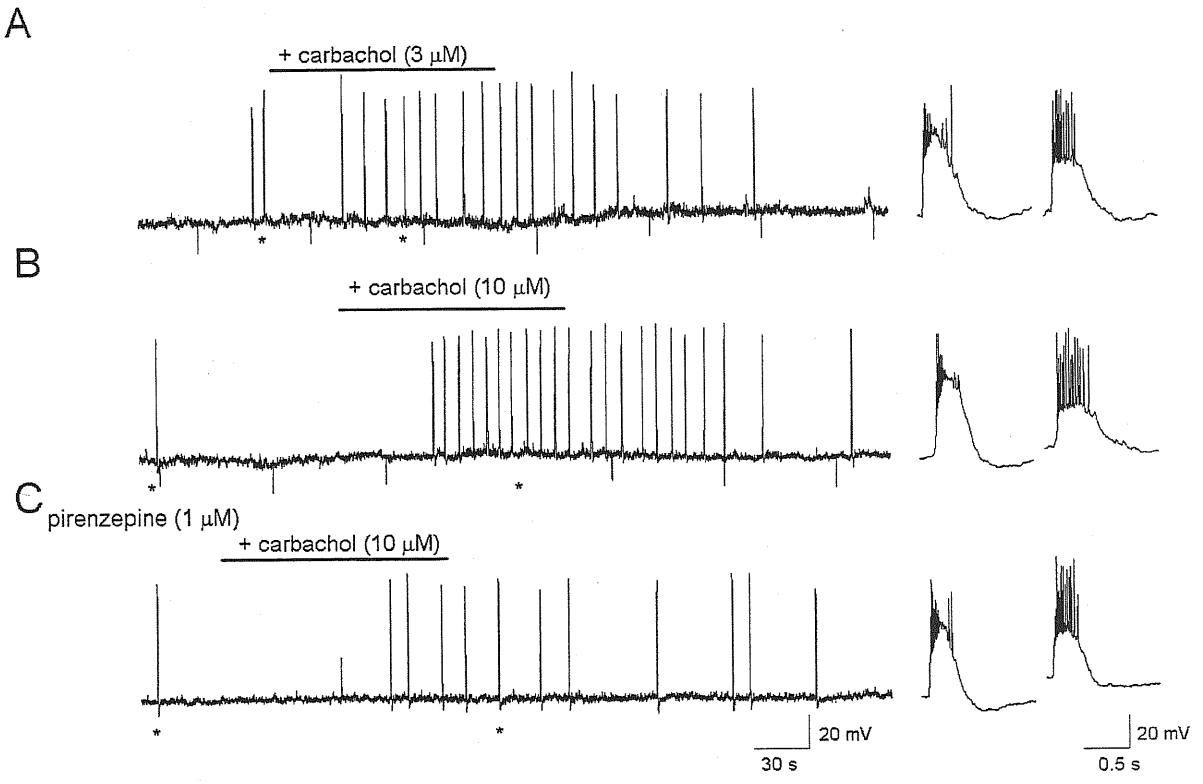

Figure 4.28 Carbachol enhances interictal discharges recorded in bicuculline (at P6)
A and **B** Carbachol enhaced interictal bursts recorded in bicuculline in a concentration dependent way. **C** This effect was partially antagonized by pirenzepine (1 μM).
On the right interictal bursts recorded before and during carbachol application are shown on an expanded time scale

It is interesting to note that, in our experimental conditions, we failed to observe direct postsynaptic effects of ACh on principal cells such as the slow cholinergic EPSP and/or carbachol-induced membrane depolarization or a change in membrane resistance in the presence of TTX. This may be due to the loss of some intracellular factor during cell dialysis, after breaking into the whole cell configuration. In age-matched experiments, using conventional microelectrodes, carbachol-induced membrane depolarization associated to a decrease in membrane conductance could be easily observed in the presence of TTX (data not shown).

4.2 Cholinergic function in the hippocampus of Nerve Growth Factor (NGF) deprived animals

The septohippocampal pathway originates in the basal forebrain (BF) from the medial septal and the diagonal band of Broca nuclei. This projection provides the main cholinergic input to the hippocampus. One characteristic of basal forebrain neurons is their dependence on NGF for their survival and maintenance. Antibody studies have confirmed the role of endogenous NGF in the maintenance of the cholinergic phenotype of BF neurons. However, the functional consequences of this NGF-dependent regulation are not known. To investigate at the cellular level the role of NGF deprivation on the cholinergic function in the hippocampus, one of the target areas of BF neurons, endogenous NGF was neutralized by implanting αD11 hybridoma cells (which secrete monoclonal antibodies specific for NGF) into the lateral ventricle of rats at different postnatal ages. Control rats were injected with parental myeloma cell line, P3U. It has been shown that endogenous NGF blockade results in a reduction of BF ChAT immonoreactive neurons in newborn but not in adult rats (Holtzman et al, 1995; Vantini et al., 1987). Therefore the antibodies injections were performed at different postnatal ages to study whether the possible

effects of NGF on the cholinergic function are developmentally regulated. The level of antibodies present in the hippocampus and cortex was assessed by ELISA in the same animals used for immunohystochemical or electrophysiological experiments. One, two or three weeks after the injection, immunohystochemical experiments were performed to test the sensitivity of BF neurons to NGF deprivation. The cholinergic function in the hippocampus was assessed by electrophysiological experiments performed in the CA1 and CA3 area. ACh release, following electrical stimulation of hippocampal slices was also measured one or two weeks after antibodies injection.

4.2.1 ELISA experiments allow to detect anti-NGF antibodies in injected animals

The presence of anti-NGF antibodies in the tissue was investigated performing ELISA analysis on proteic extracts of cortices and hippocampi of hybridoma injected animals.

In all cases, one or two weeks after the injection, αD11 monoclonal antibody levels were in the range of ng/mg, independently from the age of the injection (Table 4.2). No significant differences were observed between samples from regions ipsi and controlateral to the injection site. These data indicate that after one week, the diffusion of the antibodies is quite homogenous throughout the entire brain. It is important to note that one week after the injection, the antibody

Table 4.2 Levels of anti-NGF anibodies

Age	*hippocampus*	*cortex*
P15-P18 (P2)	1.3 ± 0.4 (n=11)	2.5 ± 1.3 (n=13)
P21-P24 (P15)	1.1 ± 0.8 (n=7)	2.3 ± 0.6 (n=7)

ELISA method was used to detect the levels of anti-NGF antibody (expressed in ng/mg of tissue) in the hippocampus and cortex in rats implanted with αD11 cells (day of implantation in brackets). The experiments were performed at P15-P18 and at P21-P24 (n = number of animals).

level was similar in animals injected at P2 or at P15. Thus the diffusion of antibodies from the lateral ventricle to the parenchyma does not change at the different postnatal ages tested. No major difference in αD11 levels was observed between the first and the second week after the injection. The level of antibodies was in vast molar excess over the level of endogenous NGF reported in the cortex and hippocampus (Nishio et al., 1992; Korsching, 1986).

4.2.2 Immunohystochemical analysis of ChAT positive cells in BF neurons

The number of ChAT positive cells was evaluated in the basal forebrain of αD11 and myeloma injected rats. When animals were injected at P2, a large reduction in the number of ChAT positive neurons was observed one week later in rats injected with hybridoma cells respect to controls (Fig 4.29). In the septum, this effect was stronger than in the diagonal band (reduced by 71% and 57% respectively; table 4.3). Two weeks after the injection, there was a decrease of the effects of NGF deprivation: a 39% decrease of ChAT positive neurons was found in the septum whereas no differences were found in the diagonal band. After three weeks no differences could be detected between NGF-deprived animals and controls (Fig 4.30).

Table 4.3 Number of ChAT positive cells in the medial septum and diagonal band of αD11- and P3U-treated animal

Age of perfusion/ Age of injection	SEPTUM		DIAGONAL BAND	
	P3U	**αD11**	**P3U**	**αD11**
P9/P2	229 ± 25	66 ± 22 **	363 ± 20	157 ± 34 **
P15/P2	208 ± 34	126 ± 24 *	289 ± 36	276 ± 13
P24/P2	195 ± 14	183 ± 44	195 ± 14	183 ± 44
P15/P8	237 ± 30	196 ± 10	309 ± 25	302 ± 24
P22/P15	211 ± 40	207 ± 10	255 ± 40	265 ± 26

Density of the ChAT positive cells (cell/mm^2) counted in the medial septum and in the diagonal band in αD11- and P3U- rats. Data are expressed as mean ± standad deviation and are obtained from three animals for each group. Asterisks indicate the statistical significant differences (* $p<0.05$, ** $p<0.01$).

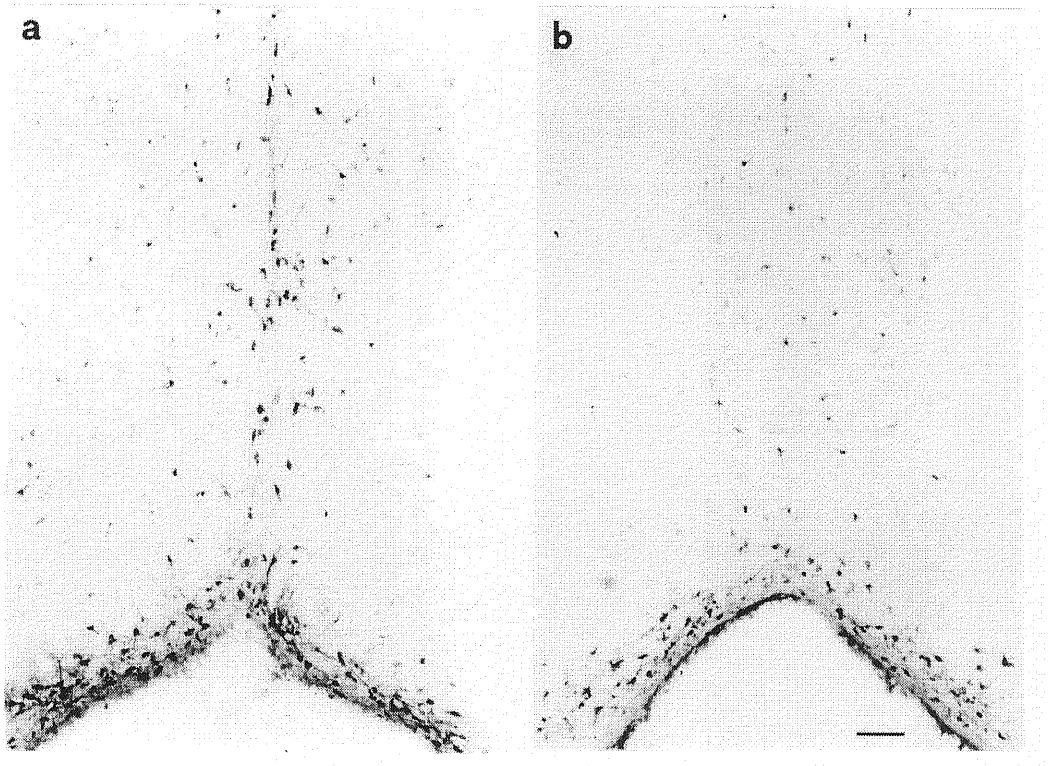

Figure 4.29 Immunohistochemistry of ChAT positive cells in the septal complex of 9 days old rats implanted with myeloma or hybridoma cells at P2.
a Labelled neurons in control rats implanted with myeloma cells. **b** Labelled neurons in rats implanted with hybridoma cells. The number of ChAT neurons in rats implanted with anti-NGF producing cells is decreased with respect to the control. Scale bar in (b) 90 μm.

When the soma size of ChAT positive neurons was analyzed, it was found that one week after the injection (at P2), the soma of the residual ChAT positive cells was smaller in NGF deprived animals respect to controls, both in the septum and in the diagonal band. Two weeks later, although there was less shrinkage, this effect was still present. Three weeks after the injection the shrinkage was present only in the diagonal band. The medians of the mean distributions of ChAT positive cells soma size data obtained from αD11- and P3U-treated animals are illustrated in Table 4.4. Summarizing (Tables 4.5), in the septum both the number of ChAT positive neurons, as well as their soma size, showed a complete recovery to control values, three weeks after the

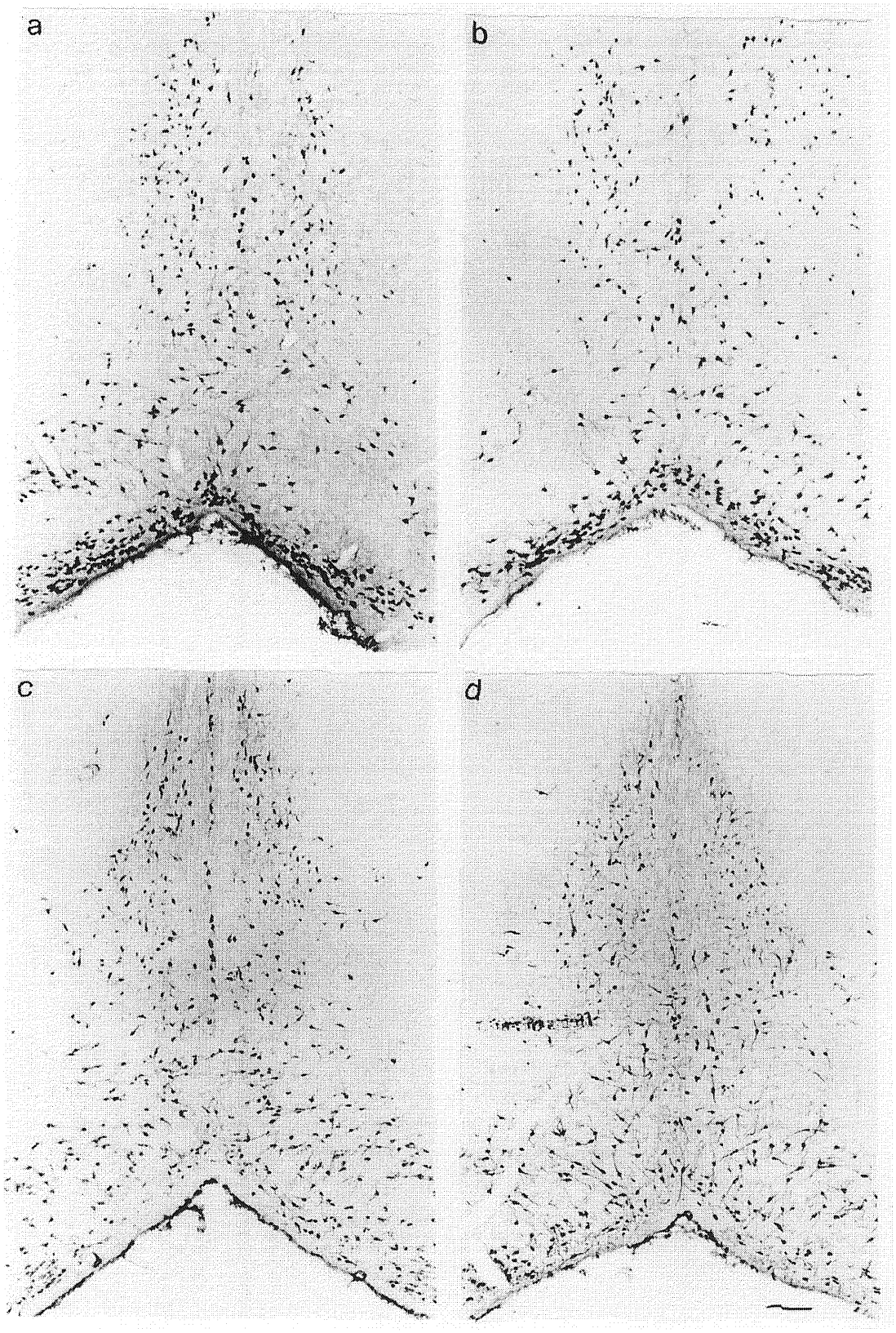

Figure 4.30 ChAT immunoreactive cells in the septal complex of rats implanted with myeloma and hybridoma cells at P2.
a and **b** Labelled neurons in the septal complex of P15 rats implanted with myeloma cells (a) or hybridoma cells (b). **c** and **d** Labelled neurons in the septal complex of P24 rats implanted with myeloma cells (c) or hybridoma cells (d). Note the small reduction of the density of ChAT positive cells only in the septum of P15 rats. Three weeks after the injection at P2 no differences in the ChAT positive cells density were observed. (scale bar 200 mm)

Table 4.4 Median of cells soma size distribution in the septum and diagonal band of αD11- and P3U-treated rats

Age of perfusion/ Age of injection	SEPTUM		DIAGONAL BAND	
	P3U	**αD11**	**P3U**	**αD11**
P9/P2	87	50	106	86
P15/P2	100	85	142	125
P24/P15	102	99	127	131

Median of a soma size distribution of pulled data. Data are expressed in μm^2, n=3 for each group of animals. Note that there is an evident shrinkage in animal injected at P2 and sacrificed one week later, in this age the index shrinkage is 27and 25 for septum and diagonal band, respectively. One week later, the shrinkage is less evident. The index shrinkage is reduced to 15 for the septum and 17 for the diagonal band

injection of the antibodies at P2, in spite of the continuous presence of αD11 antibodies. To determine whether this recovery was due to the time between the injection and the experiments, animals were injected at P8 and at P15 and analyzed one week later. At P15 (in rats injected at P8), the only difference found between NGF-deprived and control animals was a shrinkage in the neurons of the diagonal band, while at P21 (injected at P15) no differences between control and αD11-treated rats were detected. These results indicate that the recovery in the effects of NGF deprivation observed three weeks after the injection were not due to the time elapsed between the

Table 4.5 Summary of the effects of endogenous NGF neutralization on BF cholinergic neurons

Age of perfusion/ Age of injection	SEPTUM		DIAGONAL BAND	
	ChAT + cells	shrinkage	ChAT + cells	Shrinkage
P9/P2	+++	+++	++	+++
P15/P2	+	+	-	+
P24/P2	-	-	-	+
P15/P8	-	-	-	+
P22/P15	-	-	-	-

The differences between NGF deprived and control animals for different postnatal ages are summarized. The injection of hybridoma cells in the lateral ventricle of the rat affects the soma size and the number of ChAT positive cells only during the first two postnatal weeks. The effects of the injection at P2 are almost completely recovered three weeks after the injection.

injection and the experiments. These data suggest that the αD11 treatment affects the number and the soma size of ChAT positive neurons in BF during the first postnatal week and to a lesser extent during the second one. It can be concluded that this treatment exerts a transient and reversible effect on cholinergic BF neurons.

4.2.3 Cholinergic function in the hippocampus assessed by electrophysiological experiments

Most of the electrophysiological experiments were performed in rats injected at P2 and sacrificed at P15-P18. This age range was chosen as a compromise between the development of cholinergic fibers, which is almost complete after two postnatal weeks and the effects of NGF deprivation on BF neurons. Acetylcholine released from septo-hippocampal fibers exerts a complex modulatory role on hippocampal cell excitability through its action on different membrane conductances. At this age, the effects of NGF deprivation on the cholinergic function in the hippocampus was investigated in CA1 hippocampal neurons on a variety of responses. These included: i. passive and active membrane properties; ii. responses that resulted from the activation of cholinergic fibres such as slow EPSPs or block of accommodation of spike discharge; iii. responses evoked by the direct activation of both pre or postsynaptic muscarinic receptors with carbachol.

In view of immunohystochemical data showing that the maximum effect of NGF deprivation on BF neurons occurred one week after the injection (at P2), slow EPSPs evoked by stimulation of cholinergic fibers were tested in the CA1 region of the hippocampus also in this animal group. Moreover, since GABA-mediated GDPs, which occur synchronously over the entire hippocampus of neonatal animals have been shown to be modulated by endogenous ACh, in parallel experiments, GDPs frequency was analyzed in the CA3 area of NGF-deprived animals.

To conclude, in view of immunohistochemical experiments showing that BF cholinergic neurons

are sensitive to NGF regulation only when NGF is neutralized during the first two postnatal weeks, we also examined whether neurons in slices from rats injected at P15 and sacrificed at P21 exibited a different sensitivity of CA1 pyramidal cells to applied carbachol.

4.2.3.1 Rats implanted with αD11 or P3U cells at P2 and sacrificed at P15-P-18

Passive and active membrane properties of CA1 pyramidal cells.

As shown in Table 4.6, no significant ($p>0.5$) changes in resting membrane potential or input resistance were found in CA1 pyramidal neurons from slices obtained from αD11 or P3U treated animals. Single action potentials were elicited by brief (10 ms) depolarizing current pulses from a membrane potential close to the resting level (from -60 to -70 mV). Parameters such as spike threshold, amplitude, duration, and area were measured in cells from both experimental groups. Figure 4.31 shows examples of action potentials elicited in CA1 pyramidal cells from αD11 or P3U treated animals. As indicated in the figure, the threshold for action potential generation and

Table 4.6 Basic membrane properties and spike parameters in P15-P18 cells from P3U or αD11 treated rats

	P3U	*αD11*
Resting membrane potential (mV)	-66 ± 0.97 (n=17)	-66 ± 1.2 (n=16)
Input resistance (MΩ)	46 ± 4.4 (n=13)	54 ± 5.2 (n=13)
Spike threshold (mV)	-58 ± 0.72 (n=17)	-58 ± 0.71 (n=18)
Spike amplitude (mV)	83 ± 1.73 (n=12)	81 ± 1.4 (n=15)
Spike duration (ms)	1.7 ± 0.06 (n=11)	1.9 ± 0.07 (n=11) *
Spike area (ms·mV)	62.5 ± 1.8 (n=11)	68.3 ±'1.9 (n=11) *

P3U and αD11treated animals show identical passive membrane properties. Action potentials have same threshold and amplitude but different duration and area. Spike duration was measured at baseline.

* significantly different ($p<0.05$; *t*-test)

spike amplitude was approximately the same in both experimental conditions. However a small but significant ($p<0.05$) increase in spike duration (measured at baseline) and area was found in αD11-treated neurons as compared to P3U-treated cells (Table 4.6 and Figure 4.31).

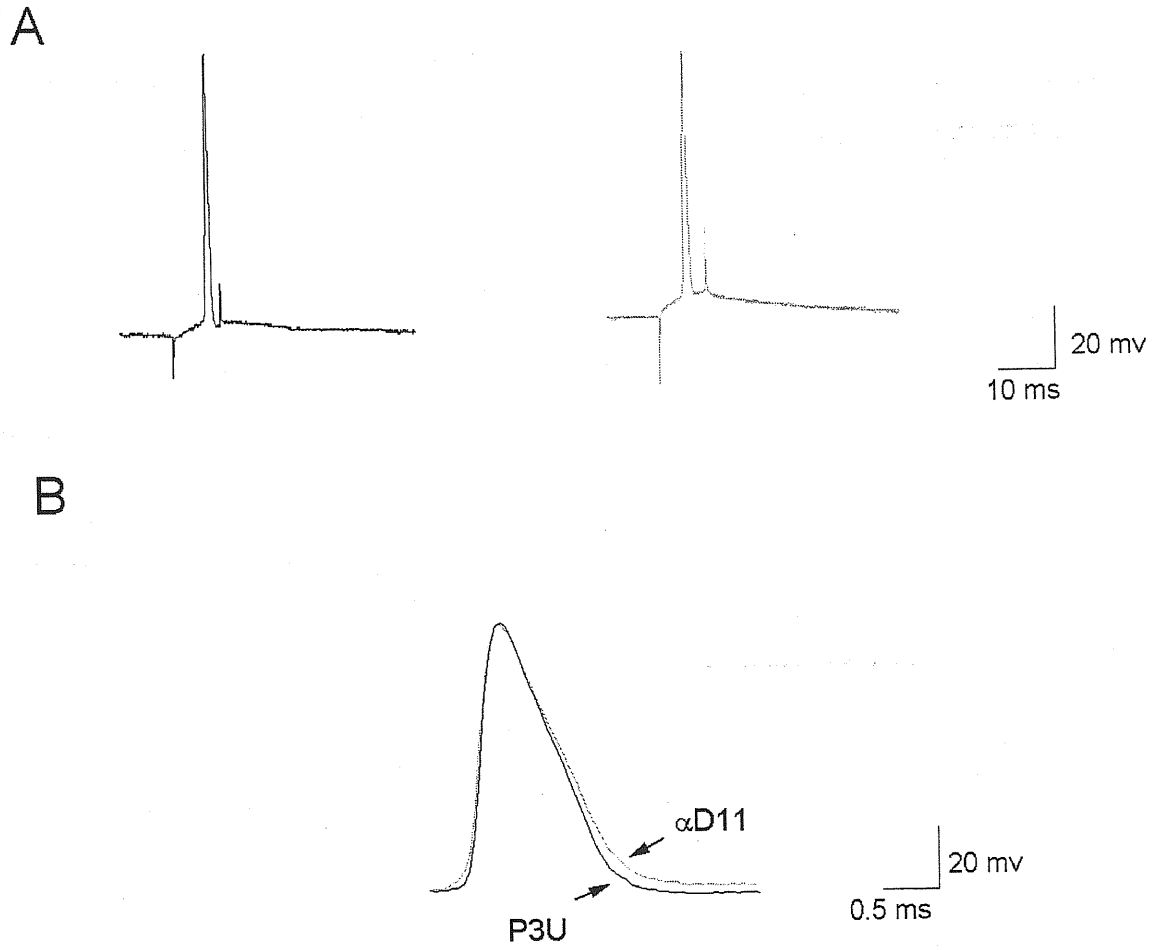

Figure 4.31 Spike broadening in αD11-treated animals.
A Action potentials elicited in P3U or αD11 rats by depolarizing current pulses of 0.2 and 0.4 nA (10 ms duration) respectively. Holding membrane potentials were -63 mV for P3U and -67 mV for αD11 cells. **B** The action potentials represented in A are superimposed. Animals were implanted at P2 and sacrificed at P15.

Slow EPSPs and changes in spike accommodation induced by stimulation of cholinergic fibers

In order to see whether chronic NGF deprivation could affect endogenous release of acetylcholine from septo-hippocampal fibres, repetitive stimulation was delivered to the stratum oriens, a region rich in cholinergic fibres. This pattern of stimulation has previously been shown to induce a slow depolarization and an increase in cell excitability, that are selectively enhanced by the cholinesterase inhibitor eserine and blocked by the muscarinic antagonist atropine (Cole and Nicoll, 1984). Slow EPSPs (n=14 in αD11 and n=13 in P3U cells) were highly variable from cell to cell in terms of amplitude and duration, probably because of differences in resting membrane potential, number of fibres stimulated, or distance between recording and stimulating electrode. In spite of this variability, slow EPSPs could be elicited in both experimental groups.

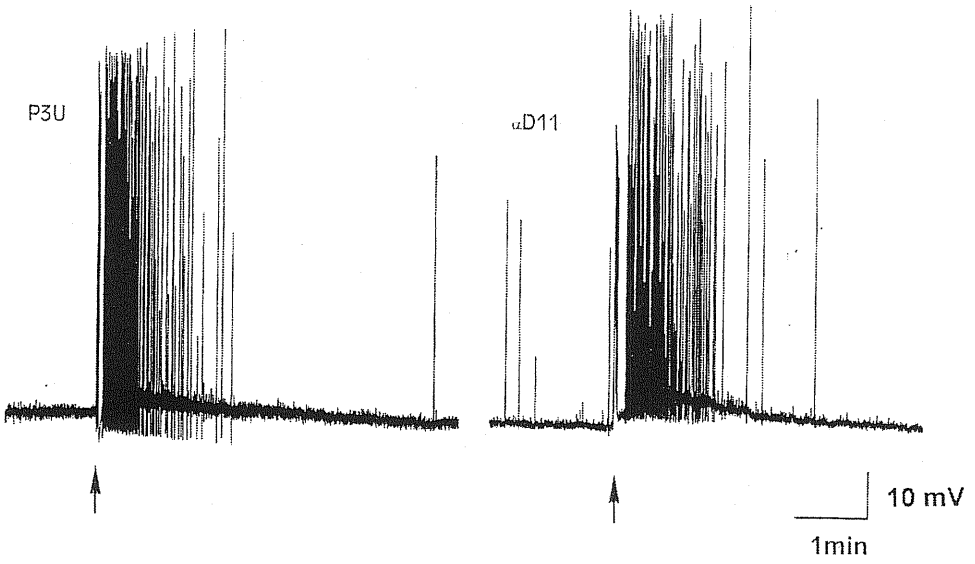

Figure 4.32 P3U and αD11-treated animals exhibit similar slow EPSPs.
Examples of slow EPSPs elicited in P17 (P3U) and P16 (αD11) neurons by repetitive stimulation (20 Hz 2.5 s, arrows) of cholinergic fibres in stratum oriens, in the presence of 3 μM eserine. Membrane potentials are -59 mV in P3U and -65 mV in αD11. Spikes display different amplitude as a consequence of digitization.

As shown in the example of Figure 4.32, repetitive stimulation of the stratum oriens (of slices obtained from both αD11- and P3U-treated animals) from a resting membrane potential ranging from -55 to -65 mV, induced a slow membrane depolarization (from 2 to 6 mV) associated to an increase in synaptic noise and cell firing that lasted for 1 to 2 minutes. These responses were markedly enhanced by 8-10 min pre-incubation with the cholinesterase inhibitors eserine (3 μM, n=17) or echothiophate (300 nM, n=5). In 5 cases (2 αD11 and 3 P3U cells), we failed to observe any slow EPSP in response to stratum oriens stimulation.

Acetylcholine released upon stimulation of cholinergic fibres has also profound effects on accommodation of spike discharges evoked by long depolarizing current pulses and on the slow afterhyperpolarization that follows the end of the pulse (Cole and Nicoll, 1984). We therefore

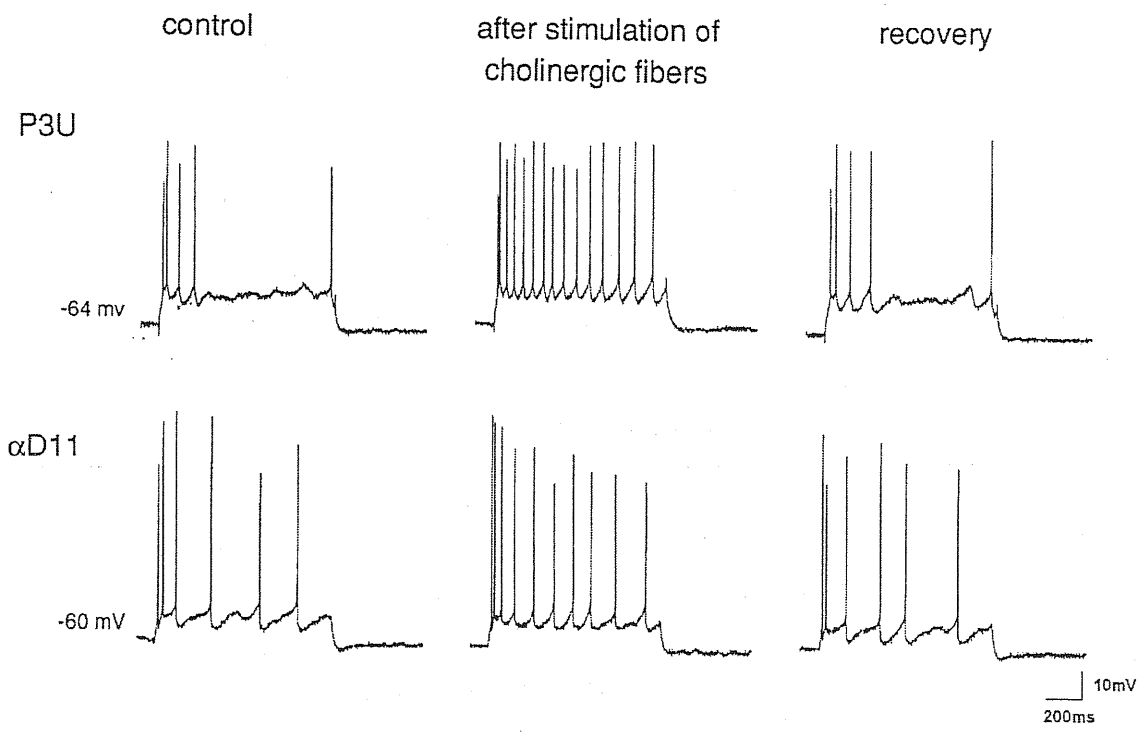

Figure 4.33 Attenuation of spike discharge accommodation in αD11-treated animals.
Spike discharge elicited by intracellular injection of depolarizing current pulses (800 ms duration) in control condition, 10-15 s after repetitive stimulation (20 Hz, 2.5 s) of cholinergic fibers, and 5 min later (recovery) in P3U and αD11-treated animals. Note that in control conditions, spike discharge accommodation was less evident in αD11 than in P3U cells. However, a more effective reduction in spike accomodation (following the cholinergic fibres stimulation) was obtained in P3U rather than in αD11-treated rats. Electrodes were filled with K-methylsulfate.

examined whether these effects could still be observed in cells from αD11-treated animals. As illustrated in the representative example of Figure 4.33, the cholinergic-induced change in spike frequency adaptation was less evident in cells from αD11-treated animals, as compared to P3U. In the absence of tetanic stimulation, accommodation of spike discharge, evoked by 800 ms depolarizing current pulses, was evaluated in ten cells by calculating the ratio between the number of spikes present in the first 200 ms and the total number of spikes: this value was 0.75 ± 0.06 (n=6) in cells from P3U and 0.55 ± 0.03 from αD11-treated rats (n=4). These values were significantly different ($p<0.05$; *t*-test). After tetanic stimulation, spike discharge accommodation was attenuated in both experimental groups. However, the degree of attenuation of spike discharge was higher in P3U than in αD11 cells. The ratio after the train was reduced by 52 % in cell from P3U implanted rat (0.36 ± 0.03, n=3), whereas only a 14% of reduction was observed in NGF deprived animal (0.47 ± 0.04, n=3). The increased number of spikes during the depolarizing current pulse was associated with a decrease in amplitude of the slow afterhyperpolarization that followed the end of the pulse.

Responses evoked by the direct activation of postsynaptic muscarinic receptors with carbachol.

In the presence of TTX (1 μM), bath application of carbachol produced (in both αD11 and P3U treated animals) a membrane depolarization, from a potential of -68 to -62 mV, associated with a decrease in membrane conductance. The decrease in membrane conductance persisted after repolarizing the membrane potential to its resting value. The conductance decrease induced by carbachol (3 μM) was 22 ± 6 % (n=6) and 44 ± 7 % (n=6) in P3U- and αD11-treated slices, respectively. These value were significantly different ($p<0.05$, *t*-test). The effects of carbachol could be seen at concentrations as low as 300 nM and were dose-dependent (Figure 4.34). With

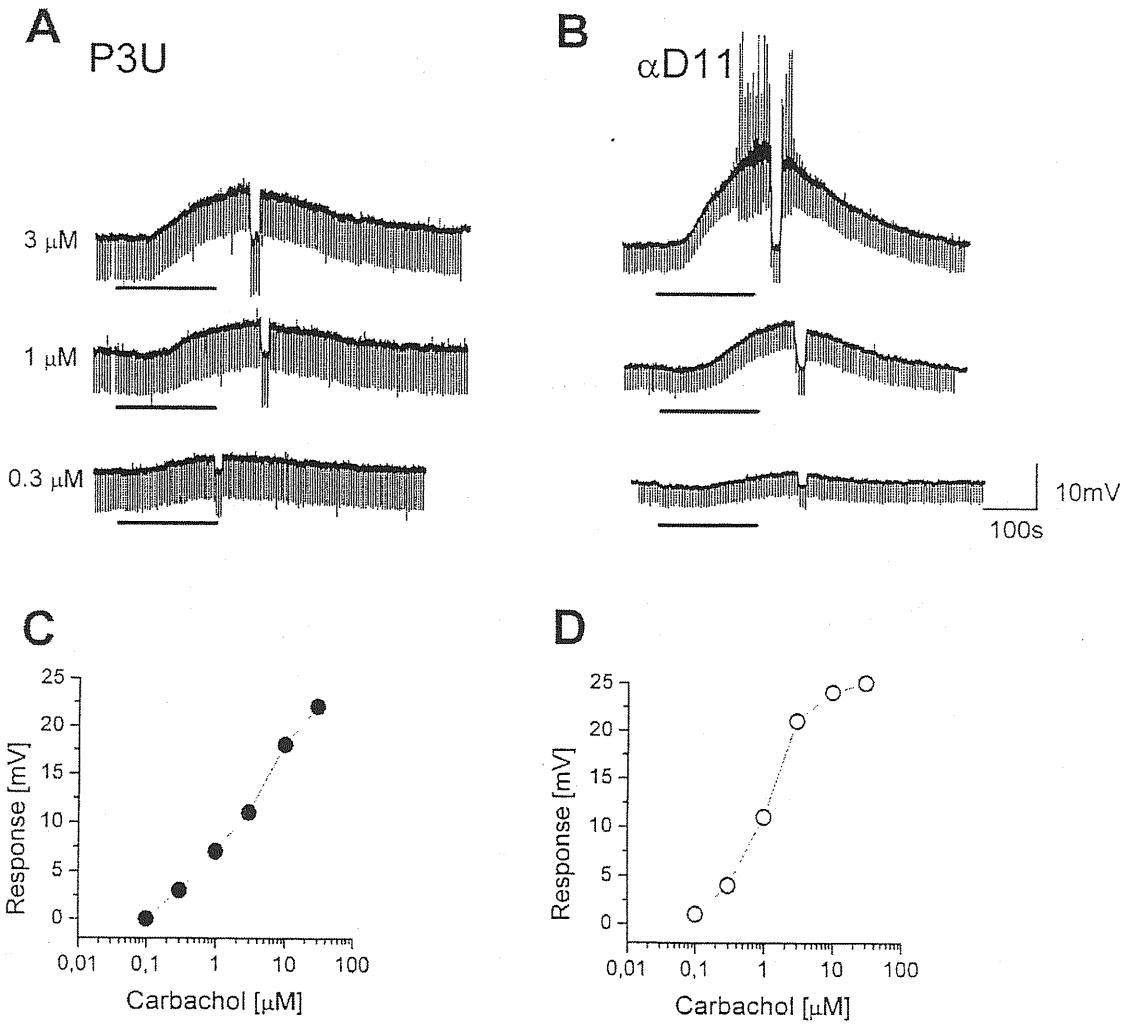

Figure 4.34 Increased sensitivity to carbachol in cells from αD11-treated animals.
A and **B** Bath application of increasing concentrations of carbachol (bars) in the presence of TTX (1 μM) in P3U- (A) and αD11- (B) treated animals. Downward deflections are electrotonic potentials resulting from the injection of a fixed current pulse through the recording electrode. Upward deflections in B are calcium action potentials. Resting membrane potential is -62 mV in A and in B. In **C** and **D** dose response curves for carbachol of cells shown in A and B, respectively. Note that the same concentration of carbachol induced larger response in αD11-treated rats

higher concentrations of the agonist, the membrane depolarization increased and reached the threshold for calcium action potentials generation. Pooled data of the effects of carbachol are shown in Figure 4.35. As shown in the graph, αD11-treated cells exhibited higher sensitivity to carbachol than P3U-treated cells, as demonstrated by the shift to the left of the dose/response

curve. The EC_{50} values for carbachol (estimated by non-linear regression fit to data) were 1.8 μM and 3.8 μM for αD11 and P3U cells, respectively. The Hill coefficient however, did not change between the two experimental groups (the n value was 1.1 and 1.2 for αD11 and P3U cells, respectively).

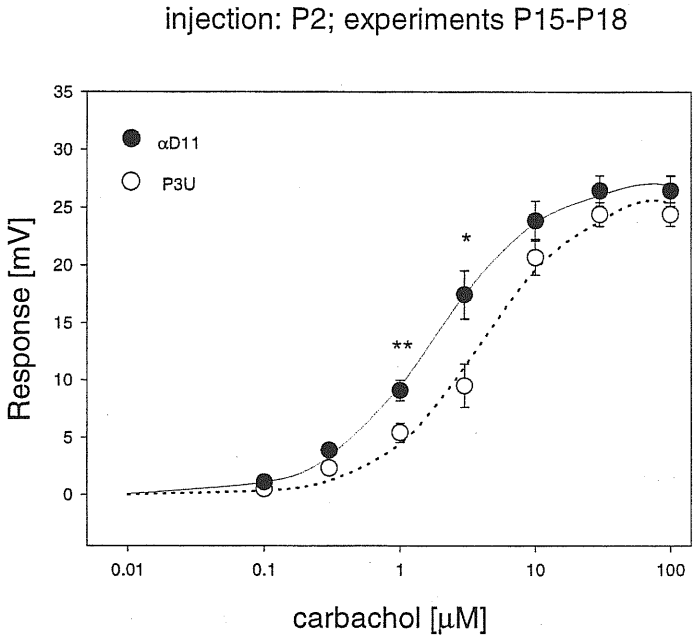

Figure 4.35 Dose-response curves to carbachol in NGF deprived and control animals.
Data points are the mean values of responses to carbachol obtained from 5-16 experiments in slices from animals implanted with αD11 or P3U cells at P2 and sacrificed at P15-P18. Bars indicate SEM. The curves are fitted with the Hill equation: $V(c) = V_{max}/[1+(EC_{50}/c)^n]$, where V is the amplitude of the response, c is the agonist concentration, V_{max} is the maximal response, EC_{50} is the effective concentration producing half maximum response and n is the Hill coefficient.
$^{*}p<0.05$; $^{**}p<0.01$ (unpaired *t*-test).

Extracellular recordings

In order to assess whether chronic NGF deprivation could also affect the function of presynaptic muscarinic receptors, which control the release of glutamate from presynaptic nerve terminals

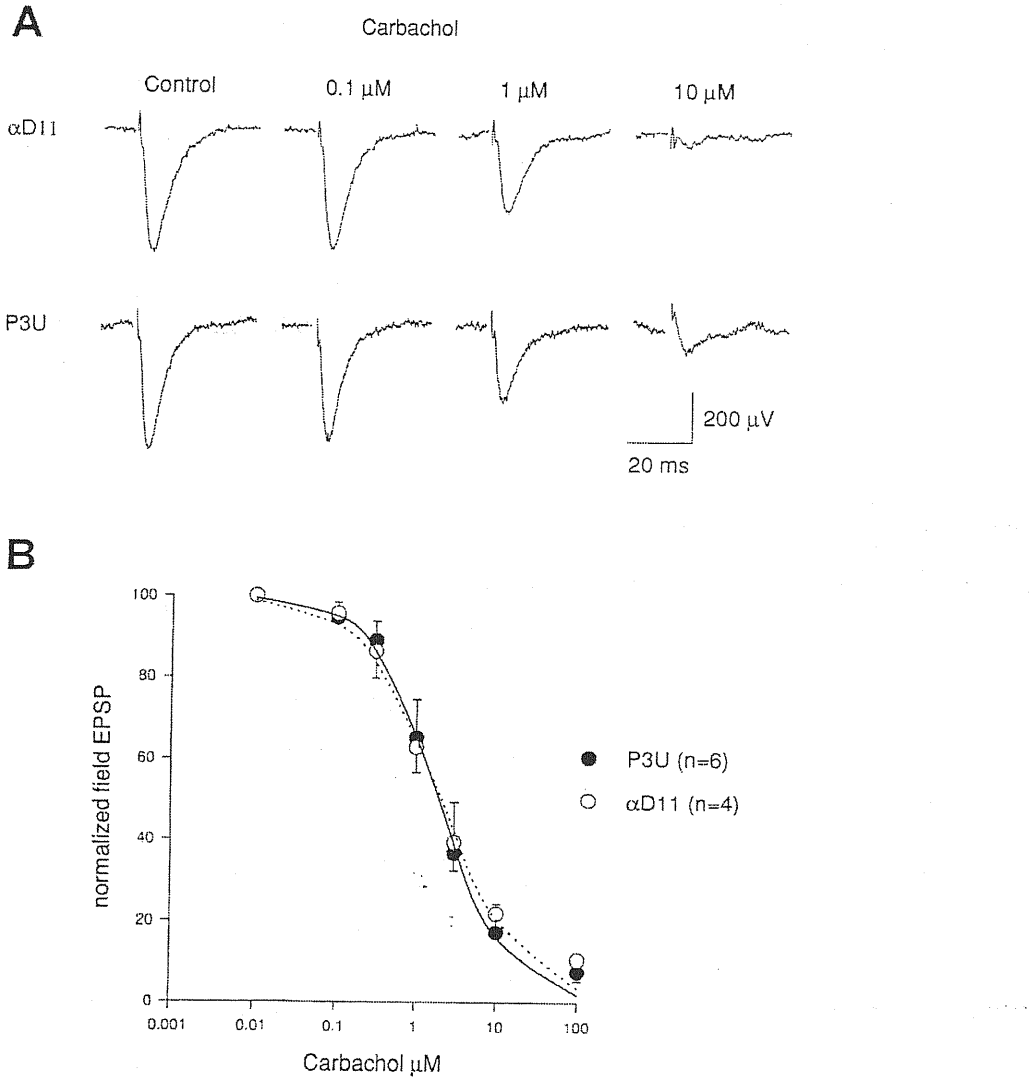

Figure 4.36 Carbachol induces a similar depression in amplitude of the field EPSP in both P3U- and αD11-treated animals.
Field EPSPs evoked in stratum radiatum by stimulation of the Schaffer collaterals in control conditions or in the presence of increasing concentration of carbachol. B. Dose response curve for the inhibitory action of carbachol on the field EPSPs in slices from P3U or αD11-treated animals. Each point is the mean of 4-6 experiments; bars are SD. Data points are fitted with the Hill equation.

(Hounsgard, 1978; Valentino and Dingledine, 1981), field EPSPs evoked by Schaffer collateral stimulation were recorded in the stratum radiatum of CA1 pyramidal neurons in the absence or in

the presence of carbachol. In agreement with previous studies, we found that superfusion of increasing concentrations of carbachol (from 0.1 to 100 μM) induced a concentration-dependent depression in the amplitude of the field EPSPs. This effect, similar to that reported by Sheridan and Sutor (Sheridan and Sutor, 1990), is considered to be presynaptic in origin. However, no significant differences ($p>0.5$, *t*-test) were detected between carbachol data groups obtained in αD11 and P3U treated rats (estimated EC_{50} values were 1 μM and 0.8 μM respectively, Figure 4.33).

4.2.3.2 Rats implanted with αD11 or P3U cells at P2 and sacrificed at P6-P11

In slices from rats implanted with αD11 cells at P2 and sacrificed one week later, GDPs were still present over the entire hippocampus. However, their frequency in the CA3 hippocampal region was significantly ($p<0.05$) lower than in controls. The mean frequency was 1.7 ± 0.32 GDPs/min (n=8) in NGF deprived animals and 3.3 ± 0.33 GDPs/min in controls (n=31).

In another set of experiments in slices from the same group of animals, the possibility to evoke slow EPSPs by stimulation of the cholinergic fibers was tested in the CA1 hippocampal region. As shown in Figure 4.37 (A1), in control conditions (P3U treated rats), the electrical stimulation of the cholinergic fibers in stratum oriens induced changes in neuronal excitability in 6 out of 8 cells. These changes consisted in increase in synaptic noise (lasting 3-7 min) associated to brief membrane depolarizations with superimposed fast action potentials. These effects were due to ACh acting on muscarinic receptors since they were enhanced by eserine (3 μM) and selectively blocked by atropine (10 μM). In one case, a slow EPSP with characteristics similar to those found in cells from P15-P18 animals was detected. In contrast, in αD11-treated rats (n=10), the

tetanic stimulation of cholinergic fibers failed to evoke responses, except for one case in which an increase in synaptic noise was observed.

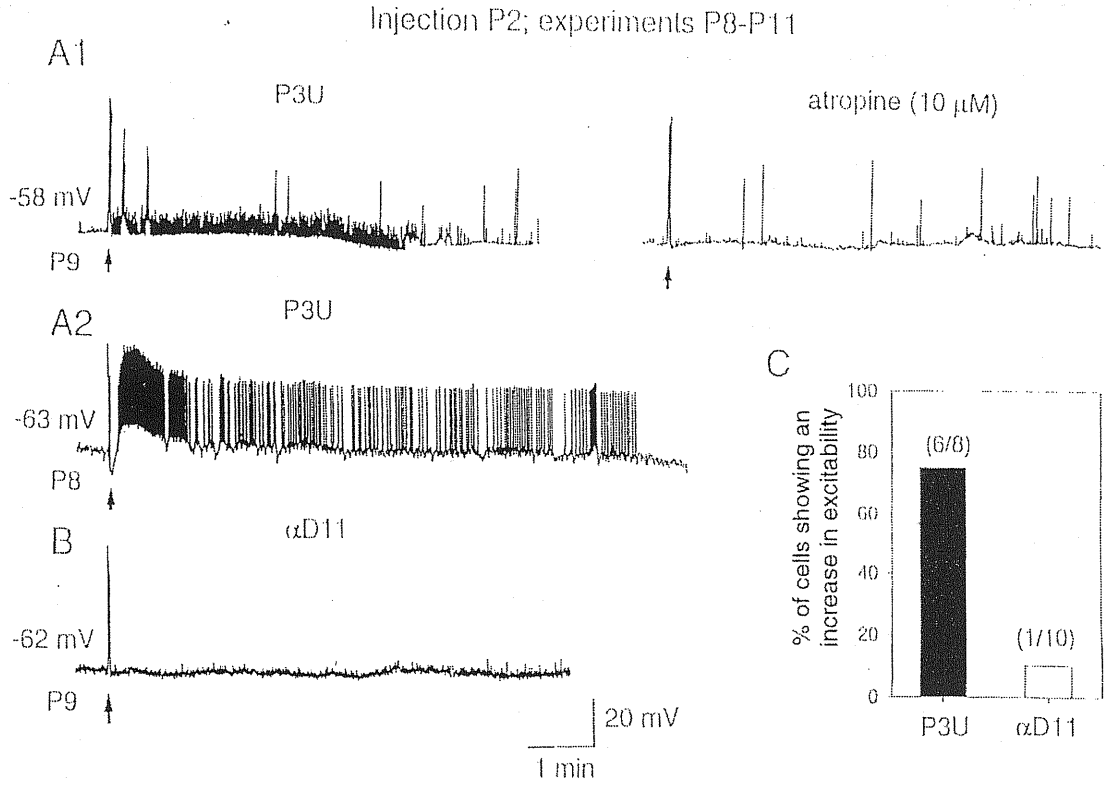

Figure 4.37 Increased cells excitability induced in P8-P9 CA1 pyramidal cells by stimulation of cholinergic fiber only in slices from P3U but not in *αD11*-treated animals.
A Tetanic stimulation of cholinergic fibers (arrows), in the presence of eserine (3 μM) induced brief membrane depolarizations with fast action potentials associated to a long lasting enhancement in synaptic noise (A1 left), effect was blocked by atropine (A1 right). In A2 the tetanic stimulation induced a slow EPSP. **B** Tetanic stimulation failed to induce a response in a cell from *αD11*-treated animal. **C** Each column represents the percentage of cholinergic responses (out of the total number of cells tested) obtained in P3U and *αD11* rats following a tetanus in the stratum oriens between P8 and P11

4.2.3.3 Rats implanted with αD11 or P3U cells at P15 and sacrificed at P21-P24

Unlike the results obtained in the group of animals implanted at P2 and sacrificed at P15 in which an increased sensitivity of principal cells to carbachol was found, in this group of animals, no significant differences ($p > 0.5$) in carbachol sensitivity between P3U (n=8) and αD11-treated

animals (n=9) were observed (Figure 4.38). Estimated EC_{50} values were 0.7 and 0.9 in αD11 and P3U treated animals, respectively. As expected from immunohistochemical experiments, the tetanic stimulation of the stratum oriens induced slow EPSPs with similar characteristics in both controls and αD11-treated rats.

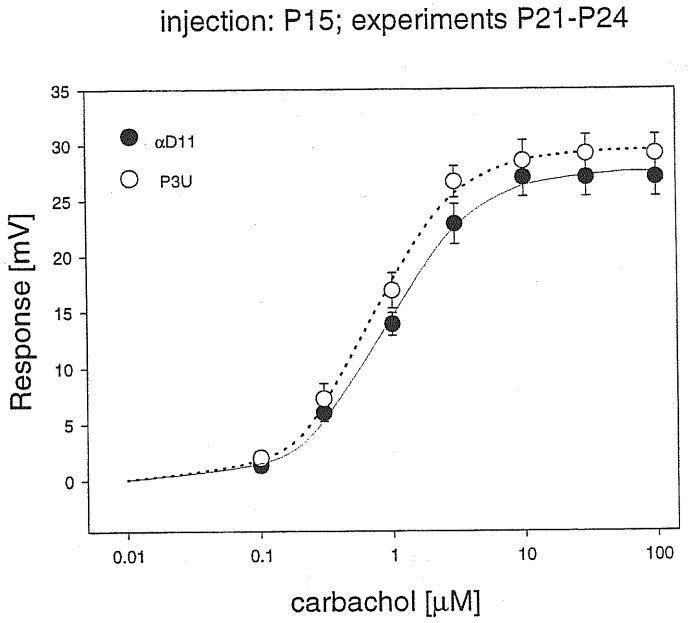

Figure 4.38. Dose-response curve to carbachol in P21-P24 αD11- or P3U-treated animals.
Dose-response curves to carbachol in slices from animals implanted with αD11 or P3U cells at P15 and sacrificed at P21-P24. Data points are the mean values obtained from 6-9 experiments. Bars indicate SEM. The curves are fitted with the Hill equation (see Figure 4.32 for comparison).

4.2.4 Releasing studies

In agreement with electrophysiological and himmunohistochemical experiments, the effect of electrical stimulation (2 Hz for 5 min) on ACh release was significantly smaller ($P<0.05$) in hippocampal slices from rats implanted with αD11 cells at P2 and sacrificed at P15-P18, in comparison with slices from P3U-treated rats (Table 4.7). In contrast, no differences ($P>0.5$)

were detected between the two experimental groups when αD11 cells were implanted at P15 and the animals were sacrificed at P21 (see Table 4.7).

In rats implanted at P2 and sacrificed a week later, successful experiments were obtained only in two cases (out of 6) for control and NGF-deprived animals. In these cases a clear reduction in the effect of stimulation on ACh release was found (about 50%)

Table 4.7 acetylcholine release from NGF-deprived and control animals

	P3U	*αD11*
P15-P18 (P2)	6.0 ± 0.9 (n=8)	3.1 ± 0.7 (n=9) *
P21-P24 (P15)	8.3 ± 1.9 (n=5)	9.0 ± 1.8 (n=7)

ACh release (pg/mg/min ± SEM) from electrically stimulated hippocampal slices from P3U or αD11 treated rats at P15-P18 (implanted at P2) and P 21-P24 (implanted at P15).
* Significantly different ($p<0.05$; *t*-test).

5. Discussion

The main findings of the present study are:

- GDPs need AMPA receptors activation for their induction. NMDA receptors play only a modulatory role but are not essential for their induction
- Achetylcoline through activation of muscarinic receptors (probably M1) positively modulate GDPs in a developmentally regulated way. The muscarinic agonist carbachol produces both an up and down regulation of the release of GABA, assessed as GDPs. These effects are due to the activation of M1 and non-M1 (possible M2) muscarinic receptors, respectively.
- In NGF deprived animals, in comparison to control, a significant reduction in GDPs frequency is observed during the first postnatal week. This may be due to a reduction in the ACh released from the septohippocampal pathway. Moreover in this period the slow cholinergic EPSP could not be evoked. Later on, at P15, an increase in the sensitivity of the postsynaptic response to carbachol is observed. This may reflect a compensatory mechanism for the loss of cholinergic innervation.

5.1 Role of ionotropic glutamate receptors in GDPs modulation

5.1.1 Role of AMPA receptors in GDPs generation

The role of AMPA and NMDA receptors in the generation of GDPs has been investigated in pharmacological experiments using selective NMDA and non-NMDA receptor antagonists. AMPA/kainate receptors activation was necessary for GDPs induction as proved by the observation that non-NMDA receptors antagonists were fully effective in blocking spontaneous GDPs. An interesting finding was that in the presence of conventional AMPA/kainate receptors

antagonists, GDPs could be still evoked by focal stimulation. Moreover spontaneous GDPs could be re-induced by application of GABA or KCl. Surprisingly they could also be reinduced by application of AMPA, even if CNQX and DNQX were used at concentrations known to block the non-NMDA component of EPSPs recorded in pyramidal cells and interneurons of adult rats (Isa et al., 1996; Neuman et al, 1988). It is possible that in our conditions, the antagonist is competitively displaced by the concentration of AMPA used. The displacement may be also induced by glutamate released by the depolarizing action of GABA during GDPs as shown by the fact that AMPA effects were abolished in the presence of bicuculline and that, in the presence of CNQX and DNQX, GDPs could be re-induced by GABA or KCl. The concentration of glutamate released during GDPs may be very high, because of the simultaneous activity of a population of cells. The fact that in double recording experiments (with KF or KCl) in the presence of kynurenic acid it is still possible to re-induce spontaneous GDPs with GABA or to evoke GDPs by focal stimulation only in the cell recorded with KCl electrode (but not with KF, in which the GABAergic component is abolished) indicates that AMPA receptors are fully blocked in pyramidal cells but not in interneurons.

The strongest evidence in favor of an essential role of AMPA receptors in GDPs generation is provided by the experiments in which the more selective AMPA receptor antagonist GYKI 53655 was used. In these experiments it was shown that GDPs were blocked and could not be re-induced by AMPA or GABA. Also the electrical stimulation was ineffective in evoking GDPs. This antagonist does not act on $GABA_A$, NMDA or metabotrobic glutamate receptors (Ouardouz and Durand, 1991). It is similar to GYKI 52466 but is more potent and does not affect kainate receptors. Moreover, unlike CNQX or DNQX, this compound is not competitive and therefore its

block is independent of agonist concentration (Donevan and Rogawski, 1993; Zorumski et al., 1993).

Kainic and domoic acid were not able to re-induce the appearance of GDPs in the presence of GYKI 53655, excluding the possibility that kainate receptors are involved in GDPs induction. After blockade of AMPA receptors with GYKI 53655, kainate has been reported to inhibit evoked GABAergic responses by presynaptic mechanisms in adult CA1 pyramidal cells (Clarke et al., 1997; Rodriguez-Moreno et al., 1997). Since GYKI 53655 is selective for AMPA receptors and does not block kainate receptors, it can not be excluded that, when AMPA receptors are already blocked, glutamate exerts an inhibitory action through kainate receptors thus preventing the re-induction of GDPs. Experiments using more selective kainate receptor agonists and antagonists (Clarke et al., 1997) would be useful in clarifying the role of this receptor in GDPs regulation.

5.1.2 Contribution of NMDA receptors to GDPs

In previous reports (Ben-Ari et al., 1997, Kazipov et al., 1997) it was proposed that NMDA receptors play a fundamental role in GDPs generation. In the present experiments NMDA antagonists only produced a transient reduction, or occasionally a transient block, of GDPs frequency (see also Gaiarsa et al, 1991). In contrast to the present results, in the CA1 region it has been recently shown (Garaschuk et al., 1998) that both CNQX and AP-5 block calcium transient associated to GDPs. Although a block of calcium oscillations does not necessary imply a block of membrane depolarization associated to GDPs (calcium could flow through NMDA channels, but see also Leinekugel et al., 1997), differences between CA1 and CA3 areas can not be excluded. The low efficacy of NMDA receptors antagonists in blocking GDPs in the CA3

region can be attributed to the lack of functional NMDAR1 subunits in the stratum lucidum (Watanabe et al., 1998, Siegel et al., 1994). .This may explain also the lack of one NMDA-dependent form of LTP at the mossy fibre-CA3 synapse (Watanabe et al., 1998, Siegel et al., 1994).

NMDA receptors contribute to network synchronization as proved by the possibility to prevent GDPs re-induction (by GABA or AMPA in the presence of CNQX and DNQX) by AP-5. It is conceivable that, in the presence of AMPA/kainate receptor antagonists, partially active AMPA receptors, would provide the membrane depolarization necessary to remove the magnesium block and to render NMDA receptors fully functional.

A crucial role of NMDA receptors in early development has been demonstrated in the CA1 hippocampal region (Durand et al., 1996; Hsia et al., 1998; Isaac et al., 1995). It has been shown that in early postnatal days, a large proportion of synapses do not bear functional AMPA receptors and only possess NMDA receptors. These synapses are functionally silent, because of the magnesium block of NMDA receptors at resting membrane potential. However, NMDA receptors would contribute to the formation of 'adult' synapses, since AMPA receptor-mediated responses can be detected after various patterns of afferent stimulation (Isaac et al, 1995; Durand et al., 1996). Differently from the CA1 region, in the CA3 area at P2, AMPA receptors are already functional, as demonstrated by the blocking or facilitating effects of CNQX and, cyclothiazide (the AMPA receptor desensitization blocker) on GDPs frequency, respectively.

As discussed above, the difference between the CA3 and the CA1 region may be ascribed to distinct receptor subunits and/or distribution. Furthermore, early in postnatal life, in the CA3 region, spontaneous synaptic activity is mainly GABA-mediated since it is completely abolished by bicuculline and almost unaffected by kynurenic acid (Hosokawa et al., 1994), whereas in the

CA1 area picrotoxin-resistant EPSCs can be detected (Hsia et al., 1998). However, it should be considered that GDPs are generated by the interplay between pyramidal cells and interneurons. Therefore we cannot exclude a difference in AMPA receptors development, properties or distribution between these two neuronal types. For example, in comparison with pyramidal cells, interneurons display on average smaller amplitude NMDA currents and calcium-permeable AMPA receptors (Freund and Buszaki, 1996). This raises the possibility that calcium enters in interneurons through AMPA receptors and this event may contribute to trigger synaptic plasticity processes involved in synapses formation during development.

5.1.3 Glutamate component of GDPs in CA3 pyramidal neurons

Having assessed the contribution of AMPA and NMDA receptors to the generation of GDPs in the network, other experiments have been performed in order to identify a possible glutamatergic component of GDPs generated on pyramidal neurons. Since the block of $GABA_A$ or AMPA receptors in the whole network would prevent GDPs generation, it was necessary to act at single cell level to dissect out the different GDPs components. To this purpose, $GABA_A$ induced responses in principal cells were blocked by perfusing the recorded neuron with fluoride (see also Khazipov et al. 1997). This procedure revealed the presence of a residual GDP component with slower kinetics. Within the first 30-40 minutes of cell dialysis with fluoride, GDPs undergo a shift in their reversal potential towards more positive values. The slope of the amplitude-voltage plot changed with time, suggesting a progressive loss of the GABAergic component. The shift in reversal was similar to that already reported for GDPs in interneurons (Khazipov et al. 1997). The residual GDPs components were characterized, in the majority of the cases, by a linear amplitude/voltage relationship. This indicates that they were mediated by the activation of

a non-NMDA receptor type, unmasked after intracellular blockade of GABA. Further support of this interpretation is provided by pharmacological experiments in which CNQX was able to completely block the residual component of GDPs (8/11cases). An NMDA component was found in only 3/11 cases. In this respect our data differ from those reported by Khazipov et al. (1997) in interneurons, where the dialysis-resistant component rectified at membrane potential more negative than -20. However, in that report no pharmacological tools were used to dissect out the different glutamatergic components and the assumption that the residual part of GDPs (which remains after intracellular dialysis with F^-) is NMDA-dependent was based only on the voltage dependency of the responses. In the present experiments, the similarity in the dose/response curves for AMPA, obtained in the presence of TTX, with intracellular solutions containing KCl or KF, excludes the possibility that the residual AMPA-mediated component of the GDPs is overestimated as a result of the interference of F^- with some phosphorylation processes (Andrews and Babior, 1984).

5.1.4 Recurrent collaterals from pyramidal cells may provide the glutamatergic drive to interneurons

As already shown (Khazipov et al., 1997; Garaschuk et al., 1998; Menendez de la Prida et al., 1998), GDPs were still present in small CA3 islands isolated from the rest of the hippocampus, implying that a local circuit consisting of a relatively small population of principal cells and interneurons was sufficient to generate them. In these cases, the glutamatergic input presumably originates from collaterals of principal cells, since the mossy fibers were disconnected from the granule cells of the dentate gyrus. Moreover, the glutamatergic component revealed in pyramidal

cells recorded with KF is also presumably due to glutamate released from recurrent collaterals, since it was present also in isolated CA3 islands.

In summary this first set of experiments suggests that GDPs generation requires activation of AMPA receptors by local release of glutamate from recurrent collaterals. Other glutamatergic components may also be involved but do not seem to be essential.

5.2 Role of muscarinic receptors in GDP modulation

5.2.1 Endogenous ACh enhances GDPs frequency acting on M1 muscarinic receptors

The present experiments have clearly shown that during the first postnatal week, endogenous ACh is able to modulate GDPs frequency and therefore the release of GABA in a developmentally regulated way through the activation of M1 muscarinic receptors. Evidence in favour of an upregulation of GDPs frequency by ACh acting on muscarinic receptors is given by the experiments with atropine, in about 50% of which GDPs frequency was reduced. Also the experiments with edrophonium strongly suggest that endogenous ACh modulates GABA release, assessed as GDPs. This compound in fact, by blocking AChE increased the levels of endogenous ACh and enhanced GDPs frequency. The effect induced by edrophonium was mediated by muscarinic receptors since it was prevented by application of atropine. We cannot rule out the possibility that edrophonium, as other anti-cholinoesterase drugs, could have a direct actions at some cholinergic receptor sites, as either agonist or antagonist (Goodman and Gilman, 1996). However studies on the heart and on airway smooth muscles suggest that edrophonium does not exert any agonist-like action on muscarinic receptors (Shibata et al., 1996; Backman et al., 1996; Endou et al., 1997).

It is not clear why immediately after washout of edrophonium a block or a reduction in GDPs

frequency occurs. A desensitization of ACh muscarinic receptors following accumulation of ACh in the tissue as the consequence of AChE inhibition by edrophonium can be excluded since the potentiating effects of edrophonium persisted when edrophonium was applied for prolonged periods of time. Another mechanism that could account for this effect is an unbalance between M1 and M2/M4 receptor activation during washout of the AChE inhibitor edrophonium. In these conditions, the concentration of ACh in the tissue would be abruptly reduced and this would cause a preferential activation of higher affinity presynaptic inhibitory M2 and M4 muscarinic receptors, which are usually associated to inhibitory responses.

Interestingly, the enhancement of GDPs frequency induced by edrophonium was developmentally regulated, as shown by the increased efficacy of the effects of this drug with age. These effects could be due to a progressive increase of both muscarinic receptors and cholinergic innervation during the first postnatal week. According to Niakas et al. (1994) at P1, the density of AChE-positive fibers is extremely low; cholinergic fibers undergo a rapid increment during the first postnatal week, they reach a pattern closely resembling the adult age conditions by P10, although they continue to increase until P30. Muscarinic receptors are already present at birth, but binding studies have shown that their number sharply increases from P4 to P10-P15 (Ben-Barak and Dudai, 1979). As for the cholinergic innervation, the total binding continues to increase gradually until P30 (Tice et. al., 1996).

The effects of ACh were mediated by M1 muscarinic receptors, as suggested by the possibility to antagonize the action of edrophonium with low concentration of pirenzepine. This drug in fact antagonized the effect of edrophonium with an EC_{50} lower than methoctramine. However, we can not exclude the possibility that, M3 receptors could be also involved. M1 and M3 receptors have been shown to be preferentially localized on the somata and dendrites of pyramidal neurons

and interneurons (Levey et al., 1995). Therefore, activation of these receptors would increase the excitability of the network probably by suppressing several potassium conductances, that causes an increase of GDPs frequency.

5.2.2 Carbachol increases and decreases GDPs frequency acting on M1 and M2 muscarinic receptors, respectively

Like those of edrophonium, the effects of carbachol were developmentally regulated. Direct application of carbachol was able to increase GDPs frequency and, after P5, to enhance the synaptic noise and to depolarize the cell. These effects were presynaptic as assessed by the fact that: i. the action of carbachol was detected also in the absence of changes in membrane potential or input resistance. ii. when the membrane depolarization was present, this was blocked by GYKI 53665 or bicuculline, implying that it was due to the release of glutamate or GABA, following activation of muscarinic receptors. As for ACh, carbachol would activate muscarinic receptors localized on pyramidal cells and/or interneurons. An increase in pyramidal cells excitability would enhance the glutamatergic drive to interneurons that would be ultimately responsible for the increased GABA release. NMDA receptors appear not to be involved in the potentiating effects of carbachol on GDPs since NMDA antagonists failed to prevent the action of carbachol. Therefore glutamate released from pyramidal cells would activate AMPA receptors. Carbachol exerts also a direct excitatory effect on GABAergic interneurons as shown by the increase in frequency of spontaneously occurring GABA-mediated synaptic potentials in the presence of GYKI 53655 and AP-5. This implies, as already described in adults (Pitler and Alger, 1992; Beherends and ten Bruggencate, 1993), a direct action of carbachol on muscarinic receptors localized on GABAergic interneurons. As for endogenous ACh, the potentiating effect

of carbachol on GDPs was mediated by M1 receptors, as suggested by the ability of pirenzepine to prevent the effects of carbachol. Carbachol-induced oscillations in adult neurons (Williams and Kauer, 1997) were blocked by pirenzepine and not by methoctramine, indicating that also in this case, M1 receptor subtypes were involved. We can not exclude the possibility that also in our case, like in adulthood, M3 receptors are also involved.

Unlike the action of endogenous ACh, carbachol had also a clear depressant presynaptic effect on GDPs. This was revealed after blockade of the excitatory effect with pirenzepine. While in juvenile and adult rats, the depressant effect of carbachol on excitatory transmitter release has been well documented (Hounsgaard, 1978; Valentino and Dingledine, 1981; Dutar & Nicoll, 1988b), in neonatal hippocampal and cortical neurons a delayed maturation of functional muscarinic receptors has been reported (Vaknin and Teyler, 1991; Milburn and Prince, 1993). Thus, at P5-P7, only a modest depressant effect of carbachol on the field EPSP has been observed in the CA1 region of the hippocampus. However the question through which muscarinic receptor this effect is mediated is still controversial (for a review see McKinney, 1993). M1 (Sheridan & Sutor, 1990), M2 (Dutar & Nicoll, 1988b; Marchi & Raiteri, 1989), M3 receptor subtypes (Hsu et al., 1995) and M4 (McKinney et al., 1993) have been suggested. In our case a non-M1, most likely a M2 receptor subtype seems to be involved as demonstrated by the experiments in which the M2 antagonist methoctramine was able to enhance the excitatory effect of carbachol, presumably by blocking the inhibitory effect of carbachol on glutamate release (and therefore on the glutamatergic drive to interneurons). The precise mechanism by which ACh diminishes glutamate release from presynaptic nerve endings is not certain. Several mechanisms can be put forward. These include: opening of potassium channels either directly (Egan & North, 1986) or indirectly through an increase in intracellular calcium (Fukuda et al.

1988), inhibition of calcium fluxes through voltage activated calcium channels (Gähwiler & Brown, 1987; Higashida et al. 1990), direct depolarization of the terminals. Interestingly both the direct effect of ACh on potassium and calcium channels are mediated by M2 and M4 receptor subtypes (McKinney, 1993).

It remains to be clarified why carbachol exerts both an excitatory and a depressant action on GABA release whereas only excitatory effects can be detected following activation of muscarinic receptors by endogenous ACh. It is conceivable that carbachol activates both synaptic and extrasynaptic receptors and the physiological properties of the latter would be different from the former.

It is interesting to notice that, in juvenile (Postlethwaite et al. 1998) or adult rats (Williams & Kauer, 1997), high doses of carbachol were shown to produce an oscillatory behaviour that closely resembled epileptic-like phenomena (Traub et al. 1996) and that was only disrupted by bicuculline. In the present experiments, bicuculline completely abolished GDPs and only towards the end of the first postnatal week was able to produce spontaneous interictal discharges, whose frequency was enhanced by carbachol as in juvenile animals (Psarropoulou & Dallaire, 1998).

5.3 Role of endogenous NGF on hippocampal function

5.3.1 NGF is necessary to maintain the cholinergic function in the hippocampus of neonatal animals

The dependence of BF neurons on NGF for the maintenance of the cholinergic phenotype is well documented. However, little is known about the functional consequences of NGF deprivation on the area targeted by the cholinergic innervation. To antagonize NGF action, we implanted

hybridoma cells secreting the monoclonal antibody αD11 (Cattaneo et al., 1988). which efficiently neutralises NGF action and which does not cross react with other neurotrophins (Gonfloni, 1995). This delivery method was previously shown to be effective in antagonizing the action of NGF in vivo on the development of the geniculo-cortical pathway (Domenici et al., 1994) and on the cholinergic phenotype of BF neurons (Molnar et al. 1997; Molnar et al. 1998). The present experiments clearly show that:

i. rats treated with anti-NGF antibodies at P2 and sacrificed one week later, present a significant downregulation (possibly ACh-dependent) of GDPs frequency ii. rats treated with anti-NGF antibodies at P2 and sacrificed two weeks later exhibit a 50% reduction in the effect on acetylcholine release following stimulation of cholinergic fibers and an increased postsynaptic sensitivity of pyramidal cells to carbachol. iii. rats treated with anti-NGF antibodies at P15 and sacrificed one week later do not show any change in the sensitivity of principal cells to carbachol or in acetylcholine release.

5.3.2 Effect observed in rat injected at P2 and sacrificed at P15

The present experiments show that rats treated with anti-NGF antibodies at P2, exhibited two weeks after implantation a 50% reduction in the effect of electrical stimulation on acetylcholine release following stimulation of cholinergic fibres and an increased postsynaptic sensitivity of pyramidal cells to carbachol. Moreover, neurons in slices from animals implanted with αD11 exhibited broader action potentials and a reduction in spike discharge accommodation. In spite of the reduction in acetylcholine release at P15, no changes in the slow cholinergic EPSP were detected. This probably reflects a compensatory mechanism, whereby a reduction in cholinergic

innervation in young animals is counterbalanced by an increase in postsynaptic sensitivity to acetylcholine.

An alteration of the cholinergic function in the hippocampus, following destruction of NGF receptor-bearing cholinergic neurons in the BF with the toxin 192-IgG-saporin, which is taken up by cholinergic terminals, (Jouvenceau et al. 1987; Heckers et al. 1994) has been recently observed. In this case however, the slow cholinergic EPSPs was abolished, probably because of the almost complete loss of BF cholinergic neurons.

It is most likely that the effects observed were due to the chronic deprivation of NGF, since the levels of anti-NGF antibodies should be sufficiently high to completely neutralise endogenous NGF (Korsching et al. 1985). The action of anti-NGF antibodies injected at P2 seems to be localized at the BF level, as suggested by the shrinkage and reduction in the number of ChAT positive cells within this region (Molnar et al. 1997; Molnar et al. 1998). Moreover, the identical basic membrane properties found with electrophysiological experiments in αD11- and P3U-treated animals, suggest no major morphological alterations of hippocampal cells. Therefore, the observed effects are most likely due to an action of the anti-NGF antibodies on BF cholinergic neurons. These cells express from birth, both high and low affinity receptors for NGF (Holtzman et al. 1992; Holtzman et al. 1995; Koh et al. 1991), while the presence of TrkA and p75 mRNA within the hippocampus is still controversial (Cellerino, 1996). In rats injected at P2 and sacrificed two weeks later, CA1 pyramidal cells of NGF deprived animal show, in comparison to control, broader action potentials, a reduction in spike discharge accommodation and an increased postsynaptic sensitivity to carbachol.

5.3.2.1 Action potential broadening

The present data also revealed a small but significant change in the shape of the action potential due to spike broadening in slices from αD11-treated animals. At this stage the mechanisms underlying this phenomenon are a matter of speculation. It has been reported that activation of muscarinic receptors by low concentrations of carbachol are capable of increasing spike duration with little or no changes in spike amplitude (Figenschou et al., 1996). This effect may involve the phosphotidylinositide second messenger cascade or direct activation of protein kinase C (Figenschou et al., 1996). Spike broadening may result from a muscarinic suppression of potassium conductances underling the I_A. Although this effect has been described in cultured hippocampal neurons, it does not appear to occur in pyramidal cells in fresh slices (Figenschou et al, 1996). We propose the possibility that changes in muscarinic receptors properties or in the second messanger cascade, following chronic NGF deprivation, may affect calcium entry through a direct or indirect action on voltage-gated calcium channels. Whatever the mechanism, such an effect may lead to an increase in calcium influx and therefore in calcium-dependent processes (Llinas et al., 1982).

5.3.2.2 Reduction in spike discharge accommodation

Cells in slices from αD11-treated animals exhibited spikes discharge that, in comparison with controls, accommodated less. However, during stimulation of cholinergic fibres, the block of accommodation was greater in cells from P3U than in αD11-treated rats. This effect was probably due to a reduction in acetylcholine release from presynaptic nerve endings of slices from αD11-treated animals. The reduction in spike discharge accommodation prior to tetanic stimulation could have similar mechanisms to those previously suggested for spike broadening.

5.3.2.3 Increased sensitivity of hippocampal cells to carbachol

The enhanced sensitivity of muscarinic receptors to carbachol found in the present experiments is similar to that observed in denervated rat hippocampus (Benson et al., 1989). However, in contrast to the present data, in denervation conditions the shift to the left of the dose/response curve to carbachol was associated with an increase in the maximum response, indicating an increased number of muscarinic receptors. In our case the apparent maximum was similar in P3U and αD11 treated rats, suggesting that the total number of receptors was unchanged in both experimental conditions. A qualitative change in receptor subtypes or changes in coupling mechanisms between the receptors and acceptors may underline the reduction in EC_{50} value found in NGF-deprived rats. It is also possible that a reduced exposure to 'ambient' acetylcholine following cholinergic denervation might induce changes in desensitization and recycling of muscarinic receptors, leading to an alteration of the EC_{50} value (Bogatkewitsch et al., 1996).

In contrast to postsynaptic muscarinic receptors, presynaptic receptors, at least in CA1 area, were not altered in NGF-deprived animals as suggested by the fact that carbachol reduced the amplitude of the field EPSPs to the same extent in both αD11 and P3U treated rats. It is well established that inhibition of glutamate release in the hippocampus is mediated by the M2 subtype of muscarinic receptors (Dutar and Nicoll, 1988b; Marchi and Raiteri, 1989) whereas the carbachol-induced membrane depolarization appears to result from the activation of the M1 subtype of muscarinic receptors (Dutar and Nicoll, 1988b). It is therefore possible that neutralization of NGF with anti-NGF antibodies selectively affects only the postsynaptic receptors belonging to the M1 subtype, while sparing the M2 subtype localized on glutamatergic

terminals. It is also likely that the effect of acetylcholine on spike discharge accommodation is mediated by M1 subtype of muscarinic receptors (Dutar and Nicoll, 1988b). In line with this, an increase in M1 but not M2 subtype of muscarinic receptors has been found in the hippocampus of animals that have received 1-2 weeks earlier a lesion of the cholinergic pathway, a cut of the fimbria-fornix or an intraventricular injection saporin Ig192 (Levey et al., 1995). This toxin binds to the low affinity receptors for NGF (and other neurotrophine of the same family) P75 (highly expressed by BF cholinergic neurons), is taken up by cholinergic terminals and cell dead occurs.

5.3.3 Effect observed in rat injected at P2 and sacrificed at P6-P11

In keeping with anatomical results, one week after the injection (at P2) of αD11 cells, the slow cholinergic EPSP could not be evoked in the CA1 area. Furthermore, in NGF deprived animals, GDPs frequency recorded in the CA3 region was significantly reduced. Since GDPs are modulated by endogenous acetylcholine, it is likely that this effect is due to a reduced ACh level in the tissue. In support of this hypothesis are the data obtained from the releasing experiments. Although, due to intrinsic technical difficulties, few experiments were performed in this animal group, very low level of ACh were detected following stimulation of hippocampal slices.

5.3.4 Lack of change in the sensitivity to carbachol of hippocampal cells from rats treated with anti NGF antibodies at P15 and sacrificed at P21

When the injection was performed at P15 and the animals were sacrificed one week later, both the sensitivity to carbachol of hippocampal cells and acetylcholine release were unchanged, in agreement with anatomical data that have shown no changes in the size and number of BF

cholinergic neurons at this time point (Molnar et al 1997; Molnar et al. 1998) and in spite of the high levels of αD11 antibodies present in the hippocampus and cortex. The shift to the left of the dose response curve to carbachol found in slices from P3U-treated animals may reflect a normally occurring developmental process. On the other hand, the unchanged sensitivity to carbachol, with respect to controls, of neurons from αD11-treated rats is consistent with the lack of alterations in the cholinergic phenotype of BF neurons under these experimental conditions.

The mechanisms underlying the transition in the sensitivity of BF neurons to NGF neutralization which occurs around P15 are still unclear. One possibility could be a switch of BF neurons in their dependence to other neurotrophic factors, a phenomenon well described in other systems (Davies, 1997). Alternatively, one may speculate that around P15, Trk A receptors may become activated in a NGF-independent way, producing a basal level of signaling, similarly to what is reported when these receptors are overexpressed in transfected cells (Hempstead, 1992). Changes in the ratio of TrkA versus $p75^{NTR}$ receptors could conceivably mediate the differential sensitivity of BF neurons to NGF deprivation before and after P15 (Bredesen and Rabizadeh, 1997). Interfering with the activity of TrkA receptors in TrkA-/- mice, leads to a partial different picture, possibly due to residual NGF signalling through p75: at P20-P25, BF cholinergic neurons are not fully mature and display a downregulation of ChAT immunoreactivity as well as a 20% reduction in the number of ChAT immunoreactive neurons (Fagan et al., 1997).

5.3.5 Conclusion

Recently in the intact *in vitro* septal-hippocampal preparation (Leinekugel et al., 1998) it has been shown that GDPs have a preferential septo-temporal propagation gradient. The septal pole, being most active, would pace the rhythm of the entire structure. Although originated within the

hippocampus, GDPs propagate to the septum, probably *via* the hippocampal-septal projection. Therefore, at a time when theta activity is not developed yet (LeBlanc and Bland, 1979), GDPs would ensure synchronization of large neuronal 'ensembles' (mainly GABAergic cells) within the developing limbic structure. By differentially regulating synaptic efficacy between neurons according to their septo-temporal distance, they may drive the formation of functional units in the septo-hippocampal complex. Synchronization of large neuronal 'ensembles' would be particularly important in synaptogenesis and would considerably enhance encoding of information during a particular period of postnatal development. ACh by activation of muscarinic receptors would further strengthen this action, thus contributing to the fine tuning of hippocampal neuronal circuitry.

References

Acsády L, Kamondi A, Sík A, Freund T and Buzsaki G (1998) GABAergic cells are the major postsynaptic targets of mossy fibers in the rat hippocampus. J. Neurosci., 18: 3386-3403

Akaike N, Hattori K, Omura Y, Carpenter DO (1985) Bicuculline and picrotoxin block γ-aminobutiric acid-gated Cl- conductance by different mechanisms. Experientia, 41: 70-71

Alger BE and Nicoll RA (1979) GABA-mediated biphasic inhibitory responses in hippocampus. Nature, 281: 315-317

Amaral DG (1993) Emerging principles of intrinsic hippocampal organization. Curr. Opin. Neurobiol., 3:225-229

Amaral DG and Dent JA (1981) Development of the mossy fibers of the dentate gyrus: I. A light and electron microscopic study of the mossy fibers and their expansions. J Comp. Neurol., 195: 51-86

Andersen P, Bliss VP and Skrede KK (1971) Lamellar organization of hippocampal excitatory pathways. Exp. Brain Res., 13:222-238

Andersen P, Silfvenius H,Sundberg SH and Sveen O (1980) A comparison of distal and proximal dendritic synapses on CA1 pyramids in guinea-pig hippocampal slices *in vitro*. J. Physiol. 307: 273-299.

Andrews PC and Babior BM (1984) Phosphorylation of cytosolic proteins by resting and activated human neutrophils. Blood, 64: 883-890

Auberger G, Heumann R, Hellweg R, Korsching S and Thoenen H (1987) Developmental changes of nerve growth factor and its mRNA in the rat hippocampus: comparison with choline acetyltransferase. Dev. Biol., 120: 322-328

Auerbach JM and Segal M (1996) Muscarinic receptors mediate depression and long-term potentiation in rat hippocampus. J Physiol., 492: 479-493

Azmitia EC and Segal M (1979) An autoradiographic analysis of differential ascending projections of the dorsal and median raphe nuclei in the rat. J. Comp. Neurol., 179: 641-668

Backman SB, Stein RD, Blank DW, Collier B and Polosa C (1996) Different properties of the bradycardia produced by neostigmine and edrophonium in the cat. Can. J. Anaesthesia, 43: 731-740

Barde YA (1989) Trophic factors and neuronal survival. Neuron, 2: 1525-1534

Behrends JC and ten Bruggencate GT (1993) cholinergic modulation of synaptic inhibition in the guinea pig hippocampus in vitro: excitation of GABAergic interneurons and inhibition of GABA-release. J. Neurophysiol., 69: 626-629

Ben-Ari Y, Krnjevic K, Reinhardt W nad Ropert N (1981) Intracellular observation on the disinhibitory action pf acetylcholine in the hippocampus. Neurosci., 12: 2475-2484

Ben-Ari Y, Cherubini E Corradetti R and Gaiarsa JL (1989) Giant synaptic potentials in immature rat CA3 hippocampal neurons. J. Physiol., 416: 303-325

Ben-Ari Y, Khazipov R, Leinekugel X, Caillard O and Gaiarsa JL (1997) GABAA, NMDA and AMPA receptors: a developmentally regulated 'menage a trois'. Trends Neurosci., 20: 523-529

Ben-Barak J and Dudai Y (1979) Cholinergic binding sites in rat hippocampal formation: properties and ontogenesis. Brain Res., 166: 245-257

Benson DM, Blitzer RD, Haroutunian V and Landau EM (1989) Functional muscarinic supersensitivity in denervated rat hippocampus. Brain Res., 478: 399-402

Benson DM, Blitzer RD, and Landau EM (1988) An analysis of the depolarization produced in guinea-pig hippocampus by cholinergic receptors stimulaiton. J. Physiol., 404: 479-496

Bernard C and Wheal HV (1994) Model of local connectivity patterns in CA3 and CA1 areas of the hippocampus. Hippocampus, 4: 497-529

Bernardo LS and Prince DA (1982) Ionic mechanisms of cholinergic excitation in mammalian hippocampal pyramidal cells. Brain Res., 249: 333-344

Bland BH, Colom LV, Konopacki J and Roth S (1988) Intracellular recods of carbachol-induced theta rhythm in hippocampal slices. Brain Res., 447: 364-368

Bland BH (1986) The physiology and pharmacology of hippocampal formation theta rhythms. Prog. Neurobiol., 26: 1-54

Bogatkewitsch GS, Lenz W, Jakobs KH and Van Koppen CJ (1996) Receptor internalization delays m4 muscarinic acetylcholine receptor resensitization at the plasma membrane. Mol. Pharmacol., 50: 424-429

Bormann J (1988) Electrophysiology of $GABA_A$ and $GABA_B$ receptor subtypes. Trends Neurosci., 11: 112-116

Bormann J, Hamill OP and Sakmann B (1987) Mechanism of anion permeation through channels gated by glycine and γ-aminobutiric acid in mouse cultured spinal neurons. J Physiol, 385:243-286

Bouron A and Reuter H (1997) Muscarinic stimulation of synaptic activity by protein kinase C is inhibited by adenosine in cultured hippocampal neurons. Proc. Natl.Acad. Sci., 94:12224-12229

Bowery NG (1993) $GABA_B$ receptor pharmacology (1993). Annu. Rev. Pharmacol. Toxicol. 33: 109-147

Bragin A, Jando G, Nadasdy Z, Hetke J, Wise K and Buzsaki G (1995) Gamma (40-100 Hz) oscillation in the hippocampus of the behaving rat. J. Neurosci., 15: 46-60

Brazier MAB (1968) The electrical activity of the nervous system. Pitman Medical Publishing, third edition

Brown DA, Higashida H, Noda M, Ishizaka N, Nashii M, Hoshi N, Yokoyama S, Fukuda K, Katayama M, Nukada T, Kameyama K, Robbins J, Marsh SJ and Selyanko AA. (1993) Coupling of muscarinic receptor subtypes to ion channels: experiments on neuroblastoma hybrid cells. Annals of the New York Academy of Science, 707

Burnashev N, KhodorovaA, Jonas P, Helm PJ, Wisden W, Monyer H, Seeburg PH and SakmannB (1992) Calcium-permeable AMPA-kainate receptorsin fusiform cerebellar glia cells. Science, 256:1566-1570

Buzsaki G (1984) Feed-forward inhibition in the hippocampal formation. Prog. Neurobiol., 22: 131-153

Buzsaki G and Chrobak JJ (1995) Temporal structure in spatially organized neuronal ensembles: a role for interneuronal networks. Curr. Op. Nerobiol., 5: 504-510

Caeser M, Brown DA, Gahwiler BH and Knopfel T (1993) Characterization of a calcium-dependent current generating a slow afterdepolarization of CA3 pyramidal cells in rat hippocampal slice cultures. Eur. J. Neurosci, 5: 560-569

Cantrell AR, MA JY, Scheuer T and Catterall WA (1996) Muscarinic modulation of sodium current by activation of protein kinase C in rat hippocampal neurons. Neuron, 16: 1019-1026

Casamenti F, Scali C, Vannucchi MG, Bartolini L and Pepeu G (1993) Long-term ethanol consumption by rats: effect on acetylcholine release *in vivo*, choline acetyltransferase activity and behavior. Neuroscience 56: 465-471

Castillo PE, Malenka RC and Nicoll RA (1997) Kainate receptors mediate a slow postsynaptic current in hippocampal CA3 neurons. Nature 388:182-186

Cattaneo A, Rapposelli B and Calissano P (1988) Three distinct types of monoclonal antibodies after long term immunization of rats with mouse NGF. J.Neurochem., 50: 1003-1010

Caulfield and Birdsall (1998) International union of pharmacology. XVII. Classification of muscarinic acetylcholine receptors. Pharmachol. Rev., 50: 279-290

Cellerino A (1996) Expression of messenger RNA coding for the nerve growth factor receptor trkA in the hippocampus of the adult rat. Neuroscience, 70: 613-616

Chao MV (1992) Neurotrophin receptors: a window into neuronal differentiation. Neuron, 9: 583-593

Cherubini E and Strata F (1997) $GABA_C$ receptors: a novel receptros family with unusual pharmacology. News Physiol. Sci., 12:136-141

Cherubini E., Gaiarsa JL, Ben-Ari Y (1991) GABA: an excitatory transmitter in early postnatal life. Trends Neurosci, 14: 515-519

Chittajallu R, Vignes M, Dev KK, Barnes JM, Collingridge GL and Henley JM (1996) Regulation of glutamate release by presynaptic kainate receptors in the hippocampus. Nature, 379: 78-81

Clarke VR, Ballyk BA, Hoo KH, Mandelzys A, Pellizzari A, Bath CP, Thomas J, Sharpe EF, Davies CH, Ornstein PL, Schoepp DD, Kamboj RK, Collingridge GL, Lodge D, Bleakman D (1997) A hippocampal GluR5 kainate receptor regulating inhibitory synaptic transmission. Nature, 389: 599-603

Cobb SR, Buhl EH, Halasy K, Paulsen O and Somogy P (1995) Synchronization of neuronal activity in hippocampus by individual GABAergic interneurons. Nature, 378: 75-78

Cole AE and Nicoll RA (1984) Characterization of a slow cholinergic post-synaptic potential recorded *in vitro* from rat hippocampal pyramidal cells. J Physiol., 352: 173-188

Colino A and Halliwell JV (1993) Carbachol potentiates Q current and activates a calcium-dependent non specific condunctance in rat hippocampus *in vitro*. Eur. J. Neurosci., 5: 1198-1209

Davies AM, (1997) Neurotrophin switching: where does it stand? Curr. Opin. Neurobiol., 7: 110-118

Domenici L, Cellerino A, Berardi N, Cattaneo A and Maffei L (1994) Antibodies to nerve grow factor (NGF) prolong the sensitive period for monocular deprivation in the rat. NeuroReport, 5: 2041-2044

Donevan SD and Rogawski MA (1993) GYKI 52466, a 2,3-benzo-diazepine, is a highly selective, non competitive antagonist of AMPA/kainate receptors responses. Neuron, 10: 51-59

Draguhn, A., Traub, R.D., Schmitz, D and Jefferys, J.G.R. (1998) Electrical coupling underlies high-frequency oscillations in the hippocampus *in vitro*. Nature, 394: 189-192

Durand GM, Kovalchuk Y and Konnerth A (1996) Long-term potentiation and functional synapse induction in developinghippocampus. Nature, 381: 71-75

Dutar P, Bassant M-H, Senut M-C and Lamour Y (1995) The septohippocampal pathway: structure and function of a central cholinergic system

Dutar P and Nicoll RA (1988a) A physiological role for GABAB receptors in the central nervous system. Nature, 332: 156-158

Dutar P and Nicoll RA (1988b) Classification of muscarinic responses in hippocampus in terms of receptors subtypes and second-messenger system: electrophysiological studies *in vitro*. J. Neurosci., 8: 4214-4224

Edmonds B, Gibb AJ and Colquhoun D (1995) Mechanisms of activation of glutamate receptors and the time course of excitatory synaptic currents. Annu. Rev. Physiol., 57: 495-519

Egan TM and North RA (1986) Acetylcholine hyperpolarizes central neurones by acting on M2 muscarinic receptor. Nature, 319: 405-407

Eichenbaum H (1996) Is the rodent hippocampus just for 'place'? Curr. Opin. Neurobiol., 6:187-195

Endou M, Tanito Y and Okumura F (1997) A comparison between chronotropic effects of neostigmine and edrophonium in isolated guinea pig right atrium. J. Pharmacol. Exp. Therap., 282: 1480-1486

Fagan AM, Garber M, Barbacid M, Silos-Santiago I and Holtzman DM (1997) A role for TrkA during maturation of striatal and basal forebrain cholinergic neurons in vivo. J. Neurosci., 15: 7644-7654

Feller MB, Wellis DP, Stellwagen D, Werblin FS and Shatz CJ (1996) Requirement for cholinergic synaptic transmission in the propagation of spontaneous retinal waves. Science, 272: 1182-1187

Figenschou A, Hu GY and Storm JF (1996) Cholinergic modulation of the action potential in rat hippocampal neurons. Eur. J. Neurosci., 8: 211:219

Freund TF and Antal M (1988) GABA-containig nerons in the septum control inhibitory internerons in the hippocampus. Nature, 336: 170-173

Freund TF and Buzsaki G (1996) Interneurons of the hippocampus. Hippocampus, 6:347-470

Frotscher M and Leranth C (1983) Cholinergic innervation of the rat hippocampus as revealed by choline acethyltransferase immunocytochemistry: a combine ligh and electron microscopic study. J Comp. Neurol. 243: 58-70

Fukuda K, Higashida H, Kubo T, Maeda A, Akiba I, Bujo H, Mishina M and Numa S (1988) Selective coupling with K+ currents of muscarinic acetylcholine receptor subtypes in NG108-15 cells. Nature 335:355-8

Gabrieli JD, Brewer JB, Desmond JE and Glover GH (1997) Separate neuronal bases of two fundamental memory processes in the human medial temporal lobe. Science, 276: 264-266

Gage FH, Wictorin K, Fisher W, Williams LR, Varon S and Bjorklund A (1986) Retrograde cell changes in medial septum and diagonal band following fimbria-fornix transection: quantitative temporal anaysis, Neuroscience: 19 241-256

Gahwiler BH and Brown DA (1987) Muscarine affects calcium current in rat hippocampal pyramidal cells in vitro. Neurosci. Lett., 76: 6-10

Gaiarsa JL, Corradetti R, Cherubini E and Ben-Ari Y (1990) The allosteric glycine site of the N-methyl-D-aspartate receptor modulates GABAergic synaptic events in neonatal rat CA3 hippocampal neurons. Proc. Natl. Acad. Sci. USA 87:343-346

Gaiarsa JL, Corradetti R, Cherubini E and Ben-Ari Y (1991) Modulation of GABA-mediated synaptic potentials by glutamatergic agonists in neonatal CA3 rat hippocampal neurons. Eur. J. Neurosci., 3: 301-309

Garaschuk, O., Hanse, E. and Konnerth, A. (1998) Developmental profile and synaptic origin of early network oscillations in the CA1 region of rat neonatal hippocampus. J. Physiol., 507: 219-236

Gonfloni S (1995) Recombinant antibodies as structural probes for neurotrophins. PhD Thesis at International School for Advanced Studies, Trieste.

Goodman and Gilmans (1996) The pharmacological basis of therapeutics.

Gray CM. Engel AK. Konig P and Singer W. (1992) Synchronization of oscillatory neuronal responses in cat striate cortex: temporal properties. Visual Neuroscience, 8: 337-47

Gray CM., Konig P., Engel AK. and Singer W (1989) Oscillatory responses in cat visual cortex exhibit inter-columnar synchronization which reflects global stimulus properties. Nature, 338: 334-337

Grover LM, Lambert NA, Schwartzkroin PA and Teyler TJ (1993) Role of HCO_3^- ion in depolarizing GABAA receptor-mediated responses in pyramidal cells of rat hippocampus. J. Neurophysiol., 69:1541-1555.

Halliwell JV and Adams PR (1982) Voltage-clamp analysis of muscarinic excitation in hippocampal neurons. Brain Res., 250: 71-92

Hebb DO (1949) Organization of behaviour. Wiley, New York.

Heckers S, Ohtake T, Wiley RG, Lappi DA, Geula C and Mesulam MM (1994) Complete and selective cholinergic denervation of rat neocortex and hippocampus but not amygdala by an immunotoxin against the p75 NGF receptor. J. Neurosci., 14: 1271-1289

Hefti F (1986) Nerve Growth Factor promotes survival of septal cholinergic neurons after fimbrial transections, J. Neurosci. 6: 2155-2162

Hempstead BL, Rabin SJ, Kaplan L, Reid S, Parada LF and Kaplan DR (1992) Overexpression of the trk tyrosine kinase rapidly accelerates nerve growth factor-induced differentiation. Neuron 9: 883-896

Higashida H, Hashii M, Fukuda K, Caulfield MP, Numa S and Brown DA (1990) Selective coupling of different muscarinic acetylcholine receptors to neronal calcium currents in DNA-transfected cells. Proc. R. Soc. London, 242: 68-74

Hohmann C and Ebner FF (1985) Development of cholinergic markers in mouse forebrain. I Choline acetyltransferase enzyme activity and acetylcholinesterase histochemistry. Brain Res., 23: 243-253

Hollman et M, Hartley M and Heinemann S (1991) CA2+ permeability of KA-AMPA-gated glutamate receptor channels depends on subunit composition. Science, 252: 851-853

Holtzman DM, Kilbridge J, Li Y, Cunningham ET, Lenn NJ, Clary O, Reichardt LF and Mobley WC (1995) TrkA expression in the CNS: evidence for existence of several novel NGF-responsive CNS neurons, J. Neurosci., 15: 1567-1576

Holtzman DM, Li Y, Parada LF, Kinsman S, Chen CK, Valletta J, Zhou J, Long JB and Mobley WC (1992) $p140^{trk}$ mRNA marks NGF-responsive forebrain neurons: evidence that trk gene expression is induced by NGF. Neuron: 9 465-478

Hopfield JJ (1995) Pattern recognition computation using action potential timing for stimulus representation. Nature, 376: 33-36

Hosokawa Y, Sciancalepore M, Strata F, Martina M and Cherubini E. (1994) Developmental changes in spontaneous $GABA_A$-mediated synaptic events in rat hippocampal CA3 neurons. Eur. J. Neurosci., 6: 805-813

Hounsgaard J (1978) Presynaptic inhibition action of acetylcholine in area CA1 of the hippocampus. Exp. Neurology, 62: 787-797

Hsia AY, Malenka RC and Nicoll RA (1998) Development of excitory circuitry in the hippocampus. J. Neurophysiol., 79:2013-2024

Hsu KS, Huang CC and Gean PW (1995) Muscarinic depression of excitatory transmission mediated by the presynaptic M3 receptors in the rat neostriatum. Neuroscience Letters, 197: 141-144

Isaac JT, Nicoll RA and Malenka RC (1995) Evidence for sylent synapses: implication for the expression of LTP. Neuron, 15: 427-434

Isa T, Itazawa S, Iino M, Tsuzuki K and Ozawa S (1996) Distribution of neurons expressing inwardly rectifying and Ca^{2+}-permeable AMPA receptors in rat hippocampal slices. J Physiol. 491: 719-733

Jaffard R and Meunier M (1993) Role of hippocampal formation in learning and memory. Hippocampus, 3:203-218

Jarolimek W and Misgeld U (1997) $GABA_B$ receptor-mediated inhibition of tetrodotoxin-resistant GABA release in rodent hippocampal CA1 pyramidal cells. J. Neurosci., 17: 1025-1032

Jefferys JGR, Traub RD and Whittington MA (1996) Neuronal networks for induced '40Hz' rhythms. TINS, 19: 202-208

Jentsch TJ (1996) Chloride channels: a molecular perspective. Curr Opin Mol Neurobiol, 6: 303-310

Johnson JW and Ascher P (1987) Glycine potentiates the nMDA response in cultured mouse brain neurons. Nature, 325:522-525

Jonas P, Racca C, Sakmann B, Seeburg PH and Monyer H (1994) Differences in CA2+ permeabilityof AMPA-type glutamate receptor channels in neocortical neurons caused by differential GluR-B subunit expression. Neuron, 12: 1281-1289

Jones S and Yakel JL (1997) Functional nicotinic ACh receptors on interneurones in the rat hippocampus. J. Physiol., 504: 603-610

Jouvenceau A, Billard JM, Wiley RG, Lamour Y and Dutar P (1994) Cholinergic denervation of the rat hippocampus by 192-IgG-saporin: electrophysiological evidence. NeuroReport, 5: 1781-1784

Kaila K, LamsaK, Smirnov S, Taira T and VolpioJ (1997) Long-lasting GABA-mediated depolarization evoked by high-frequency stimulation in pyramidal neurons of rat hippocampal slice is attributable to a network-driven, bicarbonate-dependent K^+ transient. J. Neurosci., 17:

Kamiya H and Ozawa S (1998) Kainate receptor-mediated inhibition of presynaptic Ca^{2+} influx and EPSP in area CA1 of the rat hippocampus. J Physiol., 509: 833-845

Kandler K and Katz LC (1995) Neuronal coupling and uncoupling in the developing nervous system. Curr. Op. Neurobiol., 5: 98-105

Khalilov I, Escalpez M, Medina I, Aggoun D, LamsaK, Leinekugel X, Khazipov R and Ben Ari Y (1997) A novel *in vitro* preparation: the intact hippocampal formation. Neuron, 19: 743-749

Khazipov R, Leinekugel X, Khalilov I, Gaiarsa JL and Ben Ari Y (1997) Synchronization of GABAergic interneuronal network in CA3 subfield of neonatal rat hippocampal slices. J. Physiol., 498: 763-772

Koh S and Higgins GA (1991) Differential regulation of the low affinity nerve growth factor receptor during postnatal development of the rat brain. J. Comp. Neurol., 313: 494-508

Klimesch W (1996) Memory processe, brain oscillation and EEG synchronization. Int. J. Psychophysiol., 24:61-100

Komuro, H. and Rakic, P. Intracellular (1996) Ca^{2+} fluctuations modulate the rate of neuronal migration. Neuron, 17: 275-285

Konig P Engel AK Singer W (1996) Integrator or coincidence detector? The role of the cortical neuron revisited. Trends Neurosci., 19: 130-137

Konnerth A, Durand G, Garaschuk O, Hanse, E and Kovalchuk Y (1998) Activity-dependent maturation of glutamatergic synapses. Eur. J. Neurosci. 10, supplement 10, 1.04

Korsching S, Auburger G, Heumann R, Scott J and Thoenen H (1985) Levels of nerve growth factor and its mRNA in the central nervous system of the rat correlate with cholinergic innervation, EMBO J. 4: 1389-1393.

Krnjevic K (1993) Central cholinergic mechanism and function. Prog. Brain Res. 98: 285-292

Krnjevic K, Reiffenstein RJ and Ropert N (1981) Disinhibition action of acetylcholine in the rats hippocampus: extracellular observations. Neurosci., 12: 2465-2474

Krnjevic K, Ropert N and Casullo J (1988) Septohippocampal disinhibition. Brain Res., 438: 182-192

Lacaille JC and Williams S (1990) Membrane properties of interneurones in stratum oriens-alveus of the CA1 region of the rat hippocampus *in vitro*. Neuroscience, 36: 349-359

Lancaster B and Nicoll RA (1986) Properties of two calcium-activated hyperpolarizations in rat hippocampal neurons. J Physiol, 389: 187-203

LeBlanc MO and Bland BH (1979) Developmental aspect of hippocampal electrical activity and motor behavior in the rat. Exp. Neurology, 66: 220-237

Lee MG, Chrobak JJ, Sik A, Wiley RG and Buzsaki G (1994) Hippocampal theta activity following selective lesion of the septal cholinergic system. Neuroscience, 62: 1033-1047

Leinekugel X, Khalilov I, Ben Ari Y and Khazipov R (1998) Giant depolarizing potential: the septal pole of the hippocampus paces the activity of the developing intact septohippocampal complex *in vitro*. J. Neurosci., 18: 6349-6357

Leinekugel X, Medina I, Khalilov I, Ben Ari Y and Khazipov R (1997) Ca^{2+} oscillations mediated by the synergistic excitatory actions of $GABA_A$ and NMDA receptors in the neonatal hippocampus. Neuron, 18: 243-255.

Leinekugel, X., Tseeb, V., Ben Ari, Y., and Bregestovski, P. (1995) Synaptic $GABA_A$ activation induces Ca^{++} rise in pyramidal cells and interneurones from rat neonatl hippocampal slice. J. Physiol., 487: 319-329.

Leranth C, SzeidemannZ, Hsu M and BuzakiG (1996) AMPA receptors in the rat and primate hippocampus: a possible absence of Glur2/3 subunits in most inteneurones. Neuroscience, 70: 631-652

Lerma J (1997) Kainate reveals its targets. Neuron, 19:1155-1158

Lerma J, Paternain AV, Naranjo JR and and Mellstrom B (1993) Functional Kainate-selective glutamate receptors in cultured hippocampal neurons. Proc. Natl. Acad. Sci. USA 90, 11688-11692

Levey AI, Edmunds SM, Koliatsos V, Wiley RG and Heilman CJ (1995) Expression of m1-m4 muscarinic acetilcholine receptors proteins in rat hippocampus and regulation by cholinergic innervation. J. Neurosci. 15(5):4077-4092.

Liao D, Hessler NA and Malinow R (1995) Activation of postsynaptically silent synapses during pairing-induced LTP in CA1 region of hippocampal slice. Nature 375: 400-404

Llinas R, Sugimori M and Simon S M (1982) Transmission by presynaptic spike-like depolarization in the squid giant synapse. Proc. Natl. Acad. Sci. USA, 79: 2415-2419

Lindvall O and Bjorkland A (1974) The organization of the ascendin catecholamine neurone systems in the rat brain, as revealed by the glyoxilic acid fluorescence method. Acta Physiol. Scand., 73 (suppl. 412): 1-48

Lismann JE (1997) Bursts as a unit of neural information: making unreliable synapses reliable. TINS, 20: 38-43

Lorente de No' R (1934) Studies on the structureof cerebral cortex.II. Continuation of the study of the ammonic system. J Psychol Neurol 46: 113-177

MacVicar BA and Tse FWY (1989) Local neuronal circuitry underlying cholinergic rhythmical slow activity in CA3 area of rat hippocampal slices. J. Physiol. 417: 197-212

Madison DV, Lancaster B and Nicoll RA (1987) Voltage clamp analysis of cholinergic action in the hippocampus. J neurosci., 7: 733-741

Mainen ZF and Sejnowski TJ (1995) Reliability of spike timing in noecortical neurons. Science, 268: 1503-1506

Marchi M and Raiteri M (1989) Interaction acetylcholine-glutamate in rat hippocampus: involvement of the two subtypes of M2 muscarinic receptors. J. Pharmacol. Exp. Ther., 248: 1255-1260

Markram H and Segal M (1990) Long lasting facilitation of excitatory postsynaptic potentilas in the rat hippocampus by achetylcholine. J Physiol, 427:381-393

Martina M, Strata F. and Cherubini E. (1995) Whole-cell and single channel properties of a new GABA receptor transiently expressed in the hippocampus. J Neurophysiol. 73(2): 902-906

Mattehews DA, Nadler JV, Lynch GS and Cotman CW (1974) Development of cholinergic innervation in the hippocampal formation of the rat. I Histochemical demonstration of AChE activity. Dev. Biol., 36: 130-141

McBain CJ, Eaton JV, Brown T and Dindledine R (1992) CNQX increases spontaneous inhibitory input to CA3 pyramidal neurons in neonatal rat hippocampal slices. Brain Res., 592: 255-266

McCormick DA and Pape HC (1988) Acetylcholine inhibits identified interneurons in tha cat lateral geniculate nucleus. Nature, 334: 246-248

McCormick DA and Prince DA (1986) Acetylcholine induces burst firing in thalamic neurones by activating a potassium conductance. Nature, 319: 402-405

Mc Kinney M (1993) Muscarinic receptor subtypes-specific coupling to second messengers in neuronal systems. Prog. Brain Res., 98: 333-340

Mc Kinney M, Miller JH, and Adggard PY (1993) Pharmacological characterization of the rat hippocampal muscarinic autoreceptor. J. Pharmacol. Exp. Ther. 264: 74-78.

McLean HA, Rovira C, Ben-Ari Y and Gaiarsa JL (1995) NMDA-dependent $GABA_A$-mediated polysynaptic potentials in the neonatal rat hippocampal CA3 region. Eur. J. Neurosci., 7: 1442-1448

Meister M, Wong ROL, Baylor DA and Shatz CJ (1991) Synchronous bursts of action potentials in ganglion cells of the developing mammalian retina. Science, 252: 939-943

Menendez de la Prida, L., Bolea, S. and Sanchez-Andres, J.V. (1998) Origin of the synchronized network activity in the rabbit developing hippocampus. *Eur. J. Neurosci.* 10: 899-906.

Milburn CM and Prince DA (1993) Postnatal development of cholinergic presynaptic inhibition in rat hippocampus. Dev. Brain Res., 74:133-137

Miles R, Toth K, Gulyas AI, Hajos N and Freund TF (1996) Differences between somatic and dendritic inhibition in the hippocampus. Neuron 16:815-823

Milner TA, Loy R and Amaral DG (1983) An anatomical study of the development of the septo-hippocampal projection in the rat. Dev. Brain Res., 8:343-371

Misgeld U, Bijal M, JarolimekW (1995) A physiological rolefor $GABA_B$ receptors and the effects of baclofen in the mammalian central nervous system. Prog. Neurobiol., 46: 423-462

Misgeld U, Deisz RA, Dodt HU and Lux HD (1986) The role of chloride transportin postsynaptic inhibition of hippocampal neurones. Science, 232: 1413-1415

Mladinic M (1997) Molecular investigation of a novel GABA response in developing rat hippocampus. Thesis

Molnar M, Ruberti F, Cozzari C, Domenici L and Cattaneo A (1997) A critical period in the sensitivity of basal forebrain cholinergic neurons to NGF deprivation, NeuroReport, 8: 575-579

Molnar M, Tongiorgi E, Avignone E, Gonfloni S, Ruberti F, Domenici L and Cattaneo A (1998) The effects of anti-NGF monoclonal antibodies on developing basal forebrain neurons are transient and reversible. Eur. J. Neurosci., in press

Morin F, Beaulieu C and Lacaille JC (1996) membrane properties and synaptic current evoked in CA1 interneurons subtypes in rat hippocampal slices. J. Neurophysiol., 76: 1-16

Nadel L (1991) The hippocampus and space revisited. Hippocampus, 1: 221-229

Nadler JV, Mattehews DA, Cotman CW and Lynch GS (1974) Development of cholinergic innervation in the hippocampal formation of the rat. II Quantitative changes in choline acetyltransferase and acetylcholineesterase activities. Dev. Biol., 36: 142-154

Nakajima Y, Nakajima S, Leonard RJ and Yamaguchi K (1986) Acetylcholine raises excitability by inhibiting the fast transient potassium current in cultured hippocampal neurons. Proc. Natl. Acad. Sci. USA, 83: 3022-3026

Neumann R, Ben Ari Y, Gho M and Cherubini E (1988) Blockade of excitatory synaptic transmission by 6-cyano-7-nitroquinoxaline-2,3-dione (CNQX) in the hippocampus in vitro. Neurosci. Lett., 92: 64-68

Nyakas C, Buwalda B, Kramers RJK, Traber J and Luiten PG (1994) Postnatal development of hippocampal and neocortical cholinergic and serotonergic innervation in rat: effects of nitrite-induced prenatal hypoxia and nimodipine treatment. Neuroscience, 59: 541-559

O'Keefe J. and Recce ML. (1993) Phase relationship between hippocampal place units and the EEG theta rhythm. Hippocampus, 3: 317-330

Ouardouz M and Durand J (1991) GYKI 52466 anatgonizes glutamate responses but not NMDA and kainate responses in rat abdunces motoneurons. Neurosci Lett. 125, 5-8.

Partin KM, Patneau DK, Winters CA, Mayer ML and Buonanno A (1993) Selective modulation of desensitization at AMPA versus kainate receptors by cyclothiazide and concanavalin A. Neuron, 11: 1069-1082

Paternain AV, Morales M, and Lerma J (1995) Selective antagonist fo AMPA receptors unmasks kainate receptors-mediated responses in hippocampal neurons. Neuron, 14:185-189

Penn AA, Wong ROL, Shatz CJ (1994) Neuronal coupling in the developing mammalian retina, J. Neurosci., 14: 3805-3815

Perkins KL and Wong RKS (1996) Ionic basisof the postsynaptic depolarizing GABA response in hippocampal pyramidal cells. J. Neurophysiol., 76:3886-3894

Pin JP and Bockaert J (1995) Get receptive to metabotropic glutamate receptors. Curr. Op. Neurobiol. 5:342-349

Pitler TA and Alger BE (1992) Cholinergic excitation of GABAergic interneurons in the rat hippocampal slice. J. Physiol., 450: 127-142

Pitler TA and Alger BE (1990) Activation of the pharmacologically defined M3 muscarinic receptor depolarizes hippocampal pyramidal cells. Brain Res., 534: 257-262

Postlethwaite M, Constanti A and Libri V (1998) Muscarinic agonist-induced burst firing in immature rat olfactory cortex neurons in vitro. J Neurophysiol. 79: 2003-2012

Psarropoulou C and Dallaire F (1998) Activation of muscarinic receptors during blockade of $GABA_A$-mediated inhibition induces synchronous epileptic form activity in immature rat hippocampus. Neuroscience 82: 1067-1077

Raiteri M, Leardi R and Marchi M (1984) Heterogenety of presynaptic muscarinic receptors regulating neurotransmitter release in the rat brain. J. Pharmacol. Exp. Ther., 228: 209-214

Rami A., Rabie A. and Clos J. (1989) The time course of hippocampal cholinergic innervation in the developing hypothyroid rat. A combined histochemical and biochemical study of acetylcholinesterase activity. International Journal of Developmental Neuroscience, 7: 301-308.

Recce LJ and Schwartzkroin PA (1991) Effects of cholinergic agonists on two non-pyramidal cell types in rat hippocampal slices. Brain Res., 566: 115-126

Rodriguez-Moreno A, Herreras O and Lerma J (1997) Kainate receptors presynaptically downregulate GABAergic inhibition in the rat hippocampus. Neuron, 19: 893-901.

Rotter A, Field PM and Raisman G (1979) Muscarinic receptors in the central nervous system of the rat. III Postnatal development of binding of [3h]propylbenzilylcholine mustard. Brain Res., 180: 185-205

Rouse ST and Levey AI (1996) Expression of m1-m4 muscarinic acetilcholine receptors immunoreactovity in septohippocampal neurons and other identified hippocampal afferents. Journ. of Comp. Neurology; 375:406-416.

Rovira C, Ben-Ari Y and Cherubini E (1983) Dual cholinergic modulation of somatic and dendritic field potential by the septo-hippocampal pathway. Exp. Brain Res., 49: 151-155

Rovira C, Ben-Ari Y, Cherubini E, Krnjevic K and Ropert N (1983) Pharmachology of the dendritic action of acetylcholine and further observations on the somatic disinhibition in the rat hippocampus *in situ*. Neuosci., 1:97-106

Schoepp DD and Conn PJ (1993) Metabotropic glutamate receptors in brain function and pathology. TIPS, 14: 13-20

Scoville WB and Milner B (1957) Loss of recent memory after bilateral hippocampal lesions. J Neurol Neurosurg Psychiatr, 20: 11-21

Shadlen MN and Newsome WT (1994) Noise, neuronal code and cortical organization. Curr. Op. Nuerobiol., 4: 569-579

Shatz CJ (1990) Impulse activity and the patterning of connections during CNS development. Neuron, 5: 745-756

Shelton DL and Reichardt LF (1986) Studies on the expression of the beta nerve growth factor (NGF) gene in the central nervous system: level and regional distribution of NGF functions as a trophic factor for several distinct populations of neurons. Proc. Natl. Acad. Sci. USA: 832714-2718

Sheridan RD and Sutor B (1990) Presynaptic M1 muscarinic cholinoceptors mediate inhibition of excitatory synaptic transmission in the hippocampus in vitro. Nuerosci. Lett., 108: 273-278

Shibata O, Kanairo M. Zhang S, Hasuo H, Morooka H, Fujie T and Sumikawa K (1996) Anticholinesterase drugs stimulate phosphatidylinositol response in rat tracheal slices. Anestesia & Analgesia, 82: 1211-1214

Siegel S, Brose N, Janssen WG, Gasic GP, Jahn R and Heinemann SF (1994) Regional, cellular and ultrastructural distribution of N-methyl-D-aspartate receptor subunit 1 in monkey hippocampus. Proc. Natl. Acad. Sci., USA, 91: 564-568.

Sik A, Tamamaki N and Freund TF (1993) Complete axon arborization of a single CA3 pyramidal cell in th erat hippocampus, and its relationship with postsynaptic parvalbumin-containing interneurons. Eur. J Neurosci., 5: 1719-1728

Sivilotti L and Nistri A (1991) GABA receptors mechanisms in the central nervous system. Prog. Neurobiol., 36:35-92

Skrede KK and Westgard RH (1971) The transverse hippocampal slices: a well defined cortical structure mantained *in vitro*. Brain Res., 35: 589-593

Softky WR (1995) Simple code versus efficient codes Curr. Op. Nerobiol., 5: 239-247

Softky WR and Koch C (1993) The highly irregular firing of cortical cells is inconsistent with temporal integration of random EPSPs. J. Neurosci, 13: 334-350

Spitzer, N.C. Spontaneous (1994) Ca^{2+} spikes and waves in embryonic neurons: signaling system for differentiation. Trends Neurosci. 17, 115-118

Stanley KJ (1994) The role of inwardly rectifying chloride conductance in postsynaptic inhibition. J Neurophysiol. 72:273-284

Staley KJ, Soldo BL, Proctor WR (1995) Ionic mechanisms of neuronal excitation by inhibition of $GABA_A$ receptors. Science 269:977-981

Steriade M, Contreras D and Amzica F (1996) Synchronized sleep oscillationsand they paroxismal developments. Trend Neurosci., 17:199-208

Stevens CF and Wang Y (1995) Facilitation and depression at single central synapses. Neuron, 14: 795-802

Storm JF (1990) Potassium currents in hippocampal pyramidal cells. Prog. Brain Res., 83:161-187

Strata F (1996) Giant GABAergic potentials of developing rat hippocampus: the pacemaker hypothesis. PhD Thesis SISSA

Strata F and Cherubini E (1994) Transient expression of a novel type of GABA response in rat CA3 hippocampal neurons during development. J. Physiol., 480: 493-503

Strata F, Sciancalepore M and Cherubini E (1995) cAMP-dependent modulation of Giant Depolarizing Potentials by metabotropic glutamate receptors in the rat hippocampus. *J. Physiol.*, 489: 115-125.

Strata F, Atzori M, Molnar M, Ugolini G, Tempia F and Cherubini E (1997) A pacemaker current in dye-coupled hilar interneurons contributes to the generation of gian GABAergic potential in developing hippocampus. J. Neurosci. 17: 1435-1446

Tice, MA, Hashemi T, Taylor LA and McQuade RD (1996) Distribution of muscarinic receptor subtypes in rat brain from postnatal to old age. Develop. Brain Res. 92: 70-76

Thomson SM and Gahwiler BH (1989) Activity dependent disinhibition. III. Desensitization and $GABA_B$ receptor-mediated presynaptic inhibition in the hippocampus *in vitro*. J. Neurophysiol., 61: 524-533

Toth K, Freund TF and Miles R (1997) Disinhibition of rat hippocampal pyramidal cells by GABAergic afferents from the septum. J. Physiol., 500: 463-474

Traub RD and Miles R (1991) Neuronal networks of the hippocampus. Cambridge: Cambridge Univ. Press

Traub RD Miles R and Buzsaki G (1996) Computer simulation of carbachol-driven rhythmic population oscillations in the CA3 region of the in vitro rat hippocampus. J Physiol., 451: 653-672

Umbriaco D, Watkiss WC, descarries L, Cozzari C and Hartman BK (1994) Ultrastructural and morphometric features of achetylcholine innervation in adult rat parietal cortex: an electron microscopic study in serial section. J. Comp. Neurol., 348: 351-373

Vaknin G and Teyler TJ (1991) Ontogenesis of the depressant activity of carbachol on synaptic activity in rat visual cortex. Brain Res. Bull., 26:211-214

Valentino RJ and Dingledine R (1981) Presynaptic inhibition effect of acetylcholine in the hippocampus. J. Neurosci., 1:784-792

Vannucchi MG, Casamenti F and Pepeu G (1990) Decrease of acetylcholine release from cortical slices in aged rats: investigations into its reversal by phosphatidylserine, J. Neurochem., 55: 819-825

Vantini G, Schiavo N, Di Martino A, Polato P, Triban C, Callegaro L, Toffano G and Leon A (1989) Evidence for a physiological role of nerve growth factor in the central nervous system, Neuron, 3: 267-273

Vignes M and Collingridge GL (1997) The synaptic activation of kainate receptors Nature, 388:179-182

Watanabe, M., Fukaya, M., Sakimura, K., Manabe, T., Mishina, M. and Inoue, Y. (1998) Selective scarcity of NMDA receptor channel subunits in the stratum lucidum (mossy fibre-recipient layer) of the mouse hippocampal CA3 subfield. Eur. J. Neurosci., 10: 478-487

Wisden W and Seeburg PH (1993) A complex mosaic of high-affinity kainate receptors in rat brain. J. Neurosci., 13:3582-3598

Whittington MA, Traub RD and Jefferys JGR (1995) Synchronized oscilaltions in interneuro networks driven by metabotropic glutamate receptor activation. Nature, 373: 612-615

Williams JH and Kauer JA (1997) Properties of carbachol-induced oscillatory activity in rat hippocampus. J Neurophysiol., 78:2631-2640

Wong ROL, Meister M and Shatz CJ (1993) Transient period of correlated bursting activity during development of the mammalian retina. Neruon, 11:923-938

Xie X, Hider RC, Smart TG (1994) Modulation of GABA-mediated synaptic transmission by endogenous zinc in the immature rat hippocampus *in vitro*. J. Physiol. 478: 75-86

Yakel JL (1997) Calcineurin regulation of synaptic function: from ion channels to transmitter release and gene transcription. TIPS, 18:124-34

Yuste R, Peinado A, Katz LC (1992) Neuronal domains in developing neocortex. Science, 257: 665-669

Zhang L, Weiner JL and Carlen PL (1992) Muscarinic potentiation of I_K in hippocampal neurones: electrophysiological characterization of the signal transduction pathway. J. Neurosci., 12: 4510-4520

Zohary E, Shadlen MN and NewsomeWT (1994) Correlated neuronal discharge rate and its implication for phychophysical performance. Nature, 370: 140-143

Zorumski CF, Yamada KA, Price MT and Olney JW (1993) A benzodiazepine recognition site associated with the non-NMDA glutamate receptors. Neuron, 10: 61-67